DISPERSION MODELLING DURING PARTICULATE MATTER EPISODE EVENTS IN GOLDEN, BRITISH COLUMBIA

by

Tyler Abel

B.Sc., The University of British Columbia, 2003

THESIS SUBMITTED IN PARTIAL FULFILLMENT OF THE REQUIREMENTS FOR THE DEGREE OF MASTER OF SCIENCE IN NATURAL RESOURCES AND ENVIRONMENTAL STUDIES

THE UNIVERSITY OF NORTHERN BRITISH COLUMBIA

APRIL 2011

Your file Votre référence
ISBN: 978-0-494-87568-1

Our file Notre référence
ISBN: 978-0-494-87568-1

ABSTRACT

The CALPUFF modeling system was used to investigate two episodes of high particulate matter (PM) during December 2005 and February 2006. During this time, Golden was a British Columbia Ministry of Environment (BC MOE) intensive observation site for air quality research specific to PM. Observations from 4 meteorological stations were used to characterize the winds and dispersion parameters within CALMET. Emission rates were determined from the existing Golden Emissions Inventory and receptor modelling commissioned by the BC MOE. Statistical comparison of model predicted and observed PM concentrations show that model performance compares well to similar CALPUFF studies at two of the air quality monitoring stations in Golden. The source apportionment of the CALPUFF results identified the major contributors to degraded air quality levels during the two episodes under investigation as space heating, road dust and, intermittently, Louisiana Pacific operations.

TABLE OF CONTENTS

LIST OF TABLES

LIST OF FIGURES

ACKNOWLEDGEMENTS

The author would like to thank first and foremost his supervisor Dr. Peter L. Jackson for guidance throughout this long journey. Also, his committee, Dr. Margot Mandy, Dr. Stephan Dery and Steve Sakiyama, who provided great feedback to (finally) accomplish a finished product. Many thanks to Denny Straussfogel for his help with the fieldwork and great conversation along the long road to Golden. Special thanks to Paul Willis of the BC MOE for his words of encouragement and who inspired me to do this thesis in the first place, the Town of Golden Air Quality Committee and Mike Brygger from LP.

Funding for this project was provided by the Clean Air Research Fund (CARF), the British Columbia Ministry of Environment (BC MOE) and NSERC Discovery Grant research funding via Dr. Peter L. Jackson. All contributors are greatly appreciated!

LIST OF ABBREVIATIONS

Acronym	Definition
σ	Standard deviation
ACE	Air Contaminants Emission Project
AGL	Above Ground Level
BC MOE	British Columbia Ministry of Environment
BLD	Building
BPIP	Building Profile Input Program
BURN	Burning Emissions
CONS	Construction Emissions
CORR	Correlation Coefficient
CPR	Canadian Pacific Railway; Site of Monitoring Station in Golden
D	Willmott's Index of Agreement
EI	Emissions Inventory
FAC2	Fraction of Predictions within a Factor of 2 of Observed Values
FB	Fractional Bias
FGE	Fractional Gross Error
GIS	Geographic Information System
GOLF	Golf Course Monitoring Station in Golden
km	Kilometre
LP	Louisiana Pacific Engineered Wood Products Limited
LTRFC	Local Traffic Emissions
NRMSE	Normalized Root Mean Square Error
M	metre
m/s	Meters per Second
MAE	Mean Absolute Error
MAX ERR	Maximum Error
ME	Mean Error
MED ERR	Median Error
MG	Geometric Mean Bias
MIN ERR	Minimum Error
Mix Hgt	Mixing Height
Mon-obu	Monin Obukhov Length
MSE	Mean Square Error
MM5	Fifth-Generation NCAR / Penn State Mesoscale Model
OB	Observed Measurement
PM	Particulate Matter
PM_{10}	Particulate Matter smaller than 10 microns in size

$PM_{2.5}$	Particulate Matter smaller than 2.5 microns in size
PR	Model Predictions
RDUST	Road Dust Emissions
RUC	National Oceanic and Atmospheric Association's National Center for Environmental Prediction Rapid Update Cycle Model
R1	Point at which the influence of a surface meteorological station is equal to 50 percent
Rmax,	Maximum radius of influence of surface meteorological stations in CALMET
SPCHT	Space Heating Emissions
SRC	Source
SODAR	Sonic Detection and Ranging
TEMP	Temperature
Terrad	Distance to which a terrain feature in CALMET can affect 3-D wind flows
TOWN	Townsite Monitoring Station in Golden
$\mu g/m^3$	Micrograms per Meter Cubed
US EPA	United States Environmental Protection Agency
UTM	Universal Transverse Mercator Coordinate System
VKmTs	Vehicle Kilometres Travelled
Wdir	Wind Direction
WHO	World Health Organization
Wspd	Wind Speed

1 INTRODUCTION

1.1 OVERVIEW

The public, industry and government are becoming increasingly aware of the detrimental health, economic and environmental effects associated with airborne pollutants. Growing concerns have pushed the government, communities and academia towards furthering their understanding of all processes involved in the release, dispersion of, and exposure to, airborne pollutants (British Columbia Ministry of Environment 2002).

To better understand these issues, an intensive particulate matter (PM) speciation study conducted by the British Columbia Ministry of Environment (BC MOE) was carried out in the Town of Golden, British Columbia. Golden is a small community of approximately 5000 residents situated in the northern Columbia River Basin, bordered by the Purcell Mountains to the west and the Rocky Mountains to the east (Figure 1-1). To compliment the BC MOE speciation study in Golden, this study used the CALPUFF modeling system to model the dispersion of PM in the local airshed. The CALPUFF modelling system is a diagnostic air dispersion model that utilizes meteorological conditions and wind fields calculated from the meteorological model, CALMET, to estimate pollutant concentrations in an air dispersion model called CALPUFF.

1.2 Dispersion Modeling Study Rationale

The BCMOE identified the following main goals for the Golden speciation study:

1. Ensure federal, provincial, and local air quality goals for the study are achieved.
2. Identify anthropogenic pollutants found in the Golden airshed so that an Airshed Management Plan can be optimized.
3. Provide information to allow community planners to determine the most efficient and economically viable emission reduction options.
4. Establish guidelines for future provincial PM speciation studies.

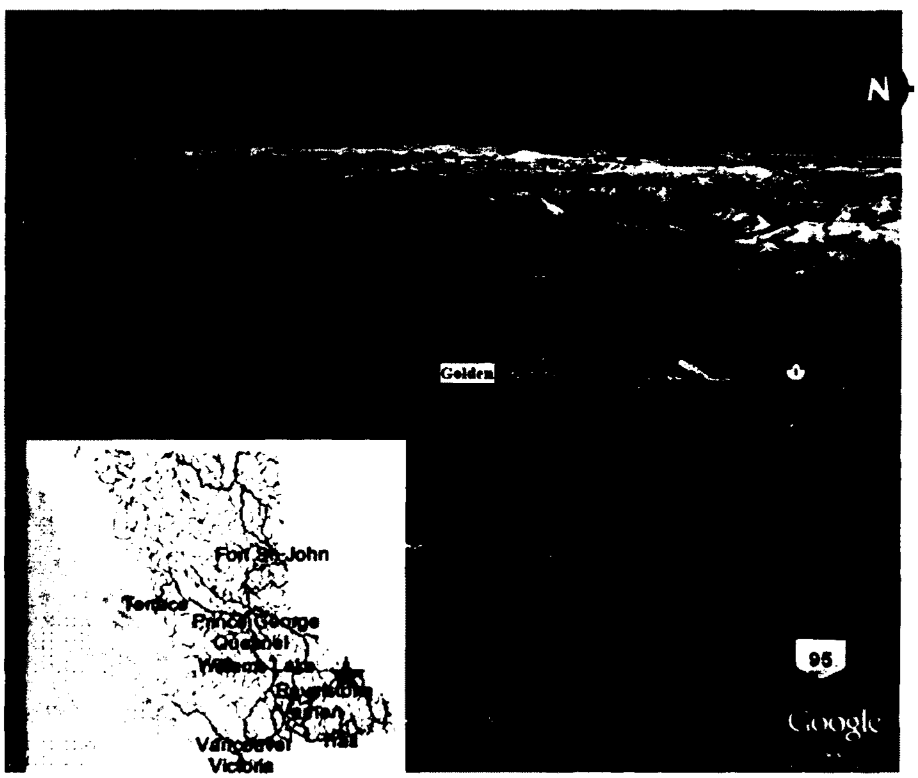

Figure 1-1 **The Northern Columbia River Basin. Golden is located at the junction of Highway 1 (Transcanada Highway) and Highway 95. Perspective view is intended to show that Golden is located in a deep valley surrounded by steep valley walls. Inset indicates Golden's location in BC (Map courtesy of Google Earth™).**

In an effort to provide a tool for future airshed management in Golden, this study used local meteorological and pollutant emission data collected in Golden to model the dispersion of PM in the Golden Airshed (Figure 1-2).

An airshed is defined here as the extent where topography and meteorology have a significant effect on hindering the dispersion of air pollutants away from the area. The airshed extent in Figure 1-2 is bounded by the Rocky Mountains to the east and the Purcell Mountains to the west. The winds in the Golden airshed predominantly flow along the the northeast to southwest orientation of the valley. The airshed north and south boundaries are based on the dispersion of potential pollutants in the airshed given the predominant wind pattern.

The data collection activities in Golden during the speciation study provided an opportunity to evaluate the CALPUFF modeling system in complex, mountainous terrain. Results from the dispersion model, can be used as a valuable tool for constructing a local air quality management plan (AQMP). It is the aim of this study to model as accurately as possible episodes of high PM. An AQMP for Golden will not solely focus on episodes of high PM. Such a plan will account for all pollutants in the airshed and take into account the acute and chronic impacts of degraded air quality on the community. Modeling PM episodes will provide insight into the meteorological and emission conditions that give rise to such episodes. In a local AQMP, this information could be used to identify when acute impacts from the major pollutant of concern in Golden, PM, are likely to occur and be used to develop strategies to reduce community exposure during these times.

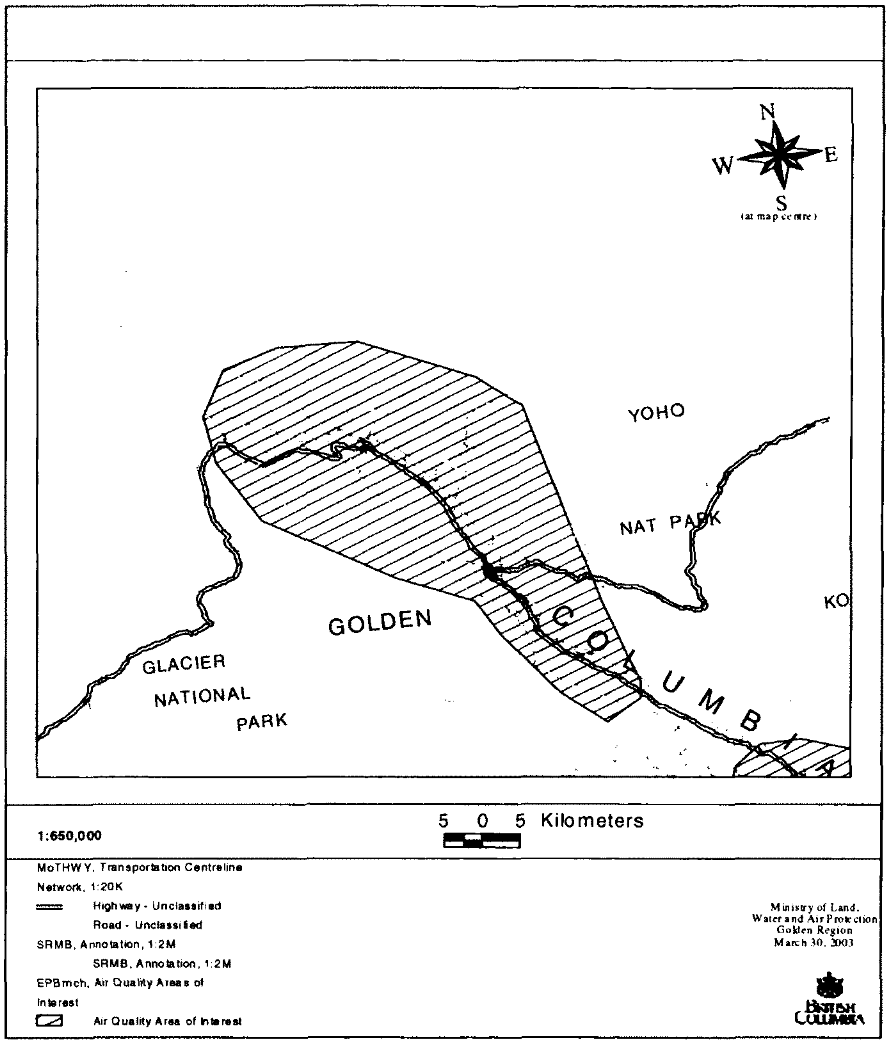

Figure 1-2 The Golden airshed. Indicated by the horizontal blue lines. Map courtesy of BC MOE.

1.3 RESEARCH RATIONALE, QUESTIONS AND GOALS

Winds in Golden tend to be terrain forced flows following the valley alignment (Figure 1-3). At low wind speeds, dispersion is expected to be influenced by the diurnal mountain wind system described in Section 2.4. Scire and Robe (1997) showed that improvements made to CALMET, the meteorological processor for the CALPUFF dispersion model, improved estimation of wind fields, wind channeling and mountain valley flows at a complex terrain site in the Columbia River Valley, when compared to other US EPA regulatory models,. It was anticipated that CALMET would be able to estimate both the main valley terrain-induced flows and the diurnal mountain wind system to model episodes of PM in Golden. Modeling conditions of low wind speeds and proper diurnal mountain wind system effects is vital. It is expected that periods of stagnation will be associated with the increase of PM during episodes.

Episodes of high PM will be modeled. CALPUFF will be used to investigate the meteorological, emission and dispersal processes that contribute to the degradation of air quality and the creation and sustenance of PM episode events. Two episodes with high concentrations of PM_{10} and $PM_{2.5}$ as well as different ratios of $PM_{2.5}$:PM_{10} will be modeled for this study. This will allow for comparison of dispersion and emission processes during each episode.

Receptor modeling results from BC MOE determined the source contribution to seasonal PM episodes (Evans and Jeong 2007). The present study will apportion sources that are contributing to two specific PM episodes by modeling individual point, area and line sources in CALPUFF.

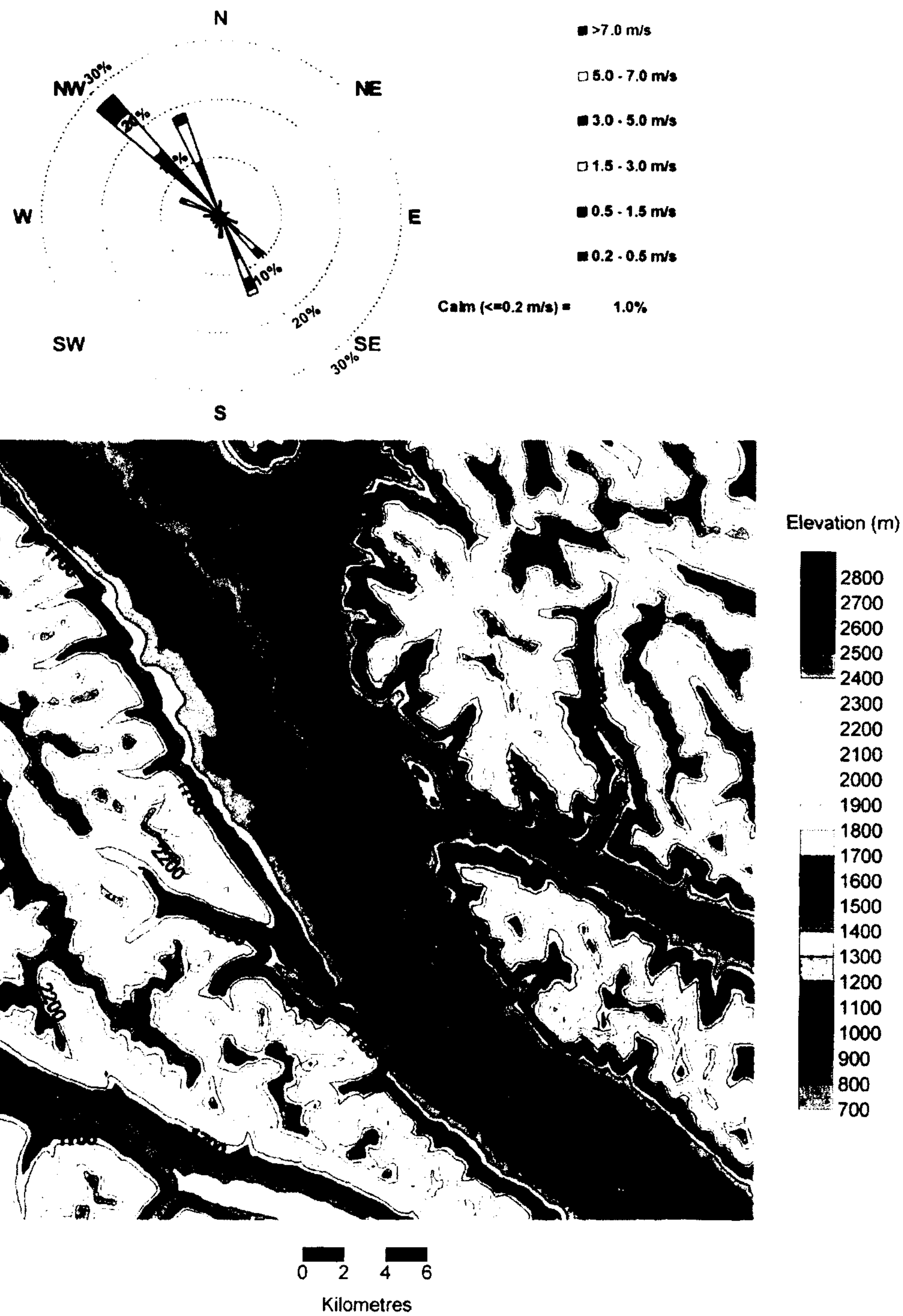

Figure 1-3 **Wind rose for Golden including all winds recorded from January 2001 through April 2005 (top). Contour map showing valley alignment for comparison with wind rose.**

A comparison of the modeled results with those from the receptor modeling will be used to evaluate CALPUFF's effectiveness as a source apportionment tool.

Along with identifying the source contributions, CALPUFF will be used to investigate boundary layer or emission processes that lead to:

- spatial differences in PM. Why does source x have a greater contribution to receptor y as opposed to receptor z in another location?
- temporal differences in PM. Why does source x contribute more to ground level concentrations when high PM concentrations are recorded as opposed to when low PM concentrations are observed?

Meeting the study goals entails answering: What are the general dispersal mechanism and emission processes that contribute to episodes of PM in Golden? It is hypothesized that evaluation of observational and modeled data will reveal that episodes are associated with low wind speeds and meteorological conditions that give rise to periods of stagnation. Diurnal variation in emission rates may also contribute to elevated PM levels.

CALPUFF modeling in Golden will evaluate the model's performance in complex topography. Of interest is CALPUFF's ability to model the dispersal and emission conditions and accurately predict PM concentrations during the episodes. Previous studies found that CALPUFF performs well in complex terrain (Scire and Robe 1997, Barna and Grimson 2002). In Golden, it is expected that CALPUFF will be able to accurately predict the observed PM concentrations. The meteorological network set up during the study period allows for evaluation of CALMET in predicting observed surface winds; and CALPUFF in simulating dispersion of PM. Previous BC MOE CALPUFF modeling efforts in Golden were hindered by using upper air data collected more than 400 kilometres away, in Kelowna. The sodar system and surface HOBO data in combination with upper air data were expected to provide more accurate local upper air data.

To review, this study sought to answer the following research questions:

- What are the dispersal mechanisms and emission processes that contribute to episodes of PM in Golden?
- Can these conditions be modeled in CALPUFF with the existing emissions information to accurately represent PM concentrations during these episodes?
- Will CALPUFF predicted PM source apportionments compare well with receptor modeling conducted by BCMOE (Evans and Jeong 2007)?

1.4 Format of Thesis

This thesis is organized by first presenting the major concepts covered in the study. This is followed by a description of the methods and modeling system. Next, a review and analysis of the episodes modeled in the study is provided. The CALMET/CALPUFF setup and evaluation is presented in the subsequent two chapters. Finally, CALPUFF source apportionment results and analysis are examined.

2 STUDY BACKGROUND

2.1 Particulate Matter

Airborne PM has been associated with a wide range of adverse human health effects (Vedal 1995). Specifically, elderly people who may have compromised cardiovascular function and younger children with asthma have been recognized as "at risk" sectors of the population (Caton and Bates 2002, Enstrom 2005). However, there is epidemiologic evidence that chronic effects from even low level exposure to PM have the potential to affect all members of the population (Vedal 1997). Over the short-term, exposure to PM leads to school absences, extreme discomfort for those with respiratory diseases, and increased hospital admission rates due to recurrences of respiratory and cardiac conditions (British Columbia Provincial Health Officer 2003). Long term effects have been associated with depressed lung function in children, increased cases of bronchitis, increased risk of lung cancer, and increased mortality due to respiratory and cardiac conditions (British Columbia Provincial Health Officer 2003, Ovadnevaite et al. 2002). Epidemiological evidence indicates that Golden and other BC interior communities should be concerned about high PM levels (British Columbia Provincial Health Officer 2003) and PM will be the focus of this modeling study.

Specifically this modeling study will focus on episodic (short-term) increases in airborne PM. A number of studies have coupled the sharp, short-term increases during episodes with significant changes in lung function and respiratory illness (Ostor, 1993; Dockery et al. 1996). In extreme cases the high PM episodes can result in immediate mortality with the US EPA estimating that the pollution-induced spike in the death rate can range from 2% to 8% for every 50 $\mu g/m^3$ increase in PM levels (US EPA, 1996). In addition, the World Health Organization (WHO) estimates that pollution episodes account for 7% – 10% of respiratory illness in children and 0.6% - 1.1% of deaths (WHO, 1994).

As the health effects of airborne PM were identified, it became apparent that smaller particles (less than 10 microns) have more significant health impacts as they can be inhaled more deeply into the lungs (British Columbia Provincial Health officer 2003). Specifically, particles with an aerodynamic diameter of less than 10 microns (and greater than 2.5 microns) have been shown to be capable of penetrating through the natural protective barriers of the human respiratory system leading to respiratory and cardiac disease (Ghose et al. 2005). Studies have indicated that the even smaller particles (less than 2.5 microns) have the ability to penetrate even further into the lungs causing more severe health effects (Kaur et al. 2005). In addition, these smallest particles are more easily able to penetrate indoors, be transported over long distances, and remain in the air for prolonged periods, as compared to larger particles (Pope 2000). Smaller particles of PM are generally associated with fossil fuel combustion from mobile sources or industrial boilers (Jansen et al. 2005, Win Lee et al. 2004).

It has been established that the size of airborne PM can serve to distinguish the origin, composition and associated health effects of particles. Coarse particles, defined as those particles with an aerodynamic diameter greater than 2.5 microns, are derived from soil and earth's crustal materials (Pope 2000). PM with an aerodynamic diameter of less than 10 microns (PM_{10}) are capable of penetrating into the lungs. Therefore, measuring PM_{10} concentrations is of interest to health officials as it will quantify soil and crustal material particulates as well as other emitted particles that affect human health. Fine particulates, defined as those particles with an aerodynamic diameter less than 2.5 microns ($PM_{2.5}$), are primarily derived from combustion during processes such as transportation, manufacturing and power generation (Pope 2000), but can also include finer dust particles. Measurement of $PM_{2.5}$, a subset of PM_{10}, is of great interest in determining the effects of these specific, generally anthropogenic, combustion processes on human health because of the noted ability of these smaller particles to penetrate deeper into the lungs causing more severe health effects than larger particles.

In an effort to reduce PM concentrations in British Columbia communities, the provincial government has instituted a province-wide 24-hour PM_{10} objective that is applicable to the Town of Golden. Table 2-1 outlines the definition of the objective as well as PM concentration targets.

Table 2-1 Provincial 24-hour Average PM_{10} air quality objective.

National Maximum Acceptable Level	Provides adequate protection against adverse effects on human health, vegetation and animals. Usually set as an intermediate objective for all existing discharges to reach within a specified time period, and as an immediate objective for existing discharges which may be increased in quantity or altered in quality as a result of process expansion or modification	50 $\mu g/m^3$

The objectives set for $PM_{2.5}$ in British Columbia were released in April 2009 and are summarized in Table 2-2.

Table 2-2 Provincial $PM_{2.5}$ ambient air quality objectives

Averaging Period	Air Quality Objective
24-hour	25 µg/m^3 *
Annual	8 µg/m^3

* based on annual 98th percentile value

In addition to adverse health effects, PM is of concern in communities, such as Golden, that rely on tourism. Particles in the air scatter light, causing a degradation of visibility (Watson 2002). Golden, a community that promotes itself as a pristine natural environment for outdoor activities ranging from skiing to eco-tourism has a great interest in having clear vistas, free of haze and smog, for its many visitors to enjoy the area.

2.2 Particulate Matter in Golden

This study focuses on dispersion modeling of PM in the Golden airshed. Specifically, two fractions of the total PM were investigated, PM_{10} and $PM_{2.5}$. Golden had the highest average concentration of PM_{10} in BC communities from 2003-2005 (Figure 2-1). $PM_{2.5}$ concentrations were also very high when compared to other BC communities (Figure 2-1).

Steep valley walls, mountain-valley winds and low wind speeds can make Golden susceptible to wintertime inversions and stagnation events throughout the year (Burkholder 2005). Local monitoring reveals that episodes of elevated levels of PM are typical during the winter months (Figure 2-2). Episodes greatly contribute to the high annual averages observed in Golden and as mentioned previously are of concern to the health of the residents of Golden, especially children, the elderly and those with respiratory illnesses who are more easily affected by higher PM levels.

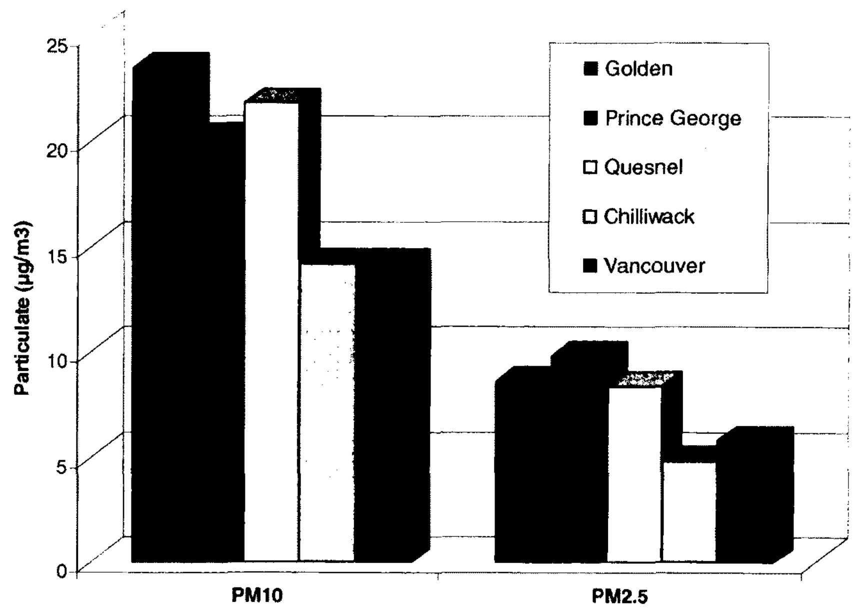

Figure 2-1 **Annual average PM_{10} and $PM_{2.5}$ concentrations in BC communities (2003-2005).**

(a) (b)

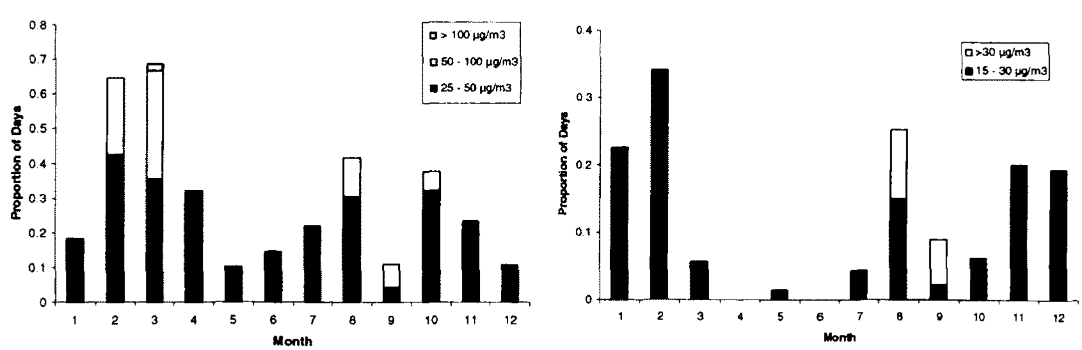

Figure 2-2 **(a) Proportion of days exceeding 25 µg/m^3, the BCMOE 24-hour objectives for PM_{10} (50 µg/m^3) and 100 µg/m^3 from 2003-2005 in Golden, BC (b) Proportion of days exceeding 15 µg/m^3 (lowest observable effects threshold) and the numeric value of the Canada Wide Standard for $PM_{2.5}$ (30 µg/m^3, 24 hour average) from 2003-2005 in Golden, BC.**

Although Golden does not have a large number of industries, it consistently ranks among the highest mean annual concentrations of PM in the province. Golden was chosen as an ideal site for the BC MOE speciation study for several reasons that also make it a challenging and interesting airshed to model with CALPUFF:

1. The Town's topography (i.e. valley bottom), climate and meteorological characteristics are typical of many communities in the interior of BC.
2. The Town's historical PM_{10} and $PM_{2.5}$ levels are well above the provincial average.
3. The Town's predominant emission sources (woodstoves, open burning, transportation, rail yards, wood processing, and road dust) are typical for communities in the interior of BC.
4. There is strong community support for the development of an air quality management plan in Golden.

(Golden Source Apportionment Study: Implementation and Planning Document May 10, 2004)

2.3 Meteorology in Golden

Dispersion models attempt to accurately estimate the meteorological conditions that disperse airborne pollutants. Meteorological conditions influence ground level PM concentrations in Golden and other communities in numerous ways. The release of PM from fugitive dust sources such as roadways is affected by rain or snowfall that can suppress or even stop the emissions from leaving the surface.

There is a greater level of emissions from residential heating during the winter or on colder fall and spring days. Dust from wind erosion increases when winds are high.

Following the release of airborne PM from the source, the dispersal pattern is determined by the meteorological conditions. The stability of the atmosphere, determined largely by the vertical temperature gradient, enhances or restricts the ability of pollutants to mix with the air above. High wind speeds can quickly disperse and dilute a source's emissions. Conversely low wind speeds may allow for the build-up of pollutants around a source and a rapid increase in PM concentrations. The creation of temperature inversions and conditions of low wind speeds are enhanced by mountainous topography, serving to trap pollutants closer to the valley bottom where communities are typically located. Thus, dispersion models attempt to incorporate meteorological, terrain and land-use data to predict the stability, wind flows and turbulence of the atmosphere. This can be especially difficult when dealing with complex terrain.

Typically, meteorology is monitored only at the Golden airport (AIRPORT) and the Golden Townsite (TOWN). However, an additional two BC MOE meteorological stations were added to the GOLF and CPR stations during the speciation study period (Figure 2-3).

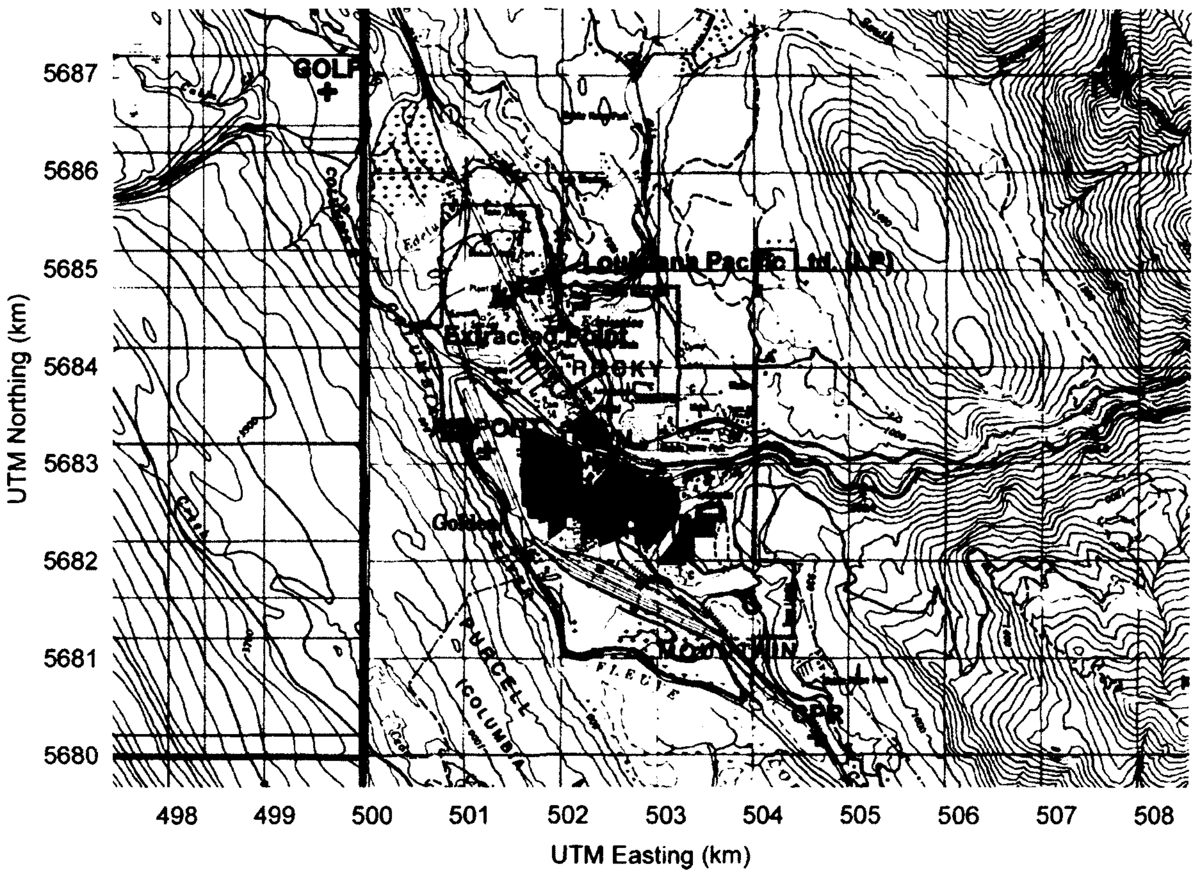

Figure 2-3 Map of Golden showing the location of the 3 within town PM and meteorological monitoring locations: the golf course north of the city; the CPR site south of the city and; the town site or central hub. Also shown is the location of the meteorological station at the airport, the extracted point used in the CALMET evaluation and the location of Lousiana Pacific Ltd. (LP)

2.4 Dispersion in Complex Terrain

Golden is located in a deep valley surrounded by steep valley walls and tributary valleys immediately east and near the north end of the main valley (Figure 1-1). Dispersion in Golden was expected to be heavily influenced by the complex topography surrounding the Town. The following section will explain the basic processes involved with dispersion in complex terrain.

There are two general types of winds associated with mountainous terrain: terrain-forced flows and diurnal mountain winds. Terrain-forced flows are produced when large-scale synoptic winds are modified or channeled by complex terrain (Whiteman 2000). Diurnal mountain winds result from the temperature contrasts that form within the mountains or between the mountains, when the elevated land surface heats and cools more rapidly, due to solar and infrared radiation, than the adjacent atmosphere. This results in horizontal pressure differences that create thermally driven circulations (Whiteman 2000). The combination of these two types of winds largely influences dispersion in complex terrain (Arya 1999).

Terrain-forced flows result as winds encounter mountain barriers. As the air flow approaches the mountain it can either be carried over, around, be forced through gaps or blocked by the mountain. Three factors will determine the path that a particular air flow will take when approaching a mountain barrier: the stability of the air, the wind speed, and the topography of the terrain (Whiteman 2000).

In boundary layer meteorology, atmospheric stability can be classified into three basic stability types: unstable, neutral and stable. The classification of stability depends on the rate of change of temperature with height above ground, and whether the air is saturated or not. In simple terms an unstable boundary layer typically occurs on hot days, where the air temperature near the surface is much greater than the temperature aloft. Any vertical motion is enhanced since the surface air rises rapidly (it is less dense that the surrounding air), and mixes. A neutral atmosphere means that there is no enhancement or suppression of vertical motion induced because of density differences – in other words, the air temperature of vertically displaced air is the same as the air temperature of the surrounding air at a given height. Unstable and neutral air masses can be carried over mountainous terrain because they are not resistant to vertical motion. Finally, a stable atmosphere means that vertical motions are suppressed. An example of stable conditions occurs during inversions, where cold air at lower elevations will remain near the surface because it is more dense than the air above.

This means that stable air masses are more resistant to lifting. Stable air is generally blocked, forced through terrain gaps or undergoes splitting as it approached mountainous terrain. Blocked stable air can be trapped on the windward side of the mountain. Splitting of the stable air mass occurs along the dividing streamline determined largely by the speed of the air mass, the surface roughness, the air's stability and the shape of the terrain. Air above the dividing streamline flows over the mountain and air below the dividing streamline flows around the mountain or is blocked (Whiteman 2000). Barriers of flow can also produce eddies that re-circulate air on either the windward or leeward side of the mountain (Arya 1999). Mountainous terrain can also greatly reduce wind speeds in deep valleys that are often protected from the prevailing winds by the topography (Oke 1997), certainly a phenomena likely to affect dispersion in Golden.

One challenge of a dispersion model is the ability to properly predict whether pollutants being dispersed towards mountains will be blocked, go over or around, be split, or be re-circulated by the barrier. CALPUFF accomplishes this through a puff-splitting scheme incorporated in the model (Scire et al. 2000).

Diurnal mountain winds are thermally driven circulations that are common in mountainous terrain. Wind generally flows upslope, upvalley and from low lying areas to the mountain in the daytime. Reverse flows are seen during the night (Whiteman 2000). These types of flows are produced by horizontal temperature differences causing winds near the surface to blow from areas with lower temperatures and higher pressures to areas with higher temperatures and lower pressures (Curry and Webster 1999). The influence of diurnal mountain winds is strongest when skies are clear and large-scale winds are weak (Whiteman 2000). In Golden, blocking of large-scale winds by the mountainous terrain may mean diurnal mountain winds are quite influential in the dispersion of pollutants.

There are three types of wind flows that define the diurnal mountain wind system in Golden:

1. The slope wind system
2. The along-valley wind system
3. The cross-valley wind system

(Whiteman 2000)

The slope wind system produces the upslope and downslope winds in mountainous areas. It is driven by the horizontal pressure gradient between the air near the slope and the air at the same elevation nearer to the center of the valley. The horizontal pressure gradient exists because of horizontal temperature differences caused by the diurnal heating and cooling of the slope surface (Whiteman 2000). The along-valley wind system is driven by pressure difference that occurs when the higher elevations in the valley generally become colder during the nighttime and warmer during the daytime compared with the air at the same altitude elsewhere in the valley. This causes an upvalley wind during the day and a downvalley wind during the night (Whiteman 2000). Cross-valley winds occur when there is a temperature difference between the two sidewalls of the valley (Whiteman 2000). These winds are more prominent during the day when the sidewalls are unequally heated by the sun. All of these flows are closed circulation flows, meaning they have an associated recirculation air flow higher above the surface.

A combination of diurnal mountain winds, terrain-forced flows and the surface heat budget contribute to a daily pattern of winds that influence the dispersion of pollutants in complex terrain. This study will focus on short time periods during episodes of high PM concentrations. Episodes usually last for several days at the most. Therefore, it is necessary to review the diurnal patterns of winds, as these winds are likely important in the creation, sustenance and degradation of PM episode events in Golden (Burkholder 2005).

During the daytime, the mixing height is quite high in the valley and may often be coupled with the atmosphere above the valley (Arya 1999), especially during summer with prominent upslope and upvalley winds and convective atmospheric conditions result in good dispersal. During the evening transition phase the slope wind system reverses and flows down the slope. This usually causes cold air to drain down the slopes and into the valley bottom and leads to the build up of an inversion (Whiteman 2000). During an inversion, dispersion of emissions released below the level of the inversion is poor as the mixing height is low, limiting vertical motion in the atmosphere. Down-slope flow and the resultant temperature difference in the valley lead to a reversal of the along-valley wind during the evening transition period (Whiteman 2000). During the night, downslope winds continue to contribute to the inversion and the down-valley winds blow within the inversion layer providing for minimal dispersion of pollutants out of the inversion layer (Whiteman 2000). During the morning, typically the reversal of both slope and along-valley flows and the convective currents from the ground combine to breakup the inversion, and thus improve dispersion (Whiteman 2000). This is a description of typical daily conditions that would be realized under surface high pressure systems with weak synoptic pressure gradients resulting in calm, clear conditions. In Golden, episodes of high PM are usually associated with a combination of high emissions and stagnant conditions that prevent the breakup of the nighttime inversions (Burkholder 2005). In this case, the night-time inversions tend to persist and mixing heights remain low for much of, or the entire day if the solar heating is weak causing pollutants to remain trapped near the surface and the population of the town.

2.5 Air Pollutant Dispersion Modelling

An atmospheric dispersion model provides a mathematical simulation of the physics and chemistry governing the transport, dispersion and transformation of pollutants in the atmosphere. A dispersion model is capable of estimating air pollution concentrations given information about the pollutant emissions and nature of the atmosphere (NIWA 2004). Air quality modeling allows researchers to simulate and assess air quality issues without the expense associated with extensive air quality monitoring networks. Air quality monitoring networks are necessary to validate dispersion modeling, however, the models can provide specific quantitative estimates of pollutant levels at many points over a wide geographical area (Scire and Godfrey 2005). The expense associated with air quality monitoring restricts measurements of ambient pollutant concentrations to only a few locations in a region.

Receptors are points in a modeling domain where concentrations of pollutants are estimated from the emissions and meteorological information supplied. Receptors can be placed anywhere within the modeling domain allowing researchers to provide more accurate estimates of pollutant concentrations in complex terrain. This allows modelling to investigate the influence of geophysical and meteorological factors on pollutant concentrations in much more detail than would ever be possible with traditional monitoring techniques. With a validated model researchers can use the modeling domain as a numerical laboratory where they can conduct experiments that would not be feasible in the real world. An accurate representation of how pollutants disperse near populated areas is useful in:

- assessing compliance of air emissions with air quality guidelines, criteria and standards;
- planning new industrial facilities;
- determining appropriate industrial stack heights;
- managing existing emissions in an airshed;
- designing ambient air quality monitoring networks;
- identifying the contributors to existing air pollution problems;
- evaluating air quality policy and pollution mitigation strategies;
- forecasting pollution episodes;
- assessing the risks of and planning for the management of rare events such as accidental hazardous substance releases;
- estimating the influence of geophysical factors on dispersion;
- running 'numerical laboratories' for scientific research involving experiments that would otherwise be too costly in the real world and;
- saving cost and time over monitoring – modeling costs are a fraction of monitoring costs and a simulation of annual or multi-year periods may only take a few weeks to assess. (NIWA 2004)

Achieving an accurate picture of air quality at a local level typically requires a model capable of correctly representing dispersion conditions, emissions and pollutant chemistry in complex terrain as well as during periods of stagnation. This stems from the fact that episodes of high pollutant concentrations are generally related to a combination of topographical effects and stagnant atmospheric conditions. With health and environmental consequences of elevated pollutant levels becoming increasingly better understood (Vedal 1995), modeling these conditions is of interest at a community health level. One advanced dispersion model capable of modeling dispersion in a non-steady state, complex terrain environment is the CALPUFF modeling system developed by EarthTech Inc. for the United States Environmental Protection Agency (USEPA) (Scire et al. 1999). CALPUFF will be used to model dispersion of PM in Golden. The following is a review of the current status of dispersion modeling with a specific emphasis on modeling during periods of high pollutant concentration and assessment of CALPUFF in a variety of applications.

2.5.1 Development of Dispersion Models

Most early mathematical models were based on the behaviour of plumes in neutral atmospheric conditions (Venkatram 1988). It was thought that under neutral conditions the structure of the planetary boundary layer could be defined through a series of theoretical assumptions based on the fundamental laws describing dispersion of windborne material presented by Pasquil (1961). However, it became apparent through experimentation that description of dispersion based on these theoretical assumptions did not always hold true (Wyngaard 1988). It has been a blend of experimentation and refinement of theory that has influenced model development over the past few decades. For short-range dispersion especially, it became evident that accurate description of constantly changing parameters, such as mixing heights, wind speed, wind direction, as well as phenomena such as the formation and breakup of temperature inversions, within the boundary layer were necessary to model the movement of air pollutants. It also became clear that modeling these parameters over complex terrain was necessary as populated areas commonly lie in valleys and mountainous, non-flat terrain. Meteorological conditions vital to dispersion in complex terrain are not defined well by models designed for, and tested in, flat terrain (Schnelle and Dey 2000).

The dispersion of pollutants in the surface boundary layer over homogeneous conditions has been captured relatively well by dispersion models such as ISC (USEPA), AUSPLUME (Environmental Protection Authority (Australia) 2000), and AERMOD (Cimorelli et al. 2005). However, flows and dispersal characteristics over complex topography have not been modeled well. Past models developed to describe dispersion over relatively flat terrain had difficulty simulating dispersion over complex terrain. Modeling difficulties in mountainous terrain are compounded by the fact these areas are prone to stagnant atmospheric conditions and terrain induced local circulation (Triantafyllou 2002). Thus, a model capable of mathematically including these phenomena has been the goal of leading air quality agencies such as the US EPA.

Most modern air pollution models are computer programs that calculate the pollutant concentration of the sources in an area using input information that is more detailed than, but relies on similar concepts, as early models. These include:

- pollutant emission rate

- characteristics of the emission source (e.g. temperature, velocity, elevation above ground)
- local topography
- meteorology of the area
- ambient or background concentrations of pollutant. (NIWA 2004)

2.5.2 Plume Models

Currently, the most commonly used dispersion models are steady-state Gaussian-plume models (e.g. Ausplume, ISC). These are based on a mathematical approximation of plume behaviour and are the easiest models to use. They incorporate a simplistic description of the dispersion process, and some fundamental assumptions are made that may not accurately reflect reality. These assumptions state primarily that as pollutants are dispersed from a source, they tend to follow a normal (Gaussian) distribution in the horizontal and vertical direction (Figure 2-4). However, even with these limitations, this type of model can provide reasonable results when used appropriately, for example in regulatory applications (Isakov 2004).

Gaussian-plume models have been useful in regulatory application (Brechler 2000), but have been shown to produce unreliable results in complex terrain and under stagnant conditions (Oettl et al. 2001, Abdul-Wahab 2004). Adaptations allowing for non-Gaussian dispersion in the vertical direction during convective conditions has allowed for certain Gaussian-plume models (e.g. AERMOD) to capture maximum concentrations of pollutants reasonably well in complex terrain (US EPA 2003). However, formulas guiding strict Gaussian-plume models are

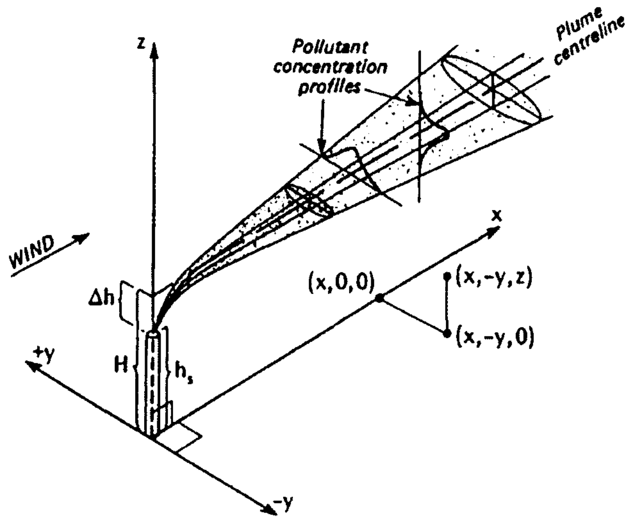

Figure 2-4 **Diagram of a typical Gaussian plume from an elevated point source. Note the normal distribution of pollutant dispersal horizontally and vertically (from Oke, 1987).**

based on "steady-state" conditions, meaning the formulas calculate concentrations for each hour based on an emission rate and meteorological conditions that are assumed to be uniform across the modeling domain (Sakiyama et al. 2005). Conditions from hour to hour can change in Gaussian models. However, each hour is treated independently of other hours, with each hour's emissions dispersing in a straight-line trajectory to the edge of the modelling domain. Although these assumptions work reasonably well under relatively steady conditions, they do not work well when there are large changes in meteorological conditions from hour to hour (Schnelle and Dey 2000). Gaussian plume models assume that a pollutant plume will have its highest concentration on a straight-line trajectory in both the horizontal and vertical direction downwind of the emission source (Whiteman 2000). The diffusion of pollutants from this straight-line maxima is dependent on dispersion coefficients usually determined over flat homogeneous terrain and follow a normal (Gaussian distribution) outwards from the maxima (Whiteman 2000) These assumptions place temporal and spatial limitations on Gaussian models that inhibit their ability to model dispersion accurately in complex terrain, because of their inability to handle spatially varying wind flows, flows from tributary valleys, terrain-induced flows or diurnal mountain winds. Gaussian models do provide some conveniences that make them appropriate for more simplistic modeling situations. The simple approach means that the models do not require significant computer resources, are user-friendly, have simple meteorological data requirements and were designed to give conservative results (NIWA 2004). However, without the ability to model complex convective and stable conditions, Gaussian models cannot effectively model causality effects (i.e. the transport time required for pollutants to reach receptors), dispersion at low wind speeds, dispersion in complex terrain, changes in atmospheric conditions, and processes, such as inversion break-up, fumigation and diurnal recycling of pollutants, varying meteorological conditions, changing pollutant dispersion coefficients, and emissions from previous hours that affect subsequent hourly concentrations of pollutants (NIWA 2004). Still, Gaussian type models have proven useful in providing a simple model of atmospheric dispersion. They allow an adequate description of the boundary layer processes affecting dispersion under homogeneous conditions.

For the most part, the less-sophisticated Gaussian plume models are used primarily for regulatory applications. Modeling for regulatory applications refers to those activities concerned with assessing compliance of emissions with ambient air quality guidelines, criteria and standards. In general, Gaussian dispersion is adequate enough to model for regulatory purposes because regulations focus on the maximum concentrations independent of where or when they occur rather than specific levels of pollutant concentrations across the modelling domain.

2.5.3 Advanced Models

New dispersion coefficients, vertical wind shear and plume behaviour in the boundary layer have been incorporated into a new generation of dispersion models capable of better estimating dispersion in complex terrain. Since many communities and their industries are located in complex terrain, the need for understanding and modeling boundary layer processes under these conditions is apparent (Sakiyama et al. 2005). For this reason, field studies over recent years have focused on improving estimates of dispersion in complex terrain (e.g. Triantafyllou 2002, Dosio et al. 2001) so more accurate estimates of important parameters such as dispersion coefficients, vertical wind shear and plume behaviour can be incorporated into these new models.

Better ways of describing the spatially varying turbulence and diffusion characteristics within the atmosphere have been, and continue to be, developed (eg. Bellasio 2005, Moraes 2005). The new generation dispersion models are capable of modeling steady-state conditions as well as non-steady state conditions (Schnelle and Dey 2000). They allow for modeling of variable and curved plume trajectories, variable meteorological conditions, retention of previous hour emissions, and better handling of low and zero wind speeds (Scire and Godfrey 2005). The models include terrain steering effects based on wind variation due to topography and surface properties balanced by an overland surface energy budget, as well as, splitting of plumes around and over hills, allowing for better representation of dispersion processes in complex terrain (Scire and Godfrey 2005).

The three most common types of advanced dispersion models are particle, puff, and grid point models. Particle models (e.g. KSP, Strimaitis 1995) represent pollutant releases by a steady stream of particles which are advected and diffused by the modeled wind fields. Puff models (e.g. CALPUFF, Scire et al. 1999) represent pollutant releases as a series of puffs which are also advected and diffused by the modeled meteorology. Grid point models (e.g. CALGRID, Yamartino et al. 1992) represent pollutant distribution by concentrations and chemical transformations on a three-dimensional grid of points (NIWA 2004). The models depend on a specific meteorological processor to determine the meteorological parameters affecting dispersion. Each of the three model-types vary in their computational efficiency and application (NIWA 2004).

An important difference between advanced models and Gaussian-plume models is the calculation of gridded wind fields, derived from vertical and horizontal winds combined with kinematic terrain effects and diurnal mountain winds in a divergence minimization scheme, that are then used to transport pollutants. Advanced models require three-dimensional meteorological fields because they do not rely on the assumption of steady state winds across the modeling domain (Scire and Godfrey 2005). The detailed wind fields produced by the meteorological processor associated with an advanced dispersion model allows for more ‘realistic’ outcomes. In many cases the meteorological data required for these models are limited or not available. The limitations of these models must be understood and modelers must take care in choosing the appropriate level of sophistication for the meteorological data available (Schnelle and Dey 2000). Even with quality meteorological input data, modeling efforts in complex terrain and under stagnant conditions can be difficult, despite the use of more advanced models. During these times low speed wind flows affecting dispersion are difficult to define. This is a result of a number of factors including anemometer thresholds (typically anemometer thresholds do not allow recording of wind speed of less than 0.5 m/s), using hourly averaged meteorological parameters and model algorithms that breakdown under low or zero wind speed conditions (i.e. CALPUFF mixing height calculation during the night).

This study will apply a dispersion model to short episodes of high PM concentration. The more advanced, new generation models are primarily concerned with modeling of non-steady state conditions, allowing for a more accurate description of the dispersion of pollutants from source to receptor. These models are designed to describe atmospheric dispersion phenomena such as terrain steering effects, inversion formation and breakup, and fumigation that allows the user to assess pollutant concentrations in complex terrain and varying dispersal, emission and chemical transformation conditions (Schmitz 2005). The advanced model selected for use in this study is the CALPUFF modeling system (Scire et al. 1999). The features of CALPUFF that suit its application in episode analysis are described below.

2.5.4 CALPUFF Modeling System Development

The CALPUFF modeling system from the US EPA (Scire et al. 1999) has been developed with the ability to model dispersion in a non-steady state, complex terrain environment. The original design specifications for the model demonstrate the intent to improve the spatial and temporal complexity of previous Gaussian-type models:

- the capability to treat time-varying point and area sources;
- suitability for modeling domains from tens of meters to hundreds of kilometers from a source;
- predictions for averaging times ranging from one-hour to one year;
- applicability to inert pollutants and those subject to linear removal and chemical conversion mechanisms and;
- applicability for rough or complex terrain situations (Scire et al. 2000)

The CALPUFF modelling system was originally developed by Earth Tech Inc. under contract from the California Air Resources Board (CARB) (Scire et al. 2000). The research team developed a modeling system that contained a meteorological modeling package, CALMET, to define the wind fields affecting dispersion. This meteorological information is then used to drive a Gaussian puff dispersion model (CALPUFF) on a gridded modeling domain to deal with a variety of modeling applications, such as complex terrain, fumigation, wet and dry deposition and building downwash (Scire et al. 2000). A peer-review of the model recommended the use of the CALPUFF modelling system in its designed application of long-range transport assessments and near-field applications (Allwine et al. 1998).

The meteorological model, CALMET, utilizes meteorological and topographical data commonly available for most regions to develop hourly wind and temperature fields on a three-dimensional, gridded modeling domain (Scire et al 2000). Scire and Robe (1997) showed that CALMET was able to reproduce key elements of wind flow in the Columbia River Valley, a complex terrain site.

The outputs from CALMET are used to drive the transport and dispersion model, CALPUFF, which advects and diffuses puffs of material emitted from sources based on the temporal and spatial variation in the meteorological fields. The three dimensional, gridded modeling domain allows for spatially and temporally varying conditions rather than the traditional Gaussian plume model that assumes uniformity over the entire hour for the plume.

Extensive hourly meteorological input parameters including wind speed and direction, temperature, cloud cover, surface pressure, relative humidity, and precipitation, as well as twice daily upper air radiosonde data, are required as inputs. Meteorological data reliability and availability within the modeling domain of interest is important to assess before CALPUFF is used (Scire and Godfrey 2005). The meteorological observations required to drive the CALMET algorithms is designed to provide a more realistic representation of wind fields and atmospheric processes used to drive dispersion within the modeling domain. However, this could be viewed as a stumbling block in proceeding with CALPUFF modeling in rural areas where such meteorological data are not regularly available. For these instances, CALMET has the option to utilize outputs from prognostic mesoscale models (e.g. RUC, MM5, or MC2 model output data) that are able to predict many of the parameters from limited data (McEwen 2003, Pielke 1998, Robe and Scire 1998). This option will not be used in the present study which focuses on using the available surface and upper air data in Golden as the only input data.

The model's effectiveness for local episode analysis applications stems from its ability to detail the major processes affecting transport, diffusion, and deposition of pollutants (Allwine et al. 1998). The transport and dispersion of pollutants follows the three-dimensional wind fields generated in CALMET. Other gridded meteorological fields including surface friction velocity, convective velocity scale, Monin-Obukhov length, mixing height, air temperature, and precipitation rate are computed using an overland boundary layer energy balance proposed by Holtslag and van Ulden (1983). Meteorological fields are determined by both upper air observations and an option for vertical extrapolation of surface observations using similarity theory during steady state conditions and probability density fluctuation during convective conditions. The model also retains previous hours' emissions, allowing pollutants to remain on the modeling grid and continue to be advected, diffused and detected as part of subsequent hours' pollutant concentrations. The retention of puffs from hour to hour also allows CALPUFF to model calm hours by simulating stagnant puffs. During hours with a zero wind speed, stagnant puffs on the modeling grid are not dispersed via advection, but may still undergo turbulence–related dispersion (Scire 2000). Furthermore, even if the measured wind speed is zero, CALPUFF accounts for other possible flow components (i.e. slope flows) during these stagnant modeling periods. The numerous algorithms used to describe dispersion processes in CALPUFF have been reasonably well assessed on an individual basis (Allwine et al. 1998). It is still necessary to evaluate how the model components perform in the Golden airshed. Evaluation of the CALPUFF modeling system is one of the goals of this study and will include a separate evaluation of CALMET and CALPUFF. Evaluating the two model components separately will help to discern what part of the disagreement between the model and observations has its roots in CALMET and what disagreement is due to CALPUFF.

2.5.5 CALPUFF Case Studies

Evaluation of CALPUFF in local scale episode analysis applications has not been extensive, but a review will provide evidence for its validity in these situations. The following examples will also demonstrate the diversity in applications of CALPUFF. CALPUFF has also been used in regulatory applications (Elbir 2003, Irwin et al. 2005), however that will not be the focus of the following assessments.

Barna and Grimson (2002) applied the CALPUFF modeling system to a wintertime PM pollution episode. In their evaluation of CALPUFF's ability to predict wintertime PM_{10} concentrations during an episode, they used the fractional gross error and fractional bias, along with the index of agreement and correlation coefficients to compare modeled results with observed PM_{10} levels.

Barna and Grimson (2002) found highly encouraging results with statistical performance tests of CALPUFF reporting good agreement between model predicted and observed PM concentrations. Differences between observed and predicted values are generally explained by peak concentrations being modeled at receptors close to, but not exactly at, the observed monitoring location. This suggests the model is accurately predicting the particulate concentrations, but is misrepresenting the location of the maxima.

CALPUFF was used to analyze a two-day wind episode in the Mexico City Basin in 1997 (Villasenor et al. 2003). The goal of the study was to simulate PM_{10} emissions from a wind-blown dust event. Wind-blown dust from agricultural lands as well as river and lake beds was thought to be an important source of PM in the city. The wind episode was carefully chosen so modelers could examine processes creating, maintaining and terminating the PM_{10} episode. Throughout the episode, CALPUFF agreed reasonably well with observed values and provided strong evidence that the hypothesis, stating that the episode arose from dust originating from wind erosion, was correct.

Levy et al. (2002) used CALPUFF to evaluate the impacts of power plant emissions on residents of Illinois. Their analysis included an assessment of the model's sensitivity to various input parameters. Estimates based on some of the most influential parameters used in CALPUFF such as background concentrations, deposition, chemical mechanisms, and size of the receptor region were found to be moderately insensitive, with the sensitivity varying based on the pollutant under question (Levy et al. 2002). According to the model creator (Joe Scire, personal communication, 2005) sensitivity tests should focus on influential CALMET parameters (e.g. R1; R2; Rmax1; Rmax2; Terrad, and; Bias). See Chapter 5 for a complete description of these CALMET parameters that largely determine the radius of influence of terrain and surface or upper air meteorological observations on the final wind fields used in CALPUFF (Scire and Godfrey 2005).

Levy and Spengler (2002) present how CALPUFF can be coupled with epidemiological evidence regarding the health benefits of reduced emission strategies. Levy and Spengler (2002) found that emission controls on two power plants in Illinois lead to a reduction of approximately 70 premature deaths per year. This reduction is associated with an overall 2% reduction in ambient secondary PM concentrations. The calculations of mortality are based on a concentration-response estimation derived from several epidemiological studies conducted by the American Cancer Society and Adventist Health among others. This type of estimation is beyond the scope of the present study, but it does highlight application of CALPUFF to emission reduction strategies.

It can be seen from the variety of studies presented that CALPUFF is diverse in its application. However, the repeated assessment of CALPUFF in similar applications is needed to test its performance against numerous data sets. Using CALPUFF in Golden will provide another evaluation of its performance in complex terrain.

3 MODELLING SYSTEM AND DATA COLLECTION

3.1 CALPUFF MODELING SYSTEM

The CALPUFF modeling system consists of three main programs and accompanying pre- and post-processors. The first component is the CALMET meteorological model; the second, the CALPUFF dispersion model; and the third, the CALPOST post-processor. There are also a number of pre-processors that prepare and merge a wide variety of data formats into CALMET input data. The modeling system is contained within a newly developed graphical user interface called CALPUFF PRO 5, but can also be used by editing the input files in a text editor. CALMET, CALPUFF, and CALPOST are briefly described below.

3.1.1 CALMET

CALMET consists of a diagnostic wind field module and a micro-meteorological module for overland boundary layers.

The CALMET diagnostic, 'mass consistent' modeling approach constructs gridded wind fields that are consistent with available terrain, land use and meteorological data, while also satisfying the governing equation for conservation of mass (Cox et al. 2005). Mass consistent wind field models represent a good compromise between accuracy and computational efficiency (Arena et al. 1997). Difficulties arise when using the mass consistent interpolation of three dimensional wind fields. The wind fields must be adjusted by minimizing divergence in the horizontal and vertical components. However, the horizontal wind velocity component is much greater than the vertical velocity component. In CALMET, then, it is necessary to define a fixed vertical velocity field based on the input surface characteristics (micro-meteorological module in CALMET) and adjust the horizontal wind components to minimize divergence in each grid cell (wind field module in CALMET).

A schematic overview of how CALMET determines the wind fields is provided in Figure 3-1. In the first step, either observational data or prognostic model outputs (e.g. Fifth-Generation NCAR / Penn State Mesoscale Model (MM5) or the National Oceanic and Atmospheric Administrations's (NOAA) National Center for Environmental Prediction Rapid Update Cycle (RUC) Model) are used to create an initial guess field in CALMET. At the edge of the domain the model applies an initial guess wind field. There is an option to include a surface station outside of the modeling domain which the model will consider in setting boundary conditions. In Golden, there are no nearby surface stations that would be representative of the edge conditions, so no observed data was used to initialize the edge of the domain. The model then uses this initial-guess wind field and adjusts it for kinematic effects of terrain, slope flows, and terrain blocking to produce a Step 1 wind field. The Step 1 wind field is then used in an objective analysis procedure that utilizes observational surface and upper air data to produce the final wind field to be used in CALPUFF.

In Step 1, the initial-guess field is used along with the geophysical data to compute the terrain steering effects. Thermodynamic blocking effects of terrain on the wind flow are parameterized in terms of the local Froude number (Scire et al 2000.) Slope flows are then computed based on the shooting flow parameterization of Mahrt (1982). The slope flow is characterized in terms of the terrain slope, distance to the crest and local sensible heat flux. The final output of CALMET's Step 1 wind field is a gridded field of 3-D wind components.

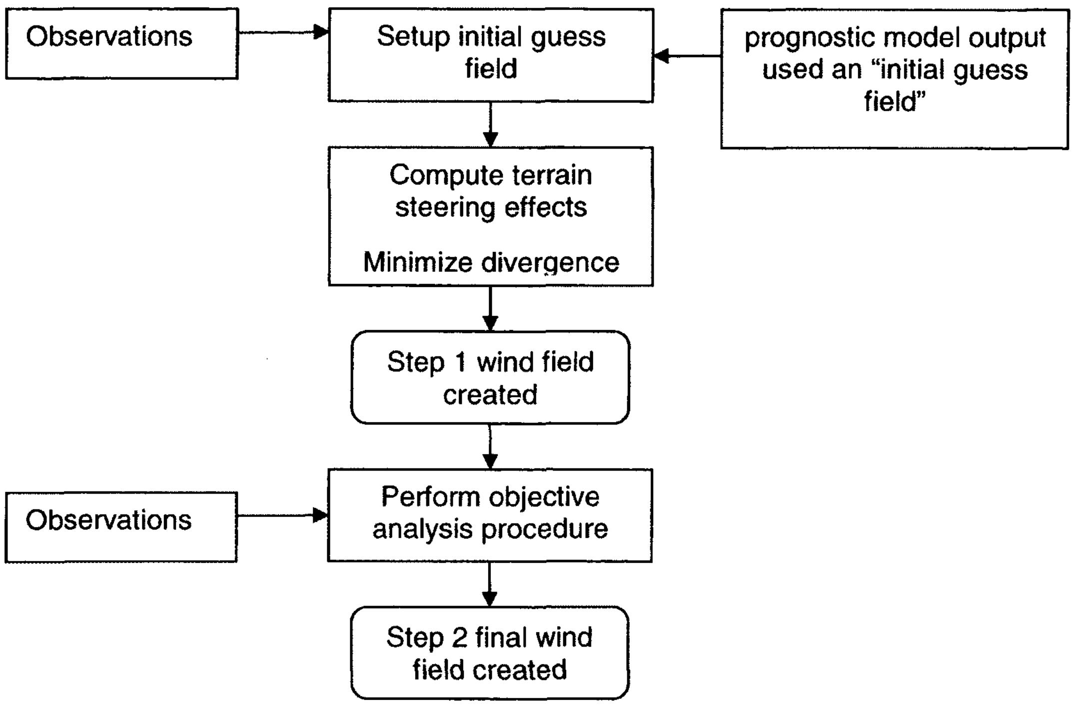

Figure 3-1 **A schematic overview of the creation of wind fields in CALMET (adapted from Scire et al. 2000).**

The second step is then performed that introduces observational data into the Step 1 wind field through an objective analysis procedure. An inverse-distance squared interpolation scheme is used which weighs observational data more heavily in the vicinity of the observational station, while the Step 1 wind fields are weighted heavily in domain areas lacking observational data. The user has control over the radius of influence of observational data. Choosing the radius of influence correctly allows an appropriate balance of observational data and the Step 1 wind fields computed by CALMET to determine the final wind fields. The final wind fields are used as the dispersal winds in the CALPUFF dispersion model.

The diagnostic nature of the CALMET model allows for minimal data requirements based on routinely collected surface and upper air meteorological observations. Although this allows easier application of the model, the hourly data lacks sufficient horizontal, vertical and temporal resolution to accurately depict atmospheric processes over the entire modeling domain. In areas where data resolution or data completeness is lacking, CALMET must rely heavily on interpolation techniques to estimate wind, temperature and turbulence fields. This inherently reduces the overall accuracy of the modelled meteorology and eventually the dispersion of the pollutants in CALPUFF.

CALMET's micro-meteorological module calculates surface friction velocity, convective velocity scale, Monin-Obukhov length, mixing height, Pasquill Gifford Turner (PGT) stability class, air temperature, and precipitation rate for each grid by using the overland boundary layer energy balance method of Holtslag and van Ulden (1983). This module describes the convective and mechanical turbulence in the boundary layer which ultimately determines the vertical extent of dispersion. The micro-meteorological module relies on both meteorological observations and assumptions of geophysical parameters based on land use type.

3.1.2 CALPUFF

CALPUFF is a puff dispersion model capable of handling multiple-layers within the atmosphere and multiple pollutant species (Scire et al. 2000). The

CALPUFF model involves more complicated and comprehensive simulation processes compared to the conventional steady-state, single-layer and single-species guassian models. The non-steady state model allows it to handle time and space varying meteorological and emission conditions. Expanded capabilities include non steady-state effects (spatial heterogeneity, causality, fumigation, etc.), complex terrain algorithms, calm and low wind speed conditions, flexible source variability options, chemical transformation, and differential advection and dispersion.

CALPUFF uses CALMET's final wind field to disperse point, line and area emission sources throughout the gridded modeling domain. The puff model represents a continuous emission source, such as a plume, as a number of discrete packets of pollutant material. The puffs are released and evolve in size according to Gaussian- like diffusion and dispersion, but the multiple puffs allow changes in meteorological and emission conditions to be captured.

3.1.3 CALPOST

CALPOST includes a number of useful features to process the data output by CALPUFF. Users define the averaging period and CALPOST processes the concentration of PM (or other pollutants modeled) at receptor sites. Data can be processed as gridded fields for mapping emissions or as data values for time series and statistical analysis.

3.2 Data Collection in Golden

Most of the observed data were collected by the BC MOE. The BC MOE had 3 monitoring locations in Golden: the golf course north of the city (GOLF); the

Canadian Pacific Railway (CPR) site south of the city; and a downtown location near the hospital (TOWN) (Figure 2-3). At each of the locations, the Ministry collected hourly meteorological data. In addition each location continuously monitored PM_{10} and $PM_{2.5}$ levels. Meteorological data were also collected at the Golden Airport (AIRPORT) by Environment Canada (Figure 2-3).

Additional equipment was added to supplement the data collection efforts of the BC MOE and Environment Canada. A SCINTEC FAS64 phased-array Doppler sodar system (SODAR) was operated at the golf course location (Figure 3-2). The SODAR system is capable of resolving the vertical wind profile by measuring the scattering of sound waves by atmospheric turbulence. The wind speed and direction is found by the Doppler effect. The SODAR transmits and receives beams of sound in different directions. By monitoring the change in frequency of the back-scattered sound, the wind speed in the direction of the beam can be found. Wind moving toward the antenna will decrease the wavelength of the reflected sound wave and wind moving away from the antenna will increase the wavelength of the reflected sound wave. The SODAR monitors this change in frequency (wavelength) of the reflected sound wave and calculates the wind speed in the particular direction of the transmitted sound. By transmitting beams in different direction the SODAR resolves the three-dimensional wind fields.

The SODAR system must be installed in an area clear of obstructions (i.e. tall buildings and trees) in the immediate area that would result in scattering of the sound waves. The system was installed beside the GOLF station that was free of large obstructions and had the available operational power requirements (Figure 3-2).

Figure 3-2 **SCINTEC FAS64 phased-array Doplar sodar system installed near the GOLF station.**

Obtaining a local vertical temperature profile in the lowest portion of the atmosphere was important as temperature lapse rates calculated from upper air stations hundreds of kilometres away would not allow for accurate prediction of mixing heights and stability classes. In order to capture a vertical temperature profile, HOBO H8 Pro temperature / RH loggers (HOBOs) were enclosed in a radiation shield and mounted on trees 1.5 metres above the ground. Six HOBOs were installed at elevations of 798 metres (1), 839 metres (2), 960 metres (3), 1036 metres (4), 1081 metres (5), and 1223 metres (6) (Figure 3-3). Locations were selected on the mountain side to the west of Golden at safely accessible locations along the road to the Kickinghorse Mountain Ski Resort.

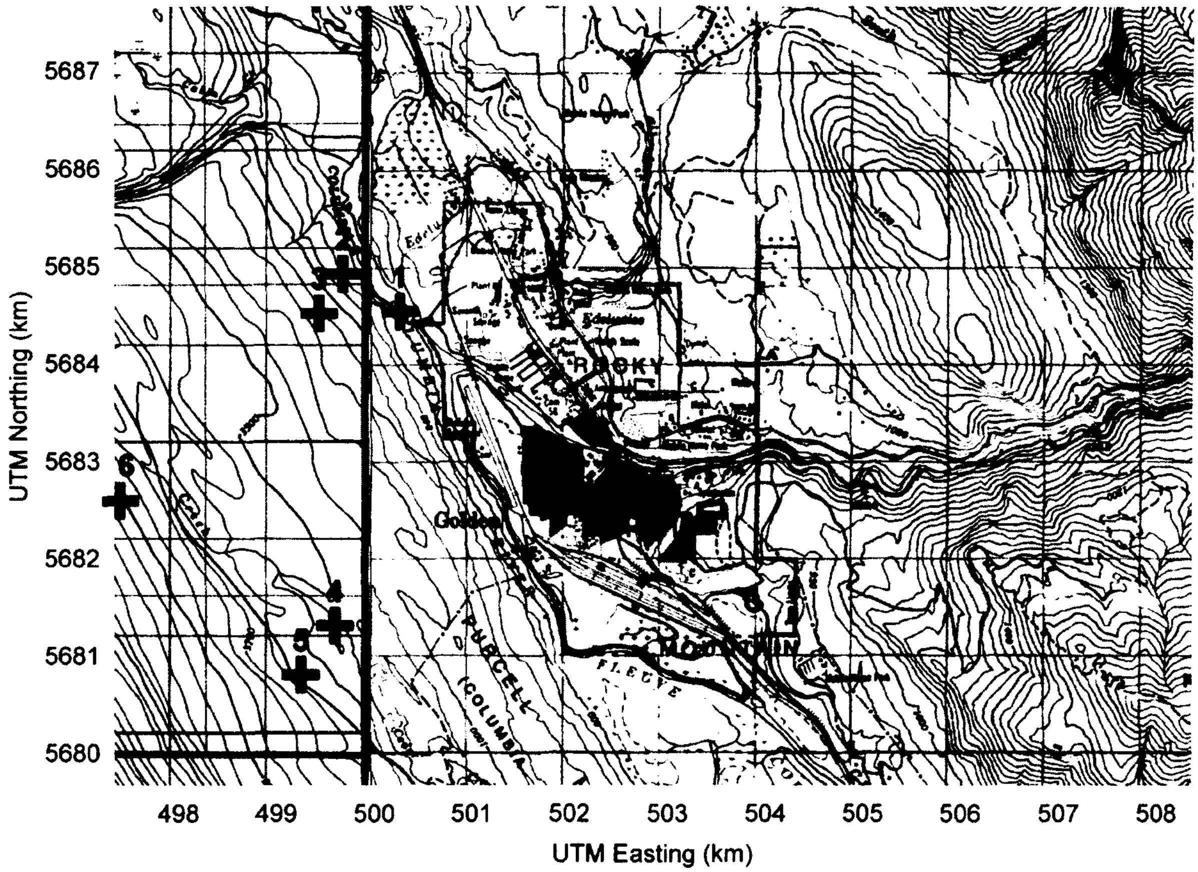

Figure 3-3 **Map of the six HOBO H8 Pro temperature / RH loggers (HOBOs) at 798 metres (1), 839 metres (2), 960 metres (3), 1036 metres (4), 1081 metres (5), and 1223 metres (6) along the road to the Kickinghorse Mountain Ski Resort to the west of Golden.**

Methods regarding the use of the collected air quality and meteorological data are provided in Chapter 5.

4 EPISODE ANALYSIS

This modeling study focused on episodes of high PM. Generally, episodes are defined as prolonged periods of elevated PM ambient concentrations above a defined threshold level. In British Columbia episodes are typically defined as periods with 24 hr PM_{10} averages above 50 µg m^{-3}, the objective for BC (Table 2-1), for at least 3 days.

During the 2005-2006 winter, PM concentrations were not as high compared to previous Golden winters. Therefore, episodes were chosen based on increases in PM_{10} and $PM_{2.5}$ concentrations compared to the 2005-2006 winter season mean data, and from inferences made regarding the ratio of $PM_{2.5}$ to PM_{10} (PM ratio). A low PM ratio indicates that most of the PM_{10} measured is larger than 2.5 microns in diameter. Therefore the emission sources creating the PM are more likely to be crustal or fugitive dust sources that create larger particles. A high PM ratio indicates that most of the PM_{10} measured is smaller than 2.5 microns in diameter. The emissions sources creating the PM in this high PM ratio period are more likely to be combustion sources that create finer particles.

An episode reasoned to be representative of a typical "wintertime" episode was chosen (December 7, 2005 – December 14, 2005. A second episode reasoned to be representative of a typical "spring-time" episode was chosen as well (February 8 – 23, 2005). Modeling an episode of each type allowed for comparison between the emission and meteorological characteristics associated with each episode.

Episodes were chosen to correspond to periods when reliable data were available from all meteorological stations, the SODAR and the PM monitors.

4.1 EPISODES MODELED

This section summarizes PM concentrations during each episode modeled and the rationale behind choosing these specific episodes.

4.1.1 Episode 1 (December 7-14, 2005)

This period exhibits higher concentrations of PM in comparison to the rest of the winter monitoring season. There are several factors that contribute to this episode being labeled as typical of wintertime. The increased PM_{10} levels are associated with an increase in the $PM_{2.5}$ fraction and high PM Ratio (Table 4-1). It was hypothesized that high PM levels during this episode were due to combustion sources (i.e. woodstoves) resulting in the $PM_{2.5}$ increase. Spatially, the highest levels of PM_{10} and $PM_{2.5}$ occur at the TOWN location, followed by CPR and the GOLF location. This supports the hypothesis that residential heating concentrated in the downtown core would be a significant contributor to episode 1. Temperatures were low during the episode, average daily minimum temperature of -9.7˚C compared to normal daily minimum of -6.1˚C in the rest of December, so many residents would likely be using wood heat appliances during this episode. Figure 4-1 shows a consistent diurnal pattern of high PM concentrations during the late afternoon and into the evening at the TOWN station.

Table 4-1 **Comparison of episode 1 average hourly PM concentrations and PM ratios ($PM_{2.5}$:PM_{10}) with hourly PM concentrations and ratios from the Winter season (2005 - 2006).**

Monitor		PM_{10} (µg/m³)		$PM_{2.5}$ (µg/m³)		PM Ratio	
		Episode 1	**Winter**	**Episode 1**	**Winter**	**Episode 1**	**Winter**
CPR	Average	16.0	12.3	10.3	5.4	0.6	0.4
	Maximum	37.0	414.6	27.0	32.0	0.8	1.0
	Minimum	3.0	0.0	1.0	0.0	0.1	0.0
	Std Dev	7.9	15.0	6.1	5.1	0.1	0.2
TOWN	Average	20.0	17.1	13.3	7.4	0.7	0.5
	Maximum	78.0	293.5	64.0	64.0	1.0	1.0
	Minimum	0.0	0.0	0.0	0.0	0.0	0.0
	Std Dev	11.2	22.8	10.1	7.8	0.2	0.3
Golf	Average	11.7	7.6	7.0	2.8	0.6	0.3
	Maximum	24.0	43.4	18.0	33.1	0.9	1.0
	Minimum	4.0	0.0	0.0	0.0	0.0	0.0
	Std Dev	4.2	4.2	3.6	3.0	0.2	0.2

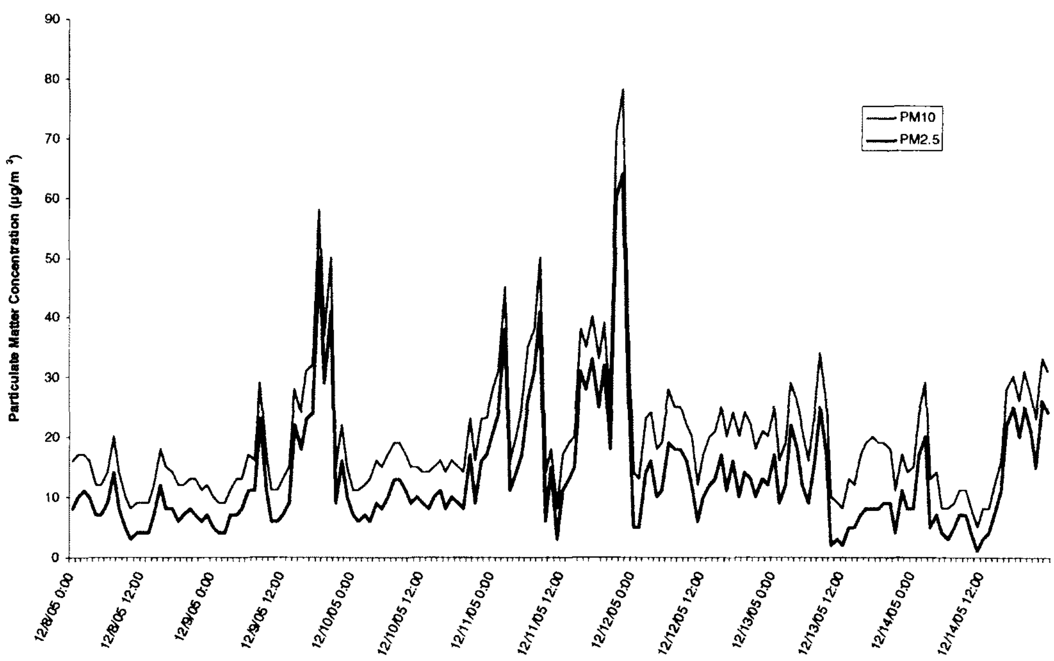

Figure 4-1 **Episode 1 profile of observed PM_{10} concentrations (µg/m³) and observed $PM_{2.5}$ concentrations (µg/m³) at the TOWN station.**

4.1.2 Episode 2 (February 8-23, 2005)

This period also exhibits higher levels of PM in comparison with the rest of the monitoring period. This episode is labelled as a springtime episode because it occurs in February and has a lower PM ratio in comparison to both episode 1 and the rest of the monitoring period (Table 4-2). It was hypothesized that high PM levels during this episode were due to emission of crustal materials (i.e. road dust, fugitive dust emissions) related to the spring thaw. However, temperatures remained low, averaging -8.0˚C, during this period as well, so it is hypothesized that there will still be a significant residential space-heating contribution to the emissions at the modeled receptors. An episode closer to the spring season would have been preferable, however data were not available. Figure 4-2 shows the same consistent diurnal pattern of high PM concentrations during the late afternoon and into the evening as was exhibited in Episode 1.

Table 4-2 **Comparison of Episode 2 average hourly PM concentrations and PM ratios ($PM_{2.5}$:PM_{10}) with hourly PM concentrations and ratios from the Winter season (2005 - 2006).**

Monitor		PM_{10} ($\mu g/m^3$)		$PM_{2.5}$ ($\mu g/m^3$)		PM Ratio	
		Episode 2	Winter	Episode 2	Winter	Episode 2	Winter
CPR	Average	26.6	12.3	7.3	5.4	0.3	0.4
	Maximum	122.9	414.6	24.3	32.0	0.7	1.0
	Minimum	1.0	0.0	0.0	0.0	0.0	0.0
	Std Dev	18.5	15.0	5.7	5.1	0.2	0.2
TOWN	Average	39.2	17.1	10.1	7.4	0.3	0.5
	Maximum	180.5	293.5	49.3	64.0	1.0	1.0
	Minimum	0.0	0.0	0.0	0.0	0.0	0.0
	Std Dev	28.7	22.8	8.3	7.8	0.2	0.3
Golf	Average	7.3	7.6	1.7	2.8	0.2	0.3
	Maximum	38.6	43.4	10.9	33.1	0.6	1.0
	Minimum	0.0	0.0	0.0	0.0	0.0	0.0
	Std Dev	4.3	4.2	2.2	3.0	0.2	0.2

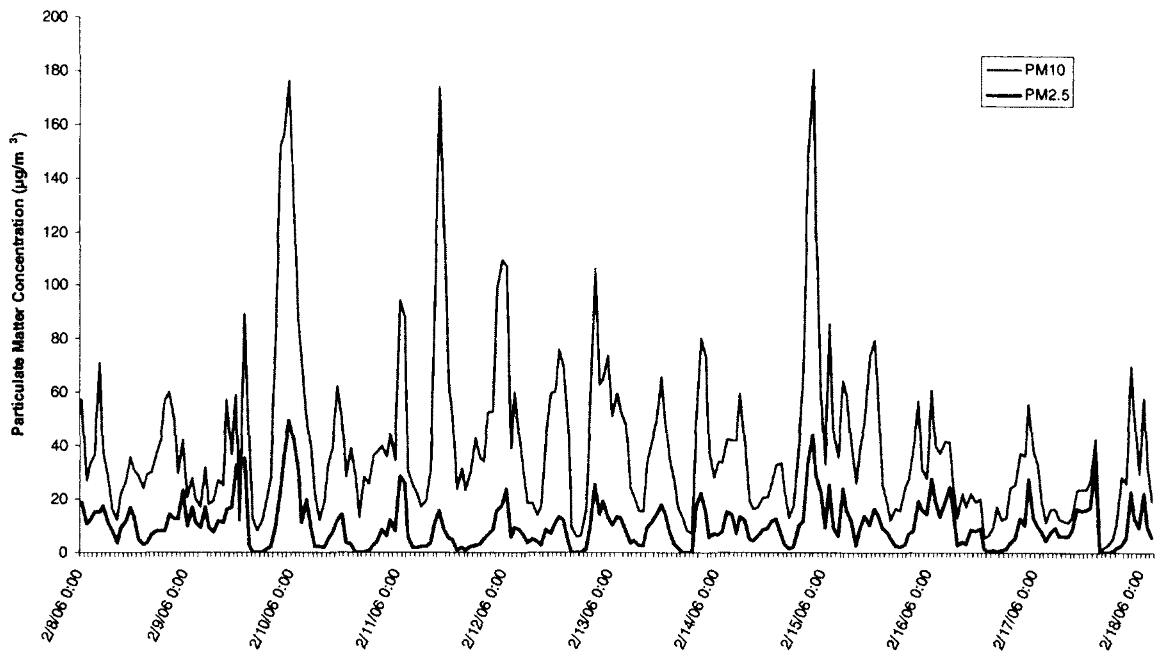

Figure 4-2 **Episode 2 profile of observed PM_{10} concentrations (µg/m^3) and observed $PM_{2.5}$ concentrations (µg/m^3) at the TOWN station.**

4.2 Comparison of Wind Characteristics During Episodic and Non-Episodic Periods

Prior to modeling, an analysis of the observational data available during the episodes was performed. Episodes usually persist when the air is stagnant. The dispersal and emission processes contributing to the two episodes of higher PM were investigated by comparing available meteorological data during the episodes with data typical of Golden on an annual, seasonal and monthly basis. This comparison helped to create hypotheses about the wind conditions contributing to the particular episodes under investigation. These hypotheses will be tested further by modeling the episodes in CALPUFF.

4.2.1 Wind Speed

PM is dispersed and diluted by wind. Low wind speeds will result in higher concentrations of pollutant as they are emitted into smaller volumes of air. Higher wind speeds help to mix and dilute the pollutant into larger volumes of air thus lowering the concentration. Typically, episodes occur during periods of stable atmospheric conditions when low wind speeds are common.

Figure 4-3 shows that both episodes occur during periods with a high frequency of calm (<0.5 m/s) and low wind speed when compared on an annual, seasonal and monthly basis. Episode 2 has a greater frequency of calm winds compared with episode 1. Each episode shows wind speeds that are consistenly low with very little diurnal variation (Figure 4-4).

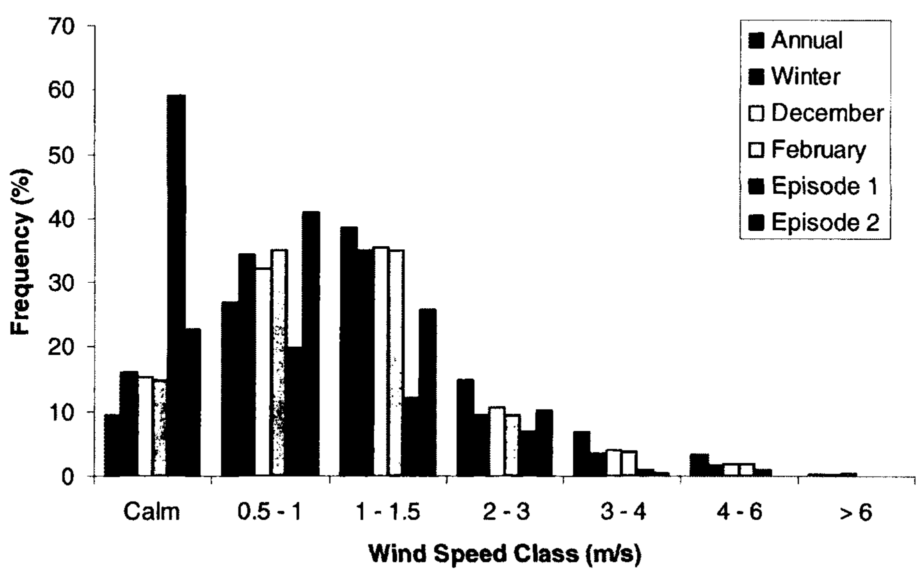

Figure 4-3 **Frequency distribution of wind speed classes (m/s) for annual, winter season, the month of December, and the month of February with those observed during episode 1 and episode 2 at the Town station. Calm winds are those with a wind speed less than 0.5 m/s. Distributions are calculated from data ranging from 2001-2005. The Town station is used because it has been operational for the longest period.**

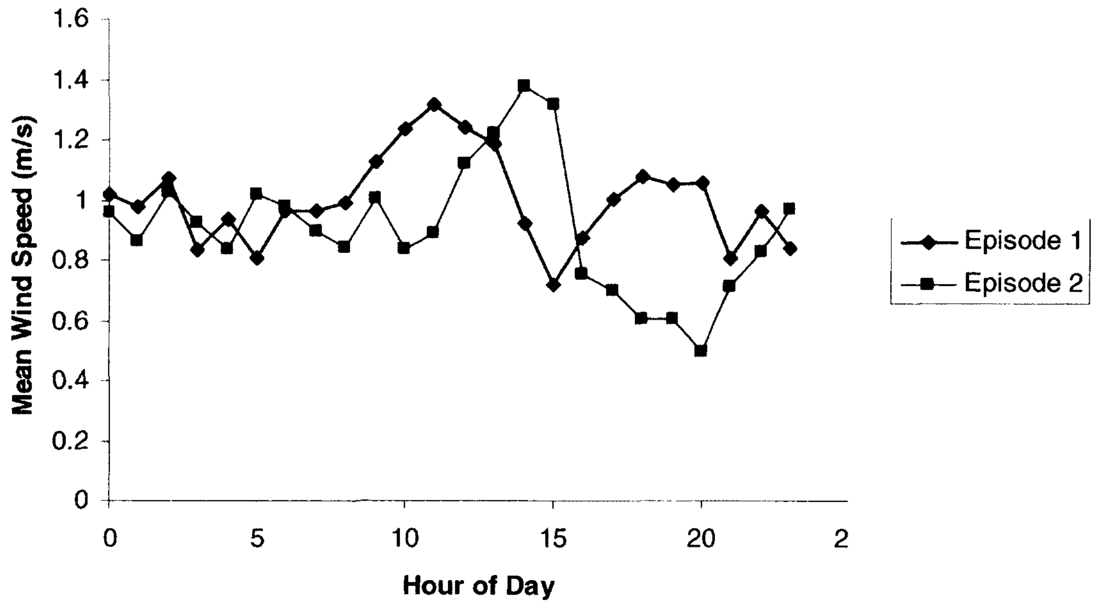

Figure 4-4 **Diurnal variation of wind speed by hour of day during each episode modelled at the Town Station. Other stations showed similar trends.**

Figures 4-5 and 4-6 demonstrate that higher concentrations of both PM_{10} and $PM_{2.5}$ occur during hours with lower mean wind speeds. At all three stations wind speed is negatively correlated to PM concentrations for both episode 1 and 2. This trend is not as evident at the GOLF station as the other two stations. This may be because the GOLF station is further away from the emission sources in Golden or that at higher wind speeds a background PM source (i.e. windblown fugitive dust) affects the GOLF station. At the other stations, periods of low wind speeds during both episodes lead to the periods of highest PM concentration.

(a)

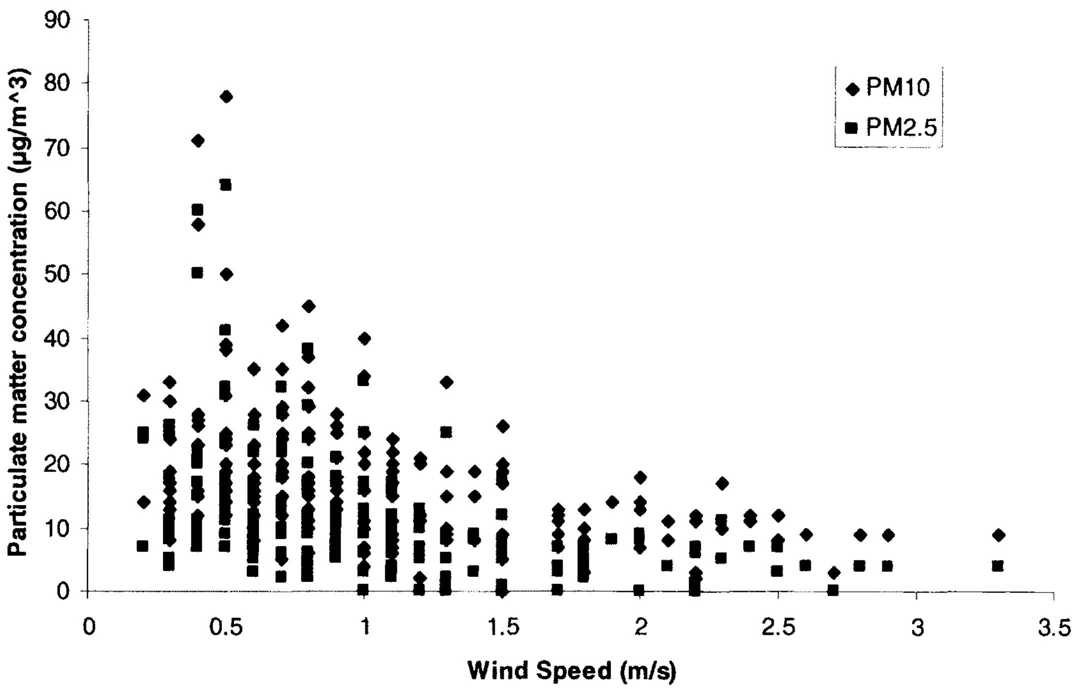

PM10
PM2.5
Particulate matter concentration (µg/m^3)
Wind Speed (m/s)
0
10
20
30
40
50
60
70
80
90
0
0.5
1
1.5
2
2.5
3
3.5

(b)

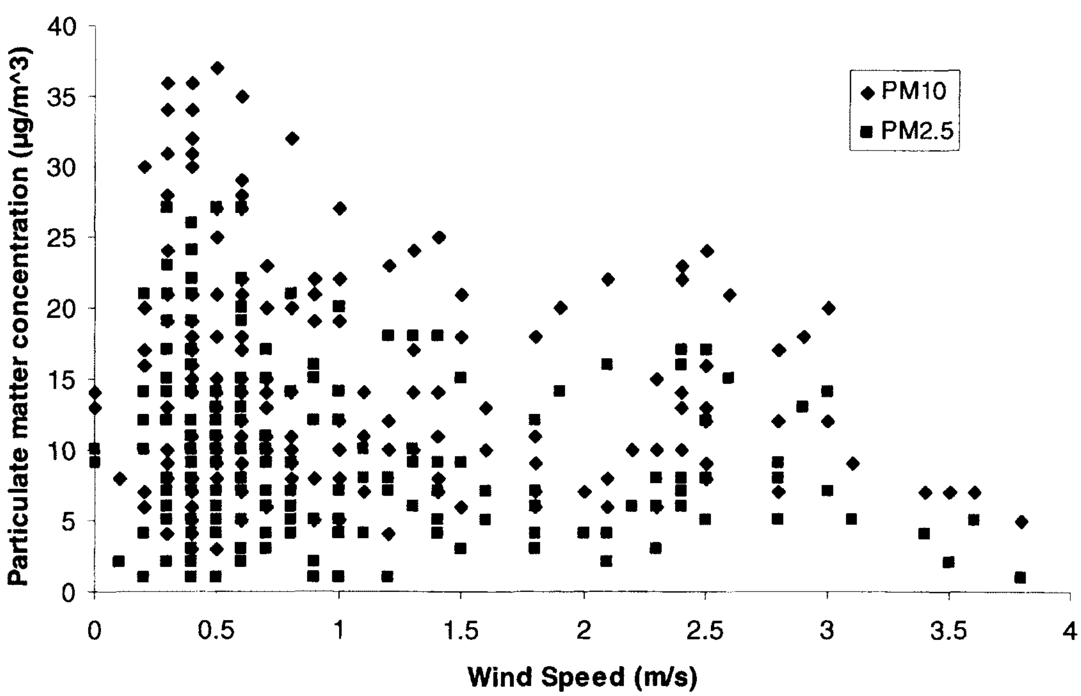

PM10
PM2.5
Particulate matter concentration (µg/m^3)
Wind Speed (m/s)
0
5
10
15
20
25
30
35
40
0
0.5
1
1.5
2
2.5
3
3.5
4

(c)

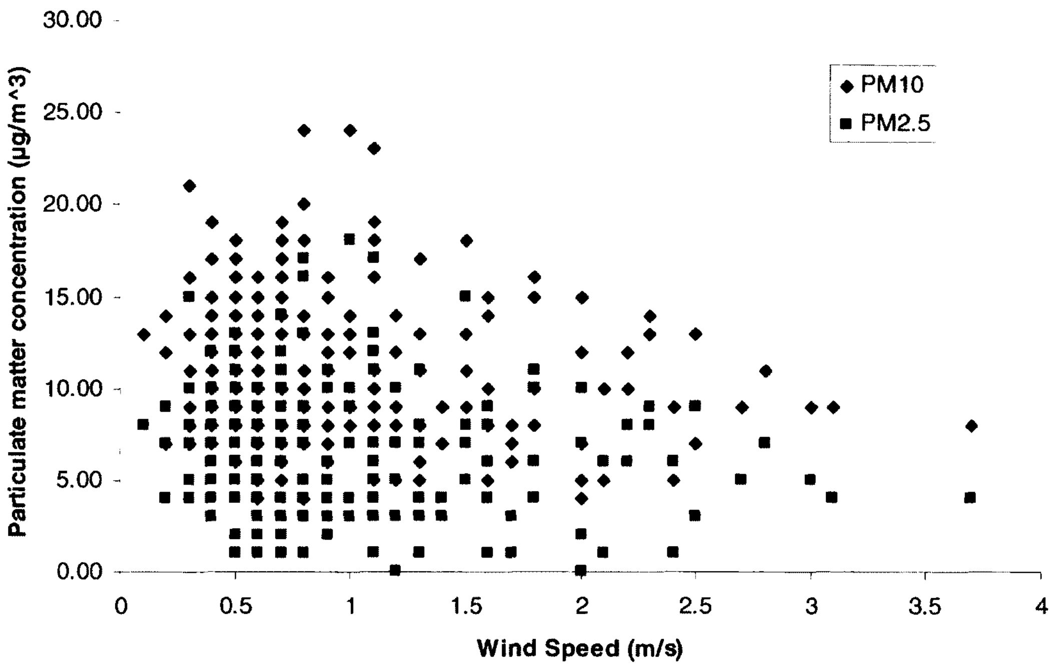

Figure 4-5 **Hourly PM concentrations and wind speed for Episode 1 at (a) Town station; (b) CPR station; (c) Golf station.**

(a)

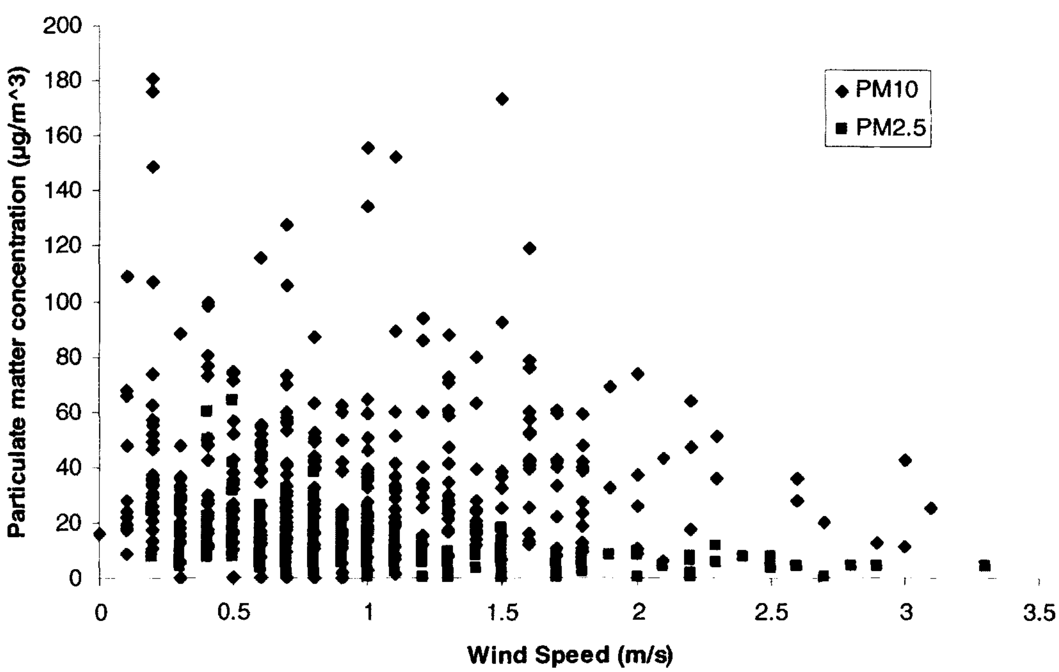

(b)

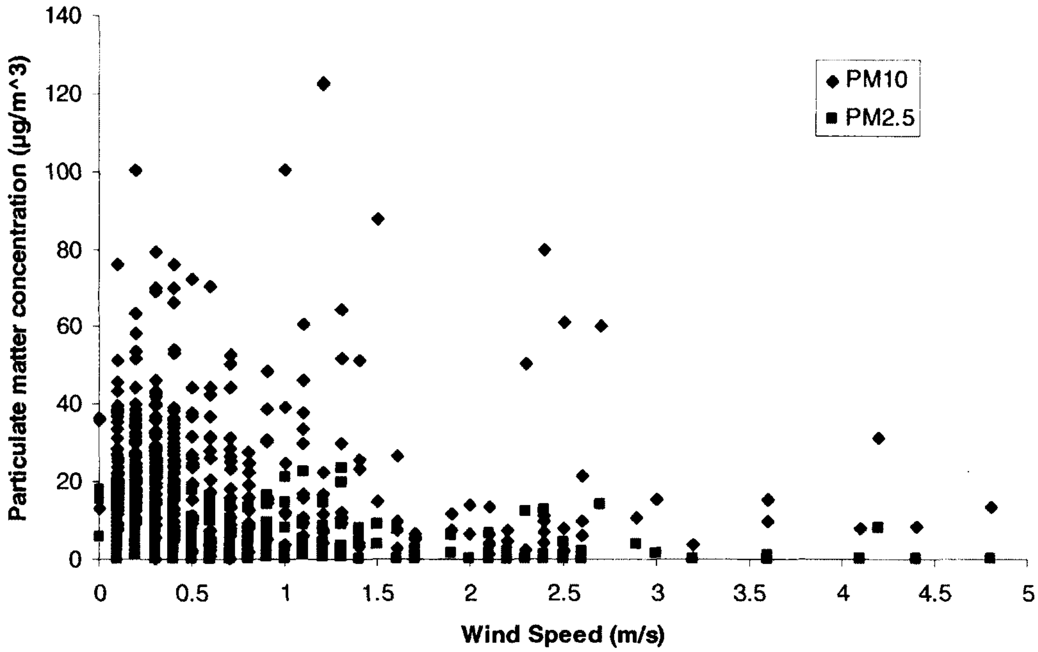

(c)

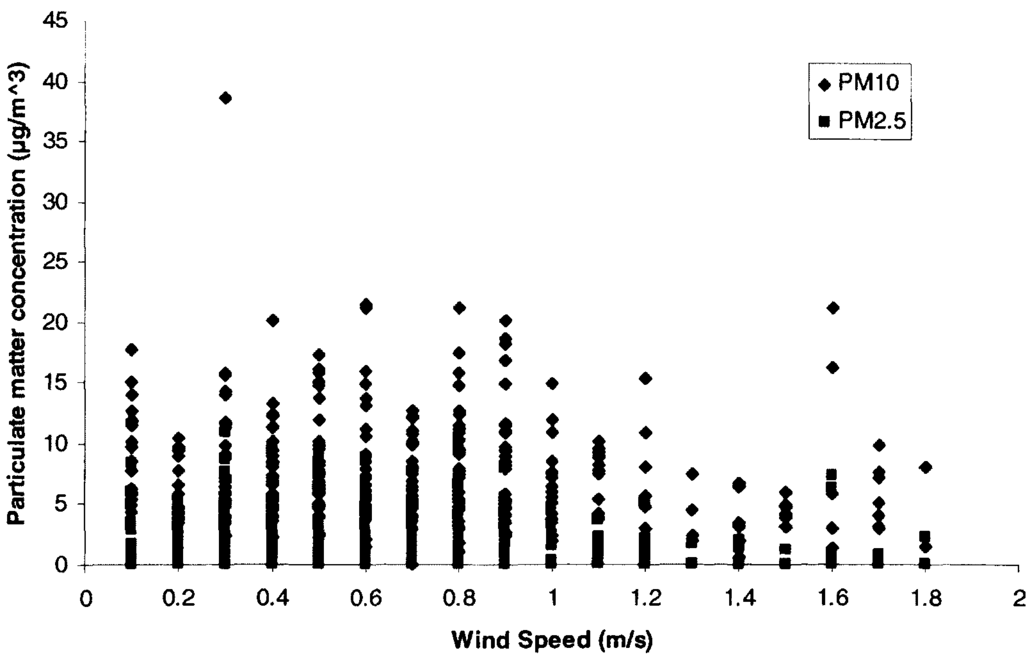

Figure 4-6 **Hourly PM concentrations and wind speed for Episode 2 at (a) Town station; (b) CPR station; (c) Golf station.**

4.2.2 Wind Direction

Variation in wind direction will disperse emissions in different directions and influence source-specific PM concentrations at the ambient monitors. For example, a north wind would likely increase Louisiana Pacific's (Figure 2-3) contribution to PM concentrations at the Town and CPR monitors, while decreasing its contribution at the Golf monitor. Southerly winds would likely result in the opposite.

Figures 4-7 and 4-8 show that high concentrations of PM are observed during both the southerly and northerly valley wind flow. An exception occurs at the Town station during the second episode where higher PM_{10} concentrations are exhibited with winds from the North.

(a)

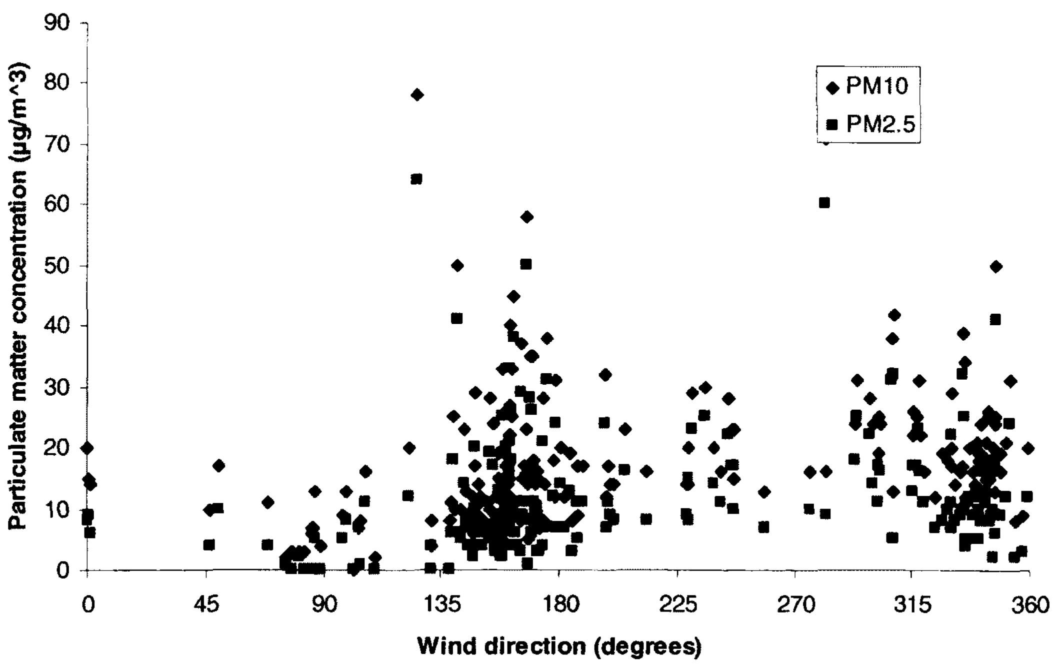

(b)

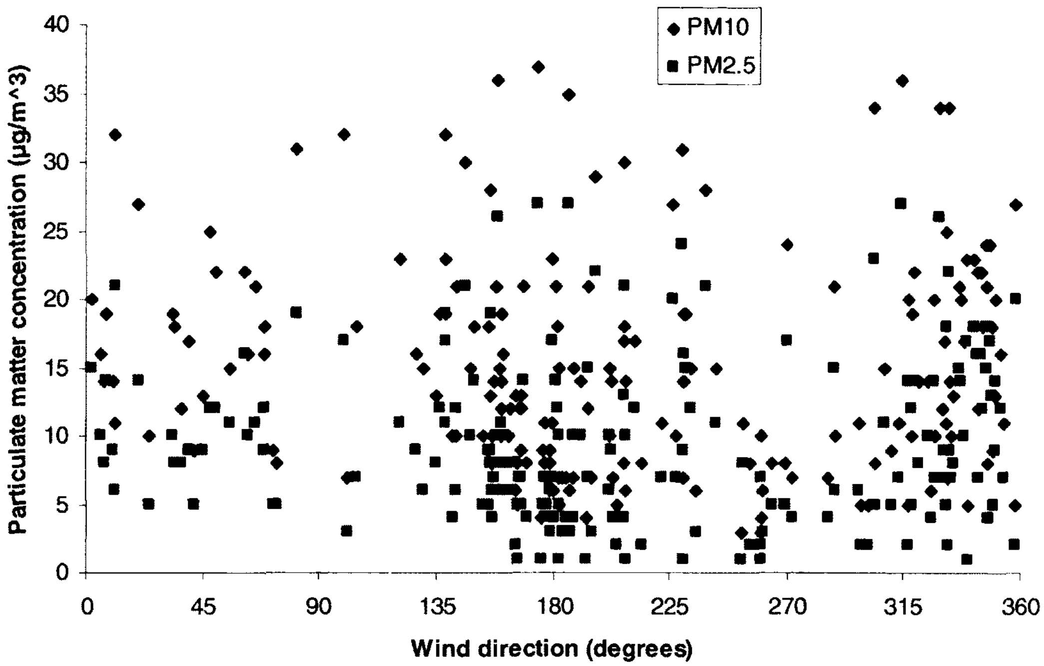

(c)

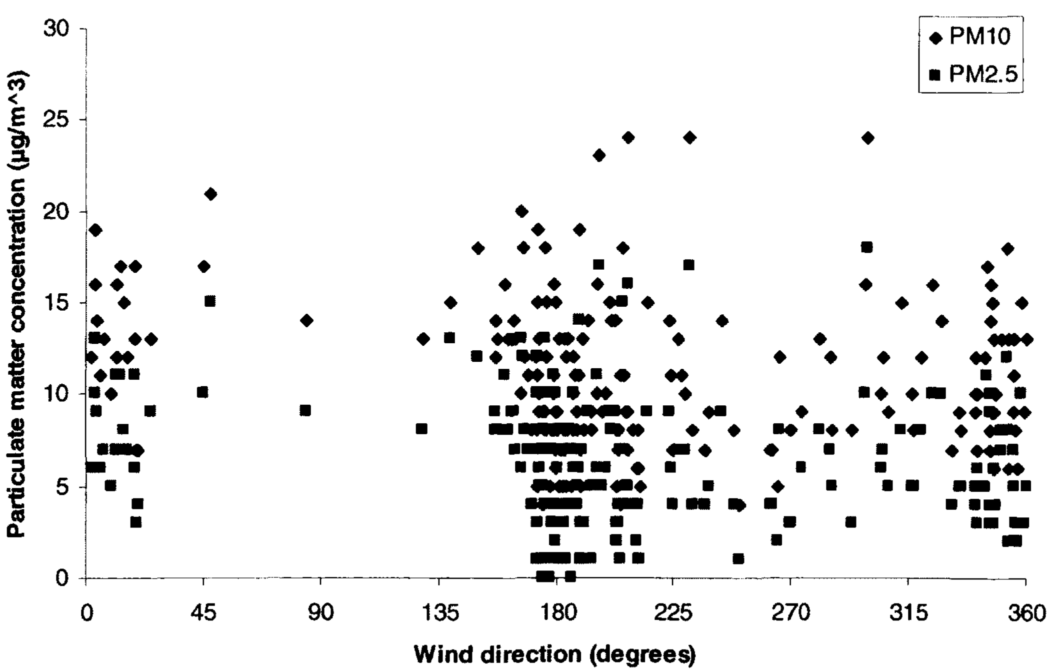

Figure 4-7 **Hourly PM concentrations and wind direction for Episode 1 at (a) Town station; (b) CPR station; (c) Golf station.**

(a)

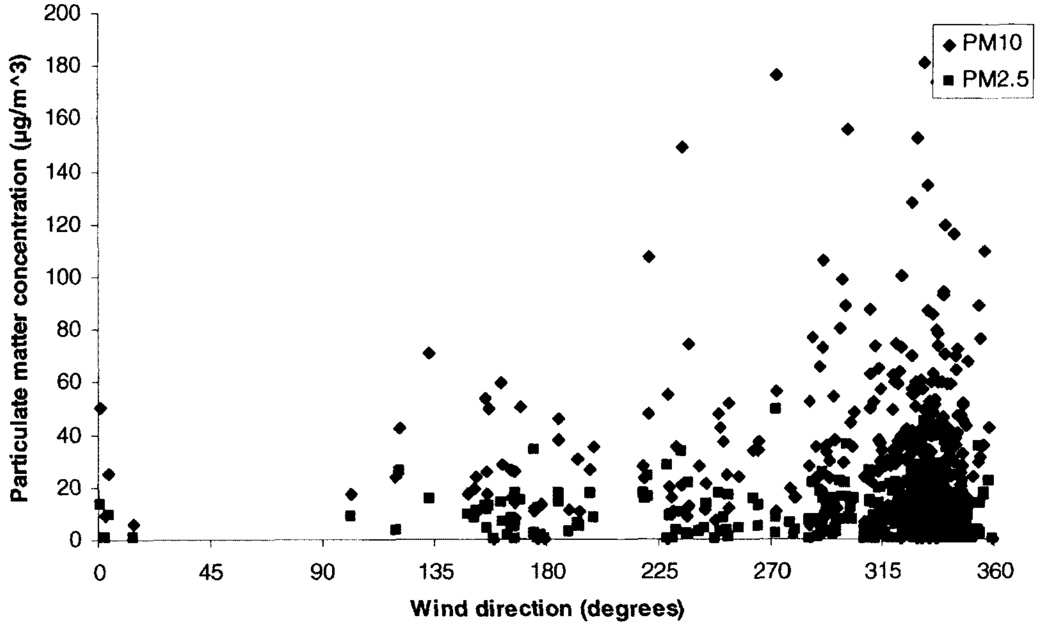
Particulate matter concentration (µg/m^3)
200
180
160
140
120
100
80
60
40
20
0
0
45
90
135
180
225
270
315
360
Wind direction (degrees)
PM10
PM2.5

(b)

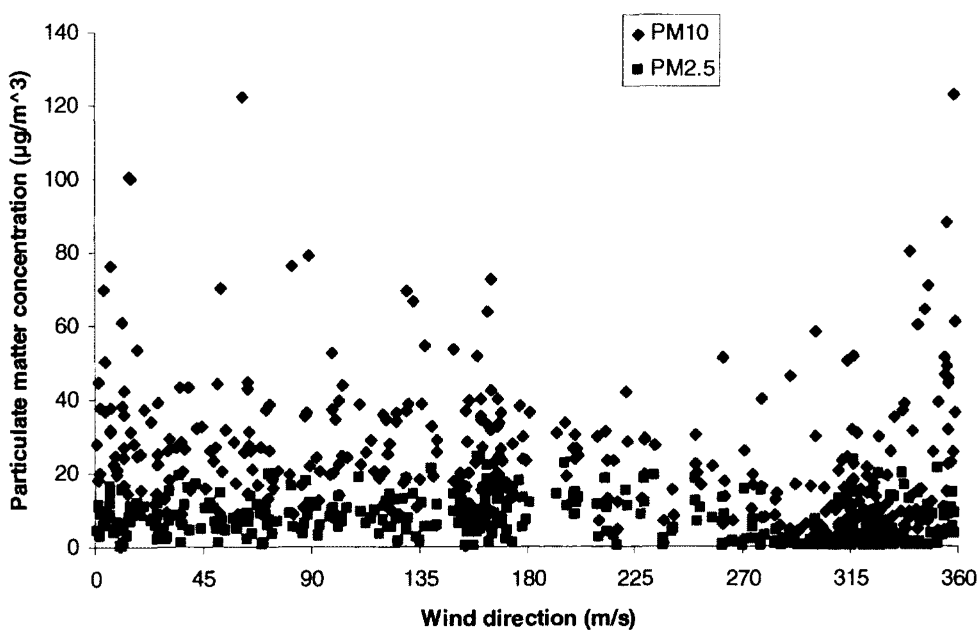
Particulate matter concentration (µg/m^3)
140
120
100
80
60
40
20
0
0
45
90
135
180
225
270
315
360
Wind direction (m/s)
PM10
PM2.5

(c)

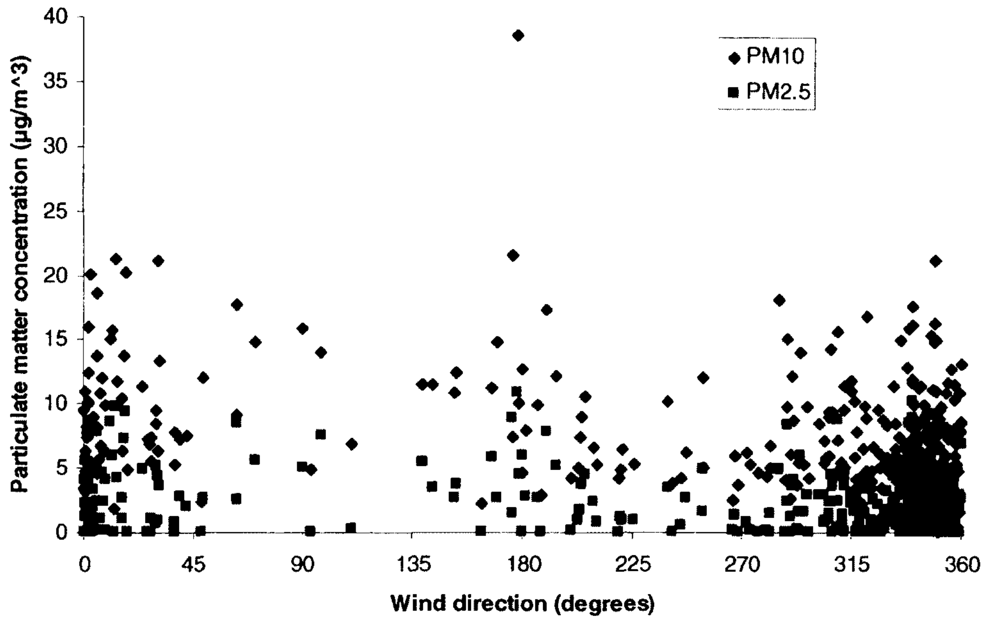

Figure 4-8 **Hourly PM concentrations and wind direction for Episode 2 at (a) Town station; (b) CPR station; (c) Golf station.**

4.2.3 Wind Rose

A wind rose shows the distribution of wind speed frequency by wind direction. All wind roses (Figure 4-9) show the terrain-forced flows along the Northwest/Southeast valley alignment. The annual flow shows a higher percentage of winds from the Northwest (Figure 4-9a). More southeasterly winds occur as during the winter (Figure 4-9b). Episode 1 (Figure 4-9c), shows the strongest influence of southeasterly winds when compared to the other wind roses. This is different than the winds displayed for the annual and winter when winds from the northwest are more prominent. Episode 2 shows more typical flows with more northwesterly winds (Figure 4-9d).

(a)

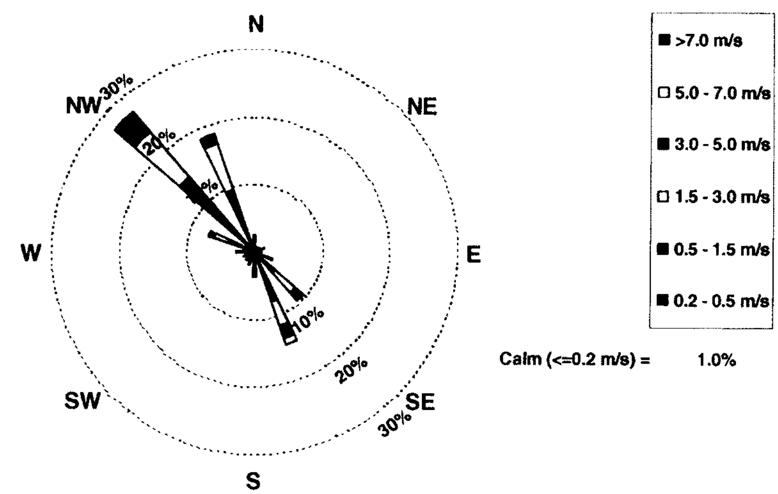
N
NE
E
SE
S
SW
W
NW
10%
20%
30%
>7.0 m/s
5.0 - 7.0 m/s
3.0 - 5.0 m/s
1.5 - 3.0 m/s
0.5 - 1.5 m/s
0.2 - 0.5 m/s
Calm (<=0.2 m/s) = 1.0%

(b)

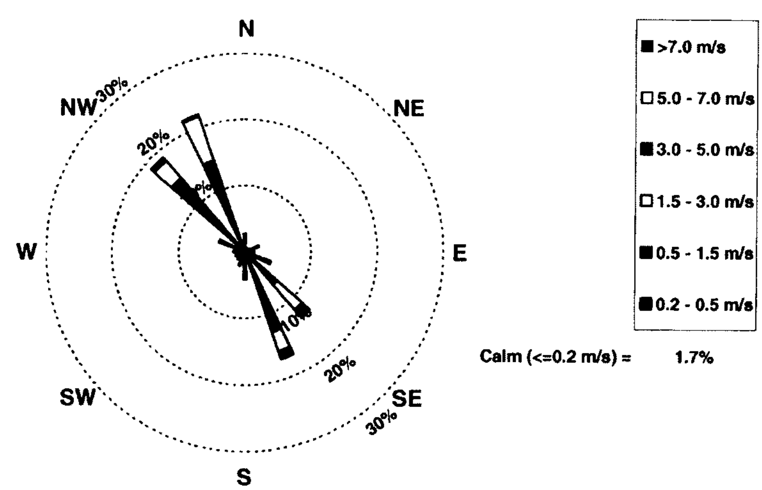
N
NE
E
SE
S
SW
W
NW
10%
20%
30%
>7.0 m/s
5.0 - 7.0 m/s
3.0 - 5.0 m/s
1.5 - 3.0 m/s
0.5 - 1.5 m/s
0.2 - 0.5 m/s
Calm (<=0.2 m/s) = 1.7%

(c)

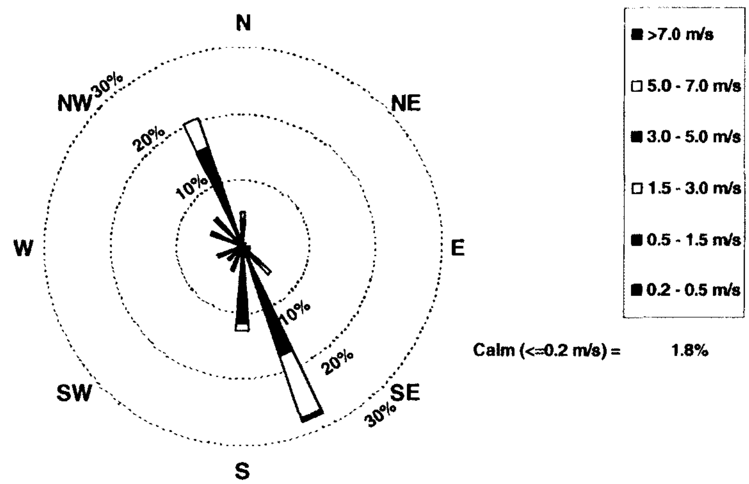

(d)

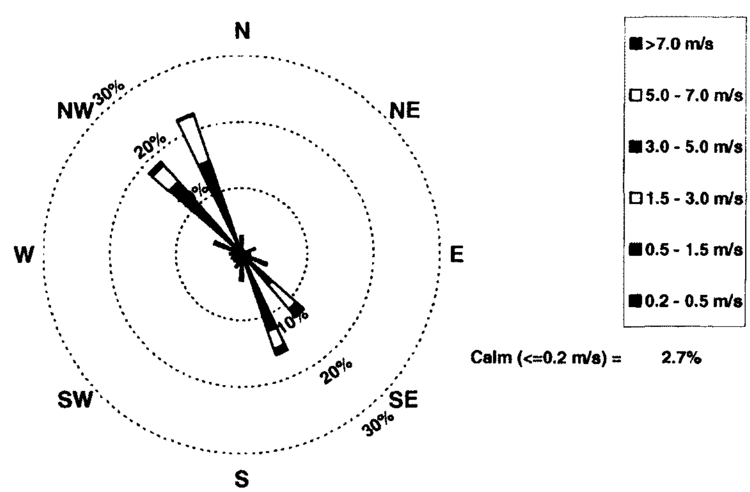

Figure 4-9 **Wind rose for Golden including (a) all winds recorded from January 2001 through December 2005; (b) all winds recorded in the winter season (November – February) from 2001-2005; (c) all winds recorded during Episode 1; (d) all wind recorded during Episode 2. The wind rose displays the distribution of wind speed frequency by wind direction. The dashed circles represent the percentage winds in each direction and the color scale corresponds to the wind speed. Each arm of the wind rose measures the incremental contribution of each wind speed class to the percentage of winds in that direction.**

4.3 Episode Analysis Discussion

The two episodes modeled using CALPUFF exhibit periods of high PM_{10} and $PM_{2.5}$ concentrations. During the episodes, pollutant concentration will be estimated using emission rates, wind characteristics and atmospheric conditions such as, stability, mixing heights and vertical temperature profile. Before analyzing the model output it is helpful to decipher any trends from the monitored data available in Golden.

The episodes occur during times of calm to light wind conditions in Golden. The synoptic, terrain-forced winds are weak and high surface pressures are observed during both episodes. Wind speeds appear to be an indicator of a potential rise in PM concentrations. During both episodes, overall mean wind speed is lower and periods of higher particulate concentrations are generally coupled with low hourly wind speed. High PM concentrations are observed primarily during typical valley aligned wind directions from the northwest and southeast.

When large-scale synoptic winds are weak, pollutants can become trapped in the local circulation and accumulate over time (Arya 1999). During these periods the local diurnal mountain winds largely determine the dispersion of pollutants in the valley. Indeed, the diurnal patterns exhibited during both episodes (Figures 4-1 and 4-2) would indicate this association. The dampened effects of the daytime diurnal circulation during the winter episodes studied can result in even lower wind speeds than periods during the summer and can contribute to the build-up of pollutants in the valley.

During both episodes, the higher PM concentrations were recorded in the late afternoon and evening. This likely occurred because of a combination of meteorological and emissions related processes. Downslope flows during this part of the day can bring emissions toward the valley floor, where PM monitors in Golden are located. In addition, theory indicates along-valley flow is typically slowing and reversing at this time (Whiteman 2000). However, it could also be the case at low wind speeds that the reversal in wind direction may not have much of an effect and dispersion is mostly hindered by the further decrease in wind speed typical of these hours of the day. This is supported by the diurnal variation exhibited during the episodes that indicates lower wind speeds in the afternoon and into the evening (Figure 4-4). Emissions also change during the late afternoon and early evening. Emissions associated with traffic increases as residents drive home from work or school and space heating emissions increase as residents burn wood, oil or gas to heat their homes upon arrival.

Wind from the northwest and southeast resulted in nearly all occurrences of high PM concentrations (Figure 4-7 and 4-8). Winds from these directions are expected given the terrain-forced flows along the valley alignment. A trend cannot be discerned that shows higher PM concentrations from either the northerly or southerly flow. The wind roses (Figure 4-9) revealed that winds in Golden are channeled over the main valley corridor. The modelled winds may show that the diurnal variation of weak winds along the valley could mean that winds that disperse pollutants down-valley at night are simply returned by the reversal of winds in the morning leading to the build-up of pollutants in the Town (Whiteman 2000).

In addition to low horizontal wind speeds, episodes typically occur during times of low mixing height, low convective activity, inversions and atmospheric stability (Malek et al. 2006). These atmospheric conditions are associated with capping and suppression of vertical motion in the boundary layer, reducing the dispersion of pollutants (Arya 1999). Since direct measurements of these atmospheric characteristics are not available in most areas, the results of validated CALMET modeling will allow for the investigation of the CALMET predictions of these parameters during the episodes.

Modeling the episodes in CALPUFF will now allow for further analysis using the CALMET predicted wind fields and atmospheric parameters causing the episodes. CALMET will calculate the winds and other meteorological fields by using the observed winds in Golden as a basis. Ultimately, CALPUFF will use the predicted winds, calculated mixing heights, stability and other atmospheric parameters to predict PM concentrations in Golden. Following the modeling, stability, mixing height and vertical wind velocity will be available as predicted model variables. This will allow for the isolation of these parameters in analysis of each episode's dispersal characteristics.

5 CALMET

This chapter describes the setup of the model and evaluation of the meteorological processor CALMET during the two PM episodes outlined (Section 4.1). Winds and other meteorological parameters output by CALMET will then be used in the dispersion portion of the modeling system, CALPUFF.

5.1 SETUP OF CALMET

CALMET used digital terrain and land use data along with data from four surface stations and a hybrid upper air station combining data from locally operated SODAR and more distant radiosonde measurements. The setup of the model is described here.

5.1.1 Modeling Domain

An air dispersion modeling domain must include all relevant emission sources and encompass an area large enough to allow the meteorological patterns of the area to develop. The CALPUFF modeling domain chosen for this study encompasses a 35 by 40 kilometer area centered at the Town of Golden (Figure 5-1). The boundaries include the entire east-west extent of the Columbia River Valley to allow CALMET to establish the main valley flow as well as any tributary flows from the Kicking Horse and Blaebarry Passes. Inclusion of the Purcell and Rocky Mountain Ranges to the west and east respectively allowed for the incorporation of steering effects from the complex terrain surrounding the Town of Golden (Figure 5-1). As described earlier, these mountain ranges act as barrier to dispersion of pollutants out of the valley and influence the dominant wind pattern in Golden, providing the basis for the airshed extent described in Figure 1-2. The modelling domain encompasses all of the sources deemed to be significant in adding to the PM loading in the Town of Golden with enough additional terrain modeled to account for the meteorological influences affecting dispersion in the airshed. The modelling domain also includes all significant receptors, namely the populated areas in the Golden airshed.

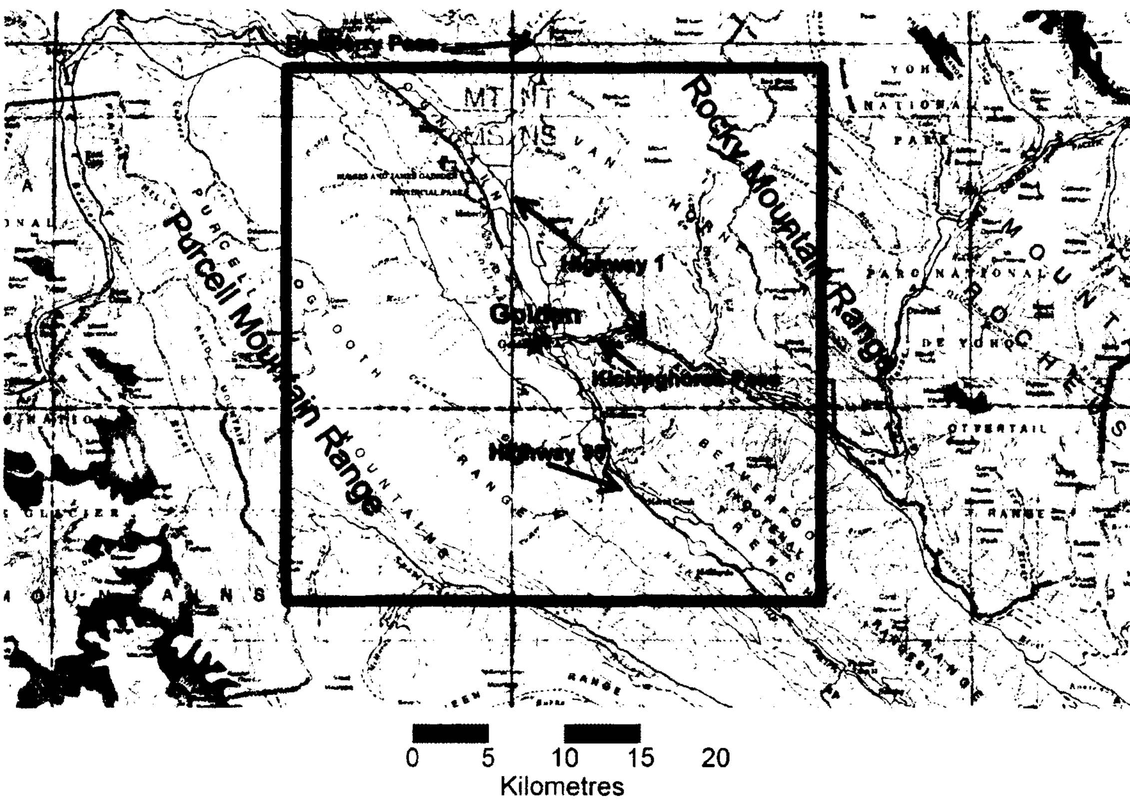

Figure 5-1 **Map showing the approximate modeling domain extent around the Town of Golden.**

A larger modeling domain would make it difficult to choose appropriate distances for critical CALPUFF parameters such as R1, Rmax, and Terrad as these are held constant across the modeling domain. For example, effects of terrain outside of the main valley may become too influential if included in the modeling domain because Terrad, the parameter that controls the terrain effects on wind fields, is set uniformly across the domain. In addition, the lack of accurate emission estimates and meteorological stations from the surrounding areas of Golden would likely reduce the accuracy of the model if the domain were expanded further. Computer processing time would also increase.

To properly characterize the terrain, the model was run with a grid spacing of 0.25 km. The same grid resolution was used by Scire and Robe (2000) in an application of CALPUFF in the Columbia River Valley. CALMET determines a wind vector for each hour in each grid cell. In addition to the 250 metre-spacing of receptors in the modeling domain, discrete receptors were located at the ambient monitoring locations (CPR, TOWN, and GOLF) in Golden (Figure 2-3). A CALPUFF receptor is placed in the centre of each grid cell. Each receptor represents a point at which CALPUFF calculates the concentration of PM. In total 22,343 gridded and discrete receptors are located in the modeling domain. The gridded receptors allow for visual display of the wind fields and dispersion results on a 3-D map created in Surfer™, the mapping program associated with CALPUFF. The statistical evaluation will focus on the three discrete receptors where continuous meteorological and PM data were collected by the BCMOE during the field study. By only looking at episodes lasting several days, the computer run time for this resolution is appropriate. Grid spacing less than this may not be appropriate considering the resolution of the terrain and land use data sets that were available.

CALMET also requires the vertical extent of the modeling domain to be defined. These are defined in layers. Ten vertical layers were defined. A more detailed description of the vertical layers is provided in Section 5.1.3c.

5.1.2 Geophysical and Land Use Data

CALMET relies on geophysical data and meteorological data to compute wind fields and dispersion characteristics. Geophysical data entered in CALMET are essential in determining the final wind fields through the internal model calculation of the terrain steering effects. Geophysical data includes terrain elevations, land use categories, surface roughness length (optional), albedo (optional), bowen ratio (optional), soil heat flux (optional), anthropogenic heat flux (optional), and leaf area index (optional). In CALMET this information is used to determine the components of the overland surface energy budget used to conserve the energy throughout the modeling system and steer the initial wind fields (Scire et al. 2000). For this study, all of the optional data listed above were estimated by CALMET using the required data of terrain elevations and land use categories. CALMET estimates the optional parameters using a series of algorithms and default values assigned for each of the land use categories. The file produced is a CALMET data file including gridded elevations, land use categories, and the optional surface parameters mentioned above.

Terrain Data were downloaded from the EarthTech, Inc. website, via the United States Geological Survey (USGS) in the form of Shuttle Radar Topography Mission data (SRTM3) (http://www.src.com/datasets/SRTM_Info_Page). These data have a resolution of approximately 90 metres in horizontal extent and 10 metres in the vertical extent because they are sampled at 3 arc-seconds. 3 arc-seconds at the equator corresponds roughly to 90 meters in horizontal extent. In the downloadable format, SRTM3 data can be processed using a pre-processor called Terrel included in the CALPUFF PRO 5 graphical user interface. Terrel transforms the terrain SRTM3 data into a useable gridded terrain field format for use in CALMET (Scire et al. 2000).

Land use/land cover data were also available from the Earthtech, Inc. website. Here, the Global Land Cover Characterization (GLCC) Database can be accessed (http://www.src.com/datasets/GLCC_Info_Page.html). Unfortunately, the resolution provided by the GLCC database was not sufficient for the modeling in Golden. More detailed landuse data were obtained from the British Columbia landuse database (resolution = 250m) and converted into CALMET landuse codes using the conversion recommended in the BC Air Dispersion Modelling Guidelines (2008) (Table 5-1). The converted land use categories are mapped in Figure 5-2. The geophysical pre-processor for CALMET, MAKEGEO, computes area weighted values for each model grid cell based on the amount of area each land use category covers in the grid cell. MAKEGEO then assigns an arithmetic average of the default geophysical parameters associated with each land use category (Table 5-2).

CALMET defines a land use category for perennial snow and ice, but does not allow for recognition of seasonal changes in snow cover. Land use categories were not changed to reflect that some areas of the Columbia River Valley are snow covered during the two episodes modelled. Certainly this is a limitation of the methods used to characterize the land use categories, as changes in the snow cover would result in a change of the default geophysical parameters (Table 5-2) assigned to each grid cell and would affect the calculated calculated overland energy budget model in CALMET.

Table 5-1 Conversion of B.C. Land Use Codes to CALMET Codes

B.C. Land Class Code	B.C. Land Use Category	CALMET Code	CALMET Land Use Category
2	Agriculture	-20	Agricultural Land –Irrigated
3	Barren Surfaces	70	Barren Land
4	Fresh Water	50	Water
5	Mining	70	Barren Land
6	Old Forest	40	Forest Land
7	Recently Logged	30	Rangeland
8	Recreational Activities	40	Forest Land
9	Residential Agriculture Mixtures	20	Agricultural Land
10	Selectively Logged	40	Forest Land
11	Urban	10	Urban
12	Wetlands	60	Wetland
13	Young Forest	40	Forest Land

Source: BC Air Dispersion Modelling Guidelines (2008)

The land use data along with the SRTM3 data from Terrel were combined in the geophysical input data file for CALMET called MAKEGEO.dat. This file includes elevations and fractional land use cover for each grid in the modeling domain.

Table 5-2 Default CALMET Land Use Categories and Associated Geophysical Parameters

Land Use Type	Description	Surface Roughness (m)	Albedo	Bowen Ratio	Soil Heat Flux Parameter	Anthropogenic Heat Flux (W/m²)	Leaf Area Index
10	Urban or Built-up Land	1.0	0.18	1.5	.25	0.0	0.2
20	Agricultural Land - Unirrigated	0.25	0.15	1.0	.15	0.0	3.0
-20*	Agricultural Land - Irrigated	0.25	0.15	0.5	.15	0.0	3.0
30	Rangeland	0.05	0.25	1.0	.15	0.0	0.5
40	Forest Land	1.0	0.10	1.0	.15	0.0	7.0
51	Small Water Body	0.001	0.10	0.0	1.0	0.0	0.0
54	Bays and Estuaries	0.001	0.10	0.0	1.0	0.0	0.0
55	Large Water Body	0.001	0.10	0.0	1.0	0.0	0.0
60	Wetland	1.0	0.10	0.5	.25	0.0	2.0
61	Forested Wetland	1.0	0.1	0.5	0.25	0.0	2.0
62	Nonforested Wetland	0.2	0.1	0.1	0.25	0.0	1.0
70	Barren Land	0.05	0.30	1.0	.15	0.0	0.05
80	Tundra	.20	0.30	0.5	.15	0.0	0.0
90	Perennial Snow or Ice	.20	0.70	0.5	.15	0.0	0.0

Source: CALMET User Guide (Scire 2008)

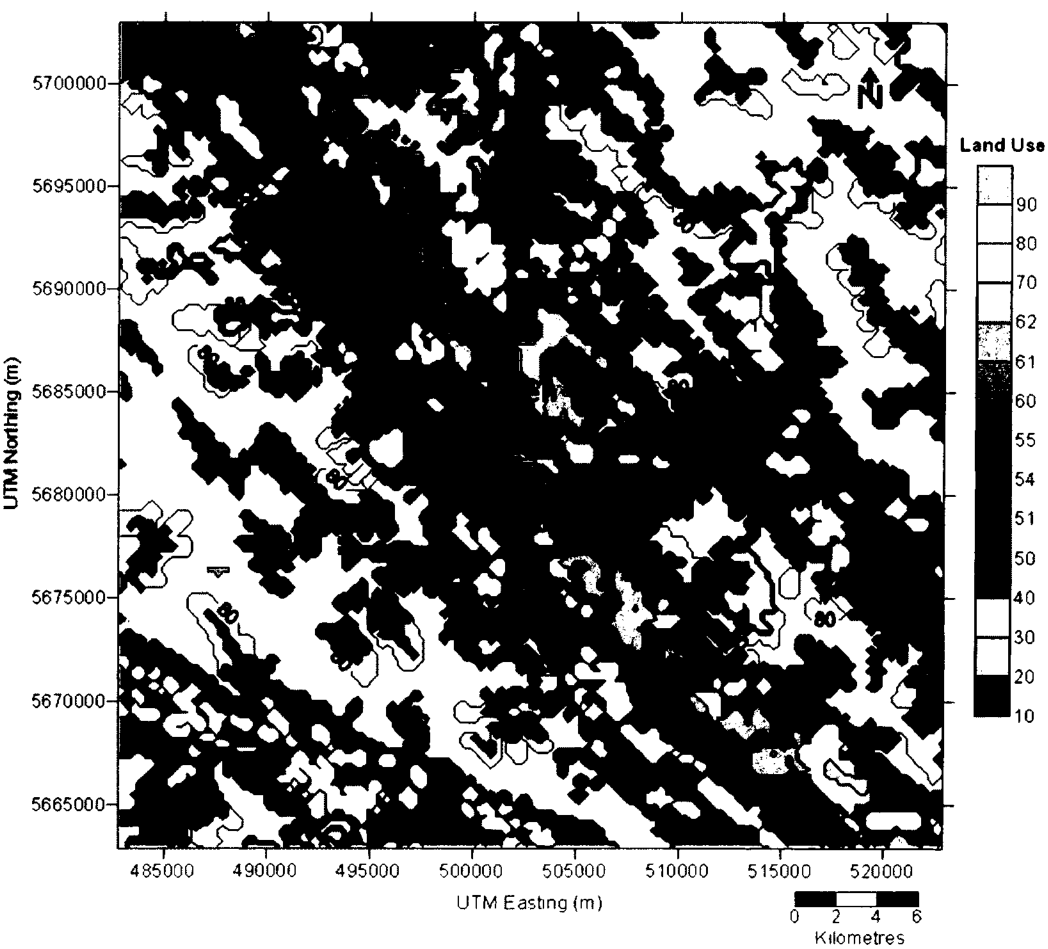

Figure 5-2 Land Use Category Map for the Modeling Domain. Land use category numbers on color scale correspond to those defined in

5.1.3 Meteorological Modeling Data

Along with the geophysical data, CALMET requires meteorological data from several sources to generate the wind fields used to drive dispersion in CALPUFF. CALMET utilizes a number of pre-processors to incorporate surface meteorological data and upper air data.

5.1.3a *Surface Station Data*

CALMET requires, at a minimum, surface observations of wind speed, wind direction, temperature, cloud cover, ceiling height, surface pressure, precipitation rates and type, and relative humidity from at least one of the four surface stations within the modeling domain for every hour modeled.

The four surface meteorological stations used in the model were located at CPR south of the Town, Lady Grey School in downtown Golden, the airport, and the Golden Golf Course north of the Town (Figure 2-3). Data for each of the parameters were available from at least one of the four surface stations for each hour of both episodes (Table 5-3). Gaps in the data at any one station were limited. The data set was as complete as can be expected.

Precipitation type was determined by coding the available precipitation data from the airport station. Precipitation rates were not determined, but effects of wet deposition are not likely to have a major influence during the episodes chosen for this study as conditions were quite dry with only one hour of precipitation recorded during Episode 1 and eight hours of precipitation recorded during Episode 2.

Cloud cover, ceiling height and pressure data were available from the airport station for daytime hours only. For overnight data, observations from the next closest airport in Revelstoke was used. Cloud cover and ceiling height were taken directly from Revelstoke. Pressure was adjusted using the hydrostatic equation to account for the difference in elevation between the Golden airport and the Revelstoke airport.

Table 5-3 Summary of the four meteorological stations used in CALMET modelling

Site Name	Elev ASL (m)	Meteorological sensors	Site UTM east (m)	Site UTM North (m)	Wind Sensor height AGL (m)
CPR	857	Temp, Wind, RH	504.8252	5679.853	10
Town	773	Temp, Wind, RH	501.9755	5682.693	10
Golf Course	795	Temp, Wind, RH, Sodar Wind	499.5356	5686.801	10
Airport	785	Temp, Wind, RH, pressure, cloud cover, ceiling height, precipitation categories	502.3239	5683.188	10

5.1.3b *Upper Air Data*

The minimum upper air data requirements for CALMET are twice-daily radiosonde releases with observed vertical profiles of wind speed, wind direction, temperature, pressure and elevation. These vertical profiles are used in combination with surface station data to predict wind fields and temperature lapse rates in the layers aloft.

Previous modeling attempts in Golden were hampered by the lack of local upper air data. To measure more locally appropriate upper air data, a SCINTEC FAS64 phased-array Doplar sodar system was operated at the golf course location

(Figure 2-3). The SODAR system resolved wind speed and direction for the lower part of the boundary layer to approximately 500 metres above ground level by measuring the scattering of sound waves by atmospheric turbulence.

Obtaining a local vertical temperature profile in the lowest portion of the atmosphere was important as temperature lapse rates calculated from upper air stations hundreds of kilometres away would not allow for accurate prediction of mixing heights and stability classes. In order to capture a vertical temperature profile, six HOBOs were installed on the mountain side to the west of Golden (Figure 3-3). It is noted here that the temperature near the surface from the HOBOs is not ideal as these measurements would be different than upper air in mid-valley, however it was the best available option. The SODAR winds and HOBO temperature profiles were combined with the twice daily radiosonde releases from the upper air station in Prince George to meet the upper air requirements for CALMET. Prince George was used as the upper air station as opposed Kelowna, the closest upper air station, as the climate normals more closely matched those in Golden. The twice-daily upper air profiles used during the two episodes modeled in this study are shown in Figure 5-3.

The combination of data from the HOBOs and SODAR system along with the Prince George upper air data reveal profiles that indicate persistent temperature inversions during both episodes. It has been hypothesized that wintertime inversions lead to episodes of high particulate matter in Golden (Burkholder 2005). The inversions depicted in the combined upper air data set may be a result of the differences in temperature from the highest station of local HOBO temperature transect and the next temperature recorded by the upper air data in Prince George. Since there were no adjustments applied to meld the data sets together, the step from the local data sets collected (SODAR wind data and HOBO temperature data) to the Prince George upper air data could compromise the integrity of the combined upper air data set if there is an artificial step change in temperature or wind introduced. Thus, it could be that the combination of data used for the upper air data is not realistic of the situation in Golden, however due to the limitations of the field monitoring with the SODAR and HOBOs and the objectives of this study to use the available meteorological data as input to CALMET, the upper air profiles in Figure 5-3 were used.

(a)

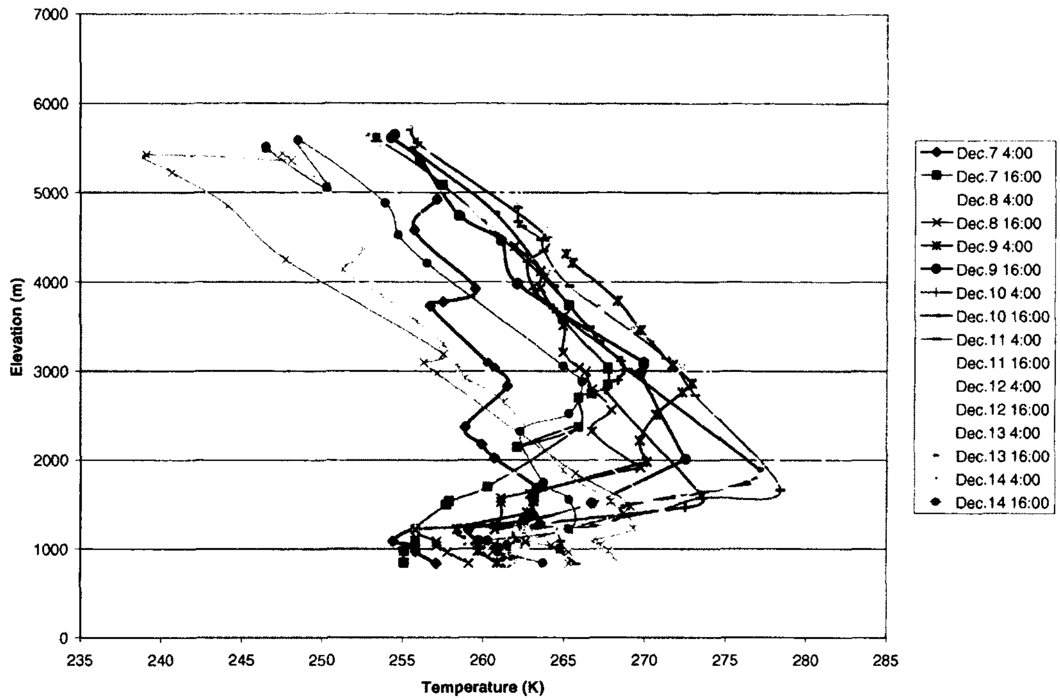

(b)

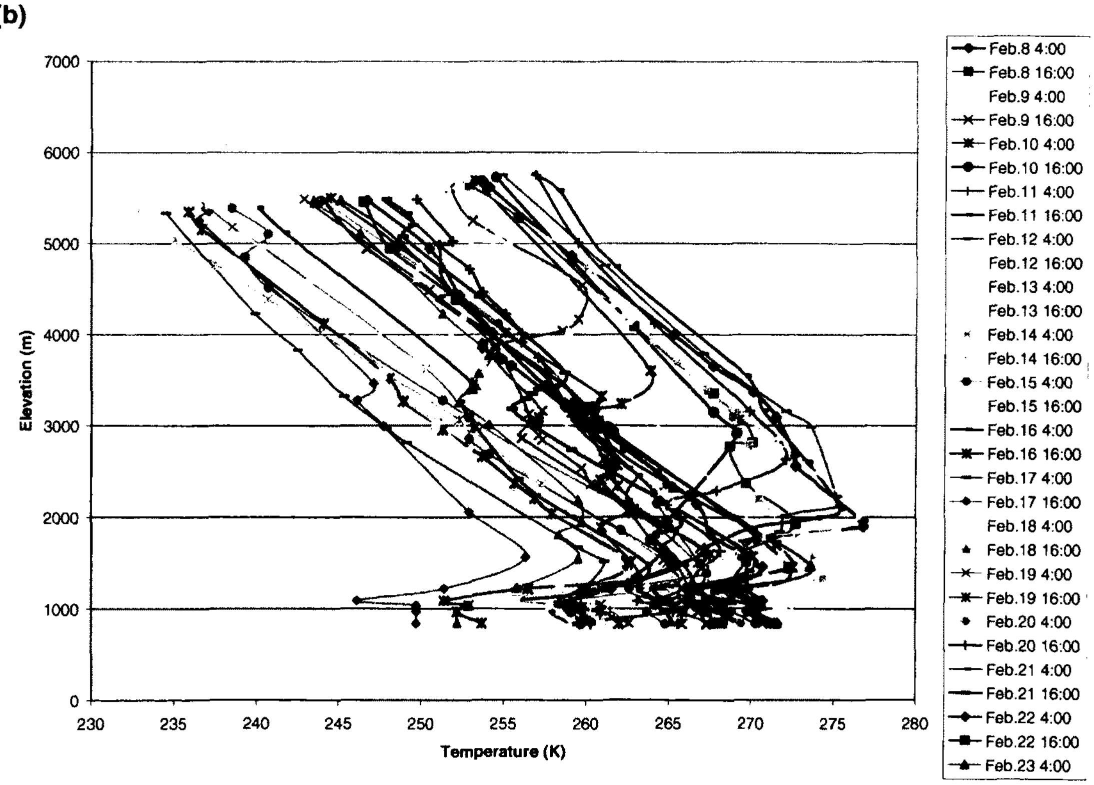

Figure 5-3 Twice Daily Upper Air Profiles for (a) Episode 1 and (b) Episode 2

5.1.3c *Weighting Factors for Surface Stations and Upper Air Stations Used in CALMET*

The model was run with 10 vertical layers. The height above ground of each of these layers is outlined in Table 5-2. Higher vertical resolution was used near the surface as these layers are more important in the immediate dispersal of pollutants in the boundary layer and ground-level pollutant concentrations that would affect the population of Golden. Higher in the valley and above the valley it is less likely that winds will be affecting the ground-level pollutant concentrations, especially during episodes when mixing heights typically remain low.

As recommended by the US EPA, the CALMET option to extrapolate surface data using similarity theory was chosen. Using the observed data and similarity theory, this method allows the influence of surface wind speed and direction to extend into the other vertical layers. In this study, winds at the surface were determined based on surface observations and the CALMET initial guess wind field. Winds in the layers aloft were derived from a combination of extrapolated surface wind data and upper air data based on the biasing option in CALMET. Biases are also outlined in Table 5-4.

The BIAS option in CALMET determines the extent to which the surface station and upper air station data influences each vertical layer in the domain. A BIAS of zero equally weights the influence of upper air station winds and surface station in the inverse distance squared interpolation of the initial guess field. A negative bias reduces the weight of the upper air station winds (i.e. a BIAS = -0.5

reduces the weight of upper air wind by 50%, while a BIAS = -1 reduces the weight of upper air wind to zero). A positive bias reduces the weight of surface station wind (i.e. a BIAS = +0.5 reduces the weight of surface station wind by 50%, while a BIAS = +1 reduces the weight of surface station wind to zero).

For this study, BIAS was largely determined by the reliability of the SODAR data incorporated into the upper air data file. Recall that the SODAR was used to resolve wind speed and direction for the lower part of the boundary layer to approximately 500 metres above ground level. BIAS values were set based on the availability and reliability of the SODAR data captured. BIAS in the first two layers were weighted completely towards surface winds (BIAS = -1) because the SODAR data was unreliable at these elevations and the radiosonde data was from well outside the modeling domain. Modeled predictions improved with the two lower layers being completely weighted to surface station extrapolation. In layers 3-6, where SODAR data were consistently available, the biases set to take advantage of this local data by equally weighting surface observations and upper air data from the SODAR in these layers (BIAS =0).

Sensitivity tests showed little difference in wind vectors when bias values were adjusted for the upper-most layers. Layers 7 and 8 represent vertical layers that are still below the top of the valley, thus the BIAS was set to be weighted slightly to the surface station data (BIAS = -0.5). Layers 9 and 10 are above the top of the valley so these layers were weighted slightly to the upper air data (BIAS = 0.5)

Table 5-4 **Weighting Factors for surface stations and upper air station used in determining CALMET winds in the 10 modeled layers.**

Vertical Layer	Height at Top of Layer (m)	Bias value
1	20	-1
2	40	-1
3	80	0
4	160	0
5	320	0
6	560	0
7	1000	-0.5
8	1500	-0.5
9	2200	0.5
10	3000	0.5

5.1.4 Calmet Model Options

There are a number of user-specified input switches and options that determine how CALMET handles terrain effects, interpolation of observational input data, and other data to determine final wind fields. The options used and the reasoning behind each choice are described in this section. Where deemed appropriate, the recommended US EPA default parameters were used. Other model parameters were chosen based on iterative testing of CALMET using the meteorological, terrain and landuse data described above. Final CALMET parameters are summarized in Table 5-5.

As describe in Section 3-1, CALMET uses an inverse-distance squared interpolation scheme to introduce observational data into the Step 1 wind field. The interpolation scheme allows observational data to be heavily weighted in the vicinity of the observational station. The wind field created in Step 1 dominates in regions farther away or outside the radius of influence of the observational station. Parameters R1 and R2 specify the weighting given to the observational data in the surface layer and in the layers aloft, respectively. R1 refers to the distance in kilometers from an observational station at which the observation and the initial-guess wind field produced by the diagnostic wind field module in CALMET are weighted equally (Scire et al. 2000). RMAX values are used to exclude observational data from interpolation if the distance from the observational station to a particular grid point exceeds the user-specified maximum radius of influence. RMAX1, RMAX2 specify the parameter for the surface layer and layers aloft, respectively (Scire et al. 2000).

Iterative testing of these CALMET parameters showed that to maintain valley flow in the complex terrain R1 and R2 values that allowed observational data to dominate between the TOWN and CPR stations were most appropriate. R1 was chosen as slightly less than the distance between these two stations. Combined with an RMax value of 5 km the wind fields balanced the observational dominated valley flow with CALMET computed kinematic effects of terrain and slope flows.

Table 5-5 **CALMET wind field model options**

Parameter	**Option Selected**	**US EPA Default**
Froude number Adjustment Effects Calculated?	Yes	Yes
Kinematic Effects Computed?	Yes*	No
Surface Wind Observations Extrapolated to Upper Layers?	Yes	Yes
Surface Winds Extrapolated even if Calm?	Yes	Yes
Maximum Radius of Influence over Land in the Surface Layer (RMAX1)	5 km	No
Maximum Radius of Influence over Land Aloft (RMAX2)	8 km	No
Radius of Influence of Terrain Features (TERRAD)	2 km	No
Relative Weighting of the First Guess Field and Observations in the Surface Layer (R1)	4 km	No
Relative Weighting of the First Guess Field and Observations in the Layers Aloft (R2)	6 km	No

*Model runs with and without kinematic effects were performed with little variation between the two. It is recommended that kinematic effects not be computed as it may cause "odd" model results. Since there was little variation between the model runs, the computation of kinematic effects did not cause "odd" results in this modelling exercise, so the results with kinematic effect turned on were used.

5.1.5 Calmet Evaluation Methods

The evaluation of dispersion modeling studies focus on the model's ability to provide accurate pollutant concentration fields as a result of the complete process of emission release, transport by wind and turbulent diffusion in the atmosphere (Cox 2005). The evaluation here isolates a single element of the overall process, the ability of the model to construct valid wind fields.

Visual assessment using scatter plots and the software mapping package SURFER allowed for an effective initial gauge of CALMET's performance. Model parameters (Table 5-2) were adjusted in subsequent model runs until the most visually representative wind fields were observed in relation to the modelled terrain and the observed wind data from the three stations in Golden. Common statistical methods used in the evaluation of diagnostic wind models such as CALMET were also used to evaluate model performance as suggested in Cox et al. (2005) and are presented here.

The statistical evaluation in this study included the Mean Error (ME) and the Mean Absolute Error (MAE). ME is the average difference between observed and predicted values. The MAE is the average of the absolute differences between the observed and predicted values. A perfect model has a ME and MAE of zero. Another common accuracy measure is the mean square error (MSE) which is similar to the MAE except differences are squared making it more sensitive to larger errors and outliers (Wilks 2006). The RMSE (the square root of the MSE) is reported here as it has the same physical dimensions as the predictions and observations (Wilks 2006). The statistical distributions of the errors are further quantified by the minimum (MIN ERR), median (MED ERR) and maximum error (MAX ERR).

Bias is sometimes used to assess wind speeds, but is not an accuracy measurement and only reveals whether the model is typically over- or under-predicting the observed measurements (OB) (Wilks 2006). In this case, it is more useful to determine the accuracy of the model predictions (PR). One can use fractional bias (Fb) as an indicator of model accuracy:

$Fb = 2(OB-PR)/(OB+PR)$.

Fb is bounded by +/- 2 with the extremes meaning no agreement between the modeled and observed values. Fb indicates to what degree the model is over or under-predicting. Negative values of Fb indicate the model is over-predicting and positive values indicate under-prediction. Fb of +/- 1.00 corresponds to model prediction within a factor of 3 of observed values, whereas a value of +/- 0.67 indicates predictions are within a factor of 2 of observed values. The Fb statistic is less reliable if the model is grossly over- or under-predicting observed values as it is bounded so that higher levels of over or under prediction result in little change in the statistic (Wilks 2006).

From the initial analysis it was determined that wind speed may have a large influence on the dispersion in Golden (Section 4-2). As a measure of the accuracy of wind speed predictions, the correlation coefficient (CORR) between calculated and observed wind speeds was calculated.

In order to test the model predictions versus the observed measurements several model runs were evaluated for each episode. First, the ability of CALMET to produce wind fields consistent with the surface station input data was tested by comparing observed values with a "full" CALMET run including all surface station data as input data. This comparison simply ensures that surface station wind field remains the same in the model output. Next, one station's observed data was excluded and the model run using the three other surface station data. Following the model run, predicted data were processed from the grid cell containing the excluded observational station and compared to the observed data from that station. Three model runs were made leaving out one of the CPR, TOWN or GOLF stations each time. This "leave one-out" method allowed investigation of how accurately CALMET would capture the winds at each station's location without the data from that station being used as input data. This is an indication of how CALMET is predicting winds away from input stations. The model runs were repeated for both episodes 1 and 2. Statistics for both the "full" and leave one out methods are provided based on the observed and predicted data sets at all three stations individually, and as a complete data set (ALL). Separate analysis of episode 1 and 2 are provided for comparison.

Another method was employed to determine how accurately CALMET was predicting the wind fields and other meteorological parameters at points other than those representing the input stations. This method was used by Ostermann and Schutte (2004) in a modeling effort for Levelton Consultants in Williams Lake, BC. Using the "full" CALMET run a point was extracted to compare predicted meteorological parameters with the surface stations wind data, temperature data and predicted stability classes. The point extracted was located in the Columbia River Valley halfway between the northern GOLF station and the southern CPR station (see Figure 2-3). If data at the extracted point were comparable to the other stations it would allow for more confidence that the main valley flow was being captured reasonably well during the "full" CALMET run.

5.2 CALMET EVALUATION RESULTS

As expected, CALMET was able to very accurately reproduce the input observed data during the "full" CALMET run (Tables 5-5, 5-6, 5-9 and 5-10) since it is essentially reproducing its input data.. Wind speed shows small MAE and Fb statistics at all stations for Episode 1 and 2. Fb shows that the model is underpredicting wind speeds during the second episode. In addition the correlation coefficients are approaching 1 for all stations indicating good model performance. Wind direction also shows very low MAE. With the exception of the CPR station during Episode 2, all stations predict over 86% of wind directions, for the "full" CALMET run, within 10 degrees of the observed values.

Table 5-6 Episode 1 CALMET "full" run wind speed statistics. Sp and S_o are the wind speed predicted and observed. σ_p = standard deviation of predicted; σ_o = standard deviation of observed; ME = mean error; MAE = mean absolute error; MAX = maximum error; MED = median error; MIN = minimum error; RMSE = root mean square error; FB = fractional bias, and; CORR = correlation coefficient.

					ERR							
Station	S_p	S_o	σ_p	σ_o	ME	MAE	MAX	MED	MIN	RMSE	FB	CORR
CPR	0.98	1.01	0.82	0.84	0.03	0.05	0.96	0.03	0.00	0.10	0.03	0.995
TOWN	1.03	1.05	0.63	0.63	0.02	0.04	0.20	0.03	0.00	0.05	0.02	0.997
GOLF	0.97	0.97	0.63	0.64	0.01	0.01	0.18	0.01	0.00	0.02	0.01	0.999
ALL	0.99	1.01	0.70	0.71	0.02	0.03	0.96	0.02	0.00	0.06	0.02	0.996

Table 5-7 **Episode 1 CALMET "full" run wind direction statistics. D_p and D_o are the wind direction predicted and observed. % 10° is the percentage of winds within 10 degrees of the observed winds. % 45° is the percentage of win ds within 45 degrees of the observed winds. Refer to Table 5-5 for other parameter definitions.**

					ERR				
Station	D_p	D_o	MAE	MAX	MED	MIN	RMSE	% 10°	% 45°
CPR	206.13	206.11	3.98	58.82	2.52	0.02	6.94	91.667	99.48
TOWN	213.24	210.56	1.58	15.53	1.20	0.00	2.24	99.479	100.00
GOLF	213.42	212.07	1.23	36.29	0.76	0.00	3.00	99.479	100.00
ALL	210.93	209.58	2.25	58.82	1.25	0.00	4.55	96.875	99.83

Table 5-8 **Episode 1 wind speed statistics for CALMET using the "leave one-out" method. S_p and S_o are the wind speed predicted and observed. Refer to Table 5-5 for other parameter definitions.**

Station	S_p	S_o	σ_p	σ_o	ERR ME	ERR MAE	ERR MAX	ERR MED	ERR MIN	ERR RMSE	FB	CORR
CPR	0.98	1.01	0.60	0.84	0.04	0.45	2.61	0.27	0.00	0.68	0.04	0.603
TOWN	0.92	1.05	0.75	0.63	0.13	0.42	2.58	0.27	0.00	0.62	0.14	0.632
GOLF	0.89	0.97	0.61	0.64	0.09	0.35	1.78	0.26	0.00	0.50	0.09	0.700
ALL	0.93	1.01	0.66	0.71	0.09	0.41	2.61	0.27	0.00	0.60	0.09	0.618

Table 5-9 **Episode 1 wind direction statistics for CALMET using the "leave one-out" method. D_p and D_o are the wind direction predicted and observed. % 10° is the percentage of winds within 10 degrees of the observed winds. % 45° is the percentage of winds within 45 degrees of the observed winds. Refer to Table 5-5 for other parameter definitions.**

Station	D_p	D_o	ERR MAE	ERR MAX	ERR MED	ERR MIN	ERR RMSE	% 10°	% 45°
CPR	206.13	206.11	3.98	58.82	2.52	0.02	6.94	91.667	99.48
TOWN	213.24	210.56	1.58	15.53	1.20	0.00	2.24	99.479	100.00
GOLF	213.42	212.07	1.23	36.29	0.76	0.00	3.00	99.479	100.00
ALL	210.93	209.58	2.25	58.82	1.25	0.00	4.55	96.875	99.83

Table 5-10 **Episode 2 CALMET "full" run wind speed statistics. S_p and S_o are the wind speed predicted and observed. Refer to Table 5-5 for other parameter definitions.**

Station	S_p	S_o	σ_p	σ_o	ERR ME	ERR MAE	ERR MAX	ERR MED	ERR MIN	ERR RMSE	FB	CORR
CPR	0.66	0.69	0.75	0.78	-0.03	0.06	0.50	0.04	0.00	0.08	0.05	0.996
TOWN	0.91	0.93	0.57	0.58	-0.03	0.07	0.63	0.07	0.00	0.11	0.03	0.982
GOLF	0.68	0.68	0.37	0.37	0.00	0.01	0.11	0.01	0.00	0.02	0.01	0.999
ALL	0.75	0.77	0.60	0.61	0.02	0.05	0.63	0.02	0.00	0.08	0.03	

Table 5-11 **Episode 2 CALMET "full" run wind direction statistics. D_p and D_o are the wind direction predicted and observed. % 10° is the percentage of winds within 10 degrees of the observed winds. % 45° is the percentage of win ds within 45 degrees of the observed winds. Refer to Table 5-5 for other parameter definitions.**

Station	D_p	D_o	ERR MAE	ERR MAX	ERR MED	ERR MIN	ERR RMSE	% 10°	% 45°
CPR	198.80	186.66	11.90	154.30	4.50	0.01	25.14	69.79	98.70
TOWN	303.05	303.66	4.28	141.27	4.28	0.00	13.34	91.93	99.74
GOLF	275.59	265.27	1.69	13.83	1.23	0.00	2.55	98.70	100.00
ALL	231.93	251.86	5.93	154.30	1.56	0.00	16.50	86.81	99.48

Table 5-12 **Episode 2 wind speed statistics for CALMET using the "leave one-out" method. S_p and S_o are the wind speed predicted and observed. Refer to Table 5-5 for other parameter definitions.**

Station	S_p	S_o	σ_p	σ_o	ERR ME	ERR MAE	ERR MAX	ERR MED	ERR MIN	ERR RMSE	FB	CORR
CPR	0.94	0.69	0.64	0.78	0.25	0.61	2.24	0.47	0.00	0.78	-0.30	0.466
TOWN	0.78	0.93	0.97	0.58	-0.15	0.69	3.98	0.69	0.00	0.95	0.18	0.345
GOLF	0.77	0.68	0.60	0.37	0.09	0.32	2.20	0.23	0.00	0.48	-0.12	0.627
ALL	0.83	0.77	0.76	0.61	-0.06	0.54	3.98	0.37	0.00	0.76	-0.08	

Table 5-13 **Episode 2 wind direction statistics for CALMET using the "leave one-out" method. D_p and D_o are the wind direction predicted and observed. % 10° is the percentage of winds within 10 degrees of the observed winds. % 45° is the percentage of winds within 45 degrees of the observed winds. Refer to Table 5-5 for other parameter definitions.**

Station	D_p	D_o	ERR MAE	ERR MAX	ERR MED	ERR MIN	ERR RMSE	% 10°	% 45°
CPR	300.25	186.66	79.81	179.84	68.62	0.23	97.50	9.38	72.66
TOWN	193.25	303.66	64.42	179.70	64.42	0.02	84.51	12.50	77.34
GOLF	298.08	265.27	41.23	177.27	28.58	0.02	56.73	14.58	83.07
ALL	263.86	251.86	61.68	179.84	41.60	0.00	81.38	12.15	77.69

Using the leave one out method, the performance measures for CALMET deteriorate in comparison to the "full" CALMET run as expected (Tables 5-7, 5-8, 5-11 and 5-12). Episode 1 performance measures are much better than those during episode 2. Episode 1 wind speed shows low Fb for all stations, indicating that speeds are well within a factor of 2 of observed wind speeds. Fb is positive during Episode 1 indicating underestimation of wind speed, while during Episode 2 the overall Fb is negative indicating overestimation of wind speed. The correlation coefficients are also very reasonable with a low at the CPR station of 0.603 and a high at the GOLF station of 0.7. Wind direction predictions are within 10 degrees of the observed values only 19 % of the time during episode 1 and within 45 degrees 64% of the time. Episode 2 wind speed shows higher Fb and the correlation coefficients are lower. Wind direction predictions are within 10 degrees of observed values only 12% of the time, but within 45 degrees 78% of the time.

On a station-by-station basis the GOLF station performed the best. The correlation coefficient for wind speed was the highest at this station as well as the highest percentage of winds within 10 and 45 degrees of the observed values.

To display CALMET's predictions of wind flows around Golden, a snapshot of calculated wind vectors for level 1, 4 and 8 is provided (Figure 5-4 – 5-6). Near the surface the wind vectors are more variable in direction and speed (Figure 5-4). In general, the flow is terrain-forced along the valley. Slope flows steer vectors on the mountainsides and CALMET also shows some easterly flow coming out of the Kicking Horse Pass. At 120 m, wind vectors are calculated using equal weighting from surface station and upper air station data (Figure 5-5). The wind speeds are more uniform and direction is similar to that at the surface. At 1250 m, wind vectors are nearly uniform in speed and direction across the entire domain (Figure 5-6).

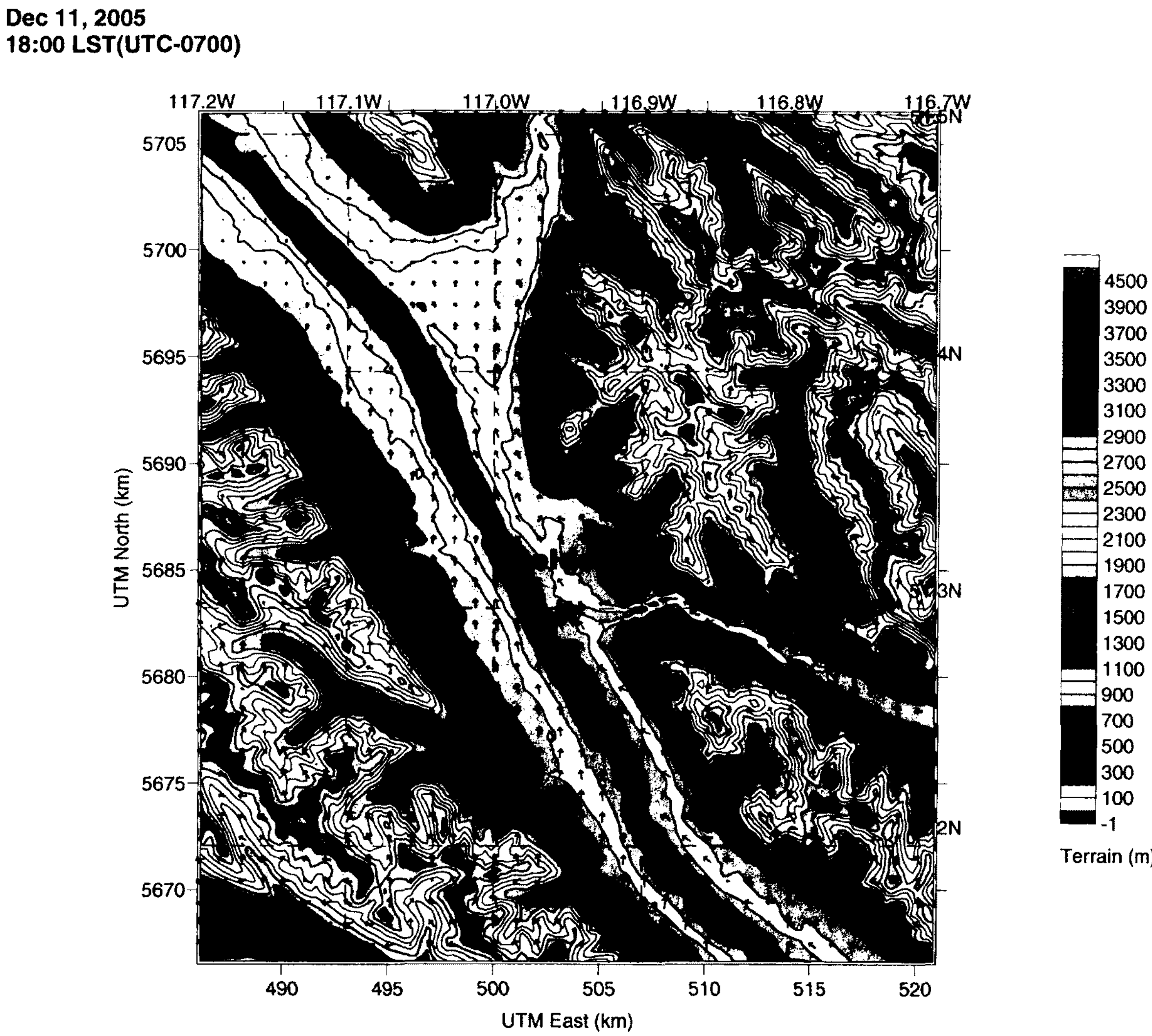

Figure 5-4 CALMET surface (10m) wind field for 18:00, December 11, 2005

Dec 11, 2005
18:00 LST(UTC-0700)

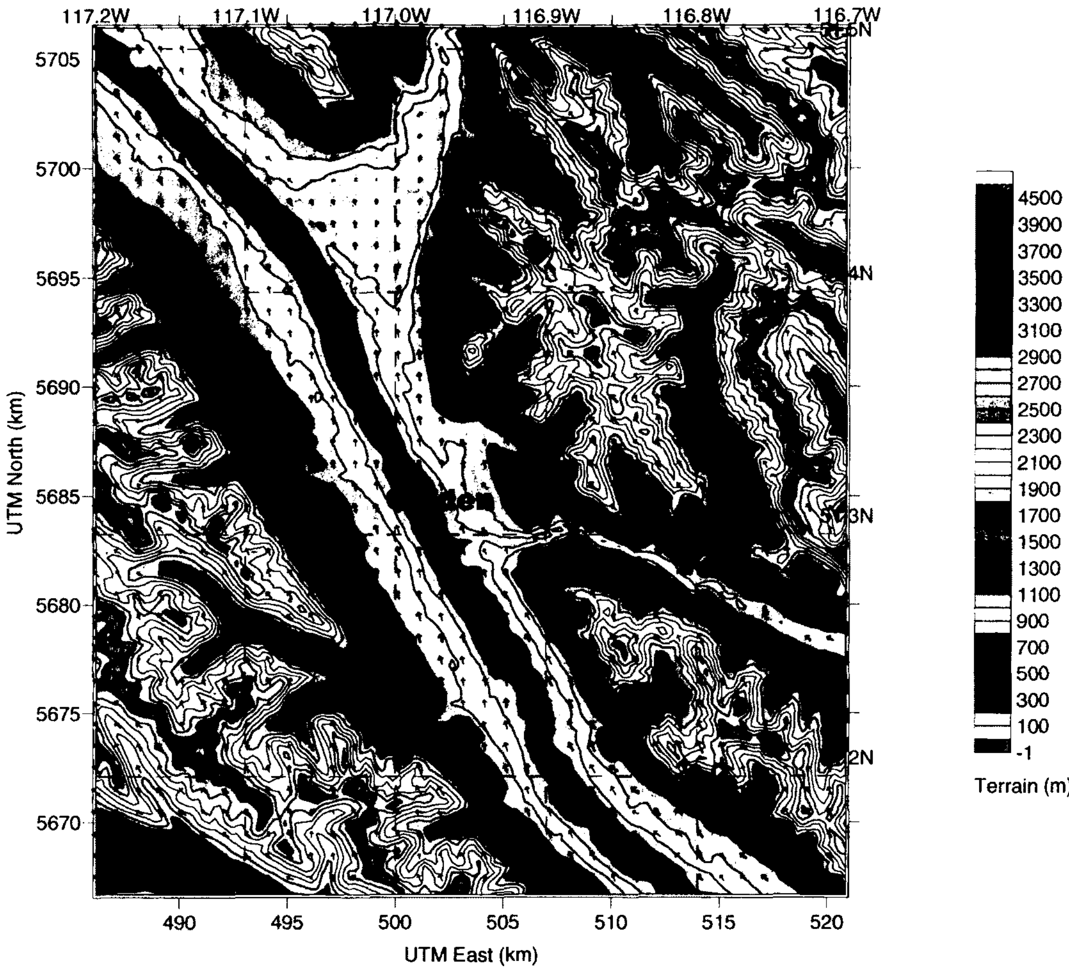

Figure 5-5 CALMET Level 4 (120m) wind field for 18:00, December 11, 2005

Dec 11, 2005
18:00 LST(UTC-0700)

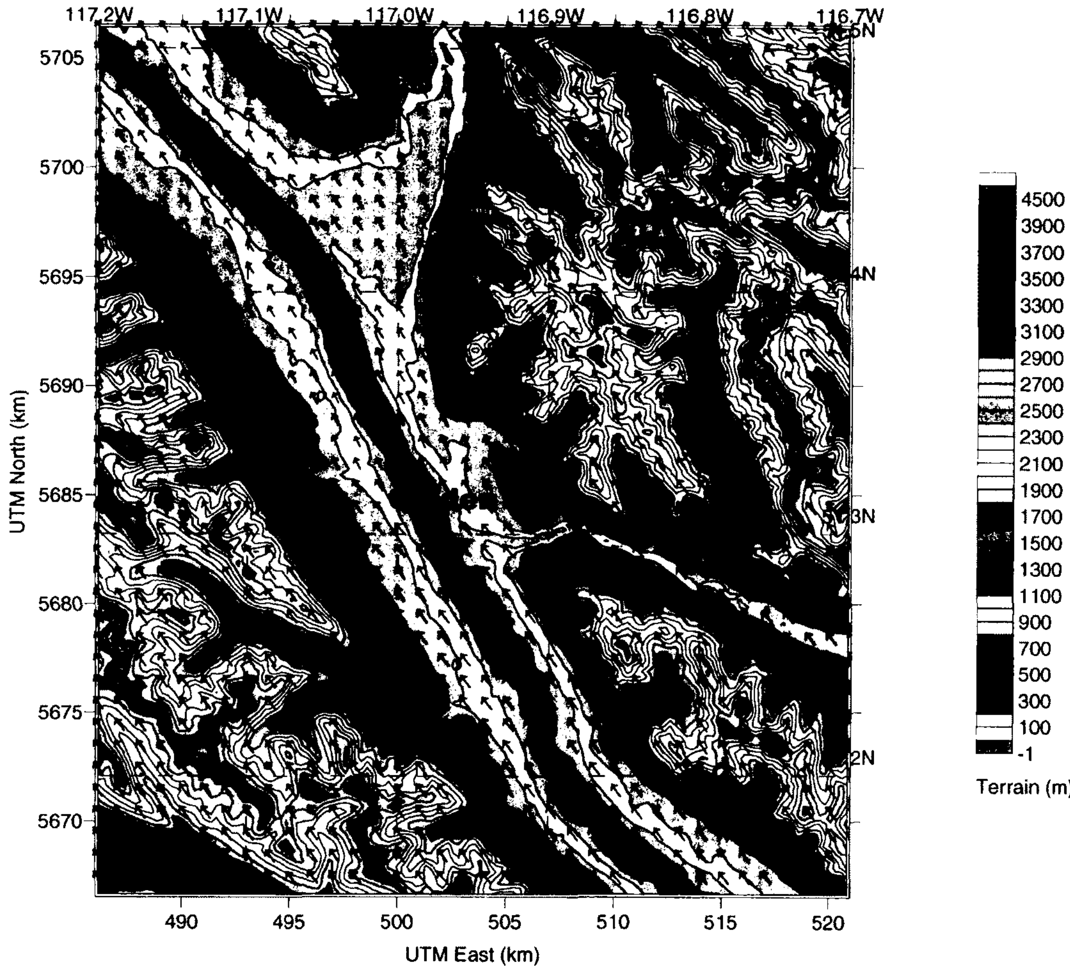

Figure 5-6 CALMET Level 8 (1250m) wind field for 18:00, December 11, 2005

The frequency distribution of the surface winds predicted at the extracted point (point location shown in Figure 2-3) are comparable to at least one input station's observed frequency in all wind speed classes (Figure 5-7). There is a reasonable distribution of wind speed classes at the extracted point with no grossly under or overestimated wind speeds. The modeled winds show the expected diurnal variation in wind speed (Figure 5-8).

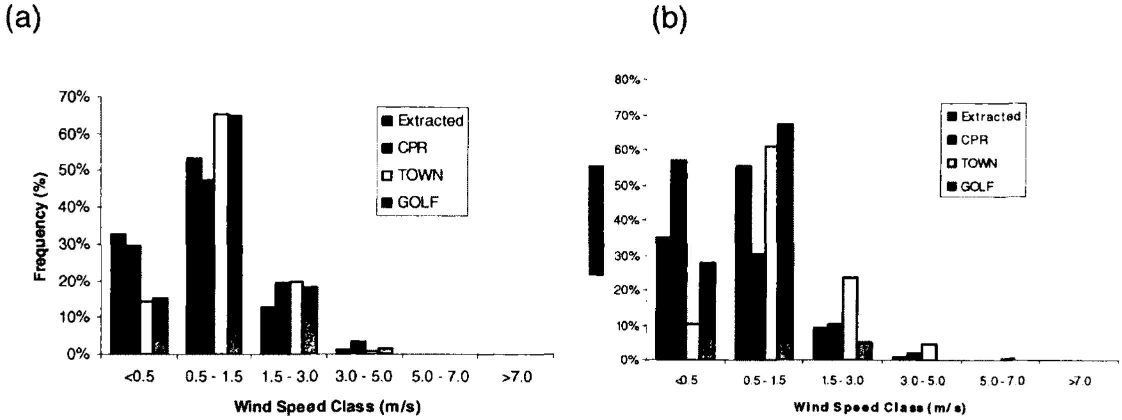

Figure 5-7 **Wind speed frequency distribution for the three surface stations and the extracted point for (a) Episode 1, (b) Episode 2.**

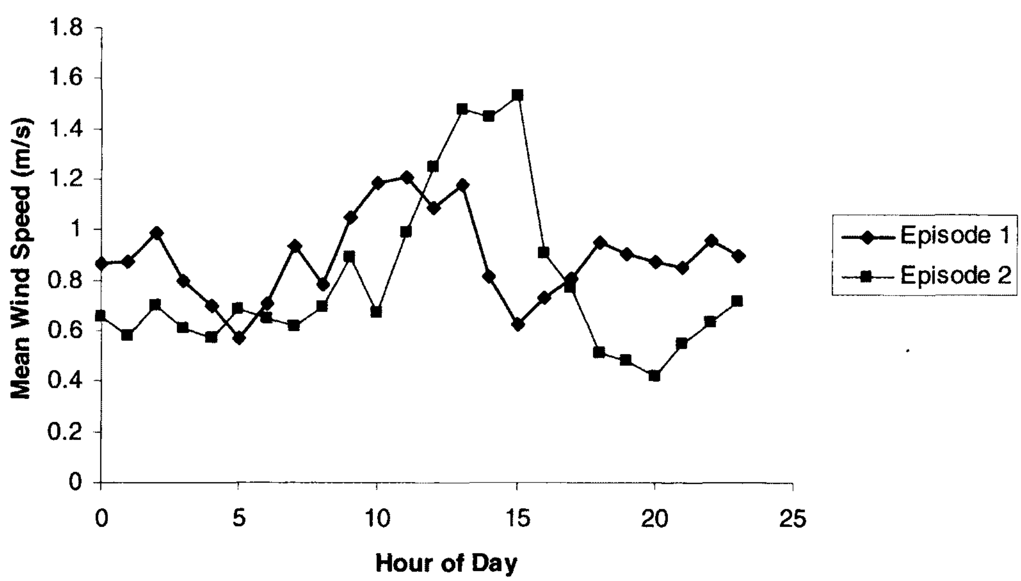

Figure 5-8 **Diurnal variation in modeled wind speeds at the extracted point during each episode.**

Wind rose for the extracted point during episode 1 (Figure 5-9a) shows good agreement with the wind rose from observed values reported at the TOWN station

(Figure 5-9c). During episode 2, the wind rose shows good agreement with the GOLF station observed surface wind rose (Figure 5-9d). This reveals northerly winds for almost the entire episode (Figure 5-9b).

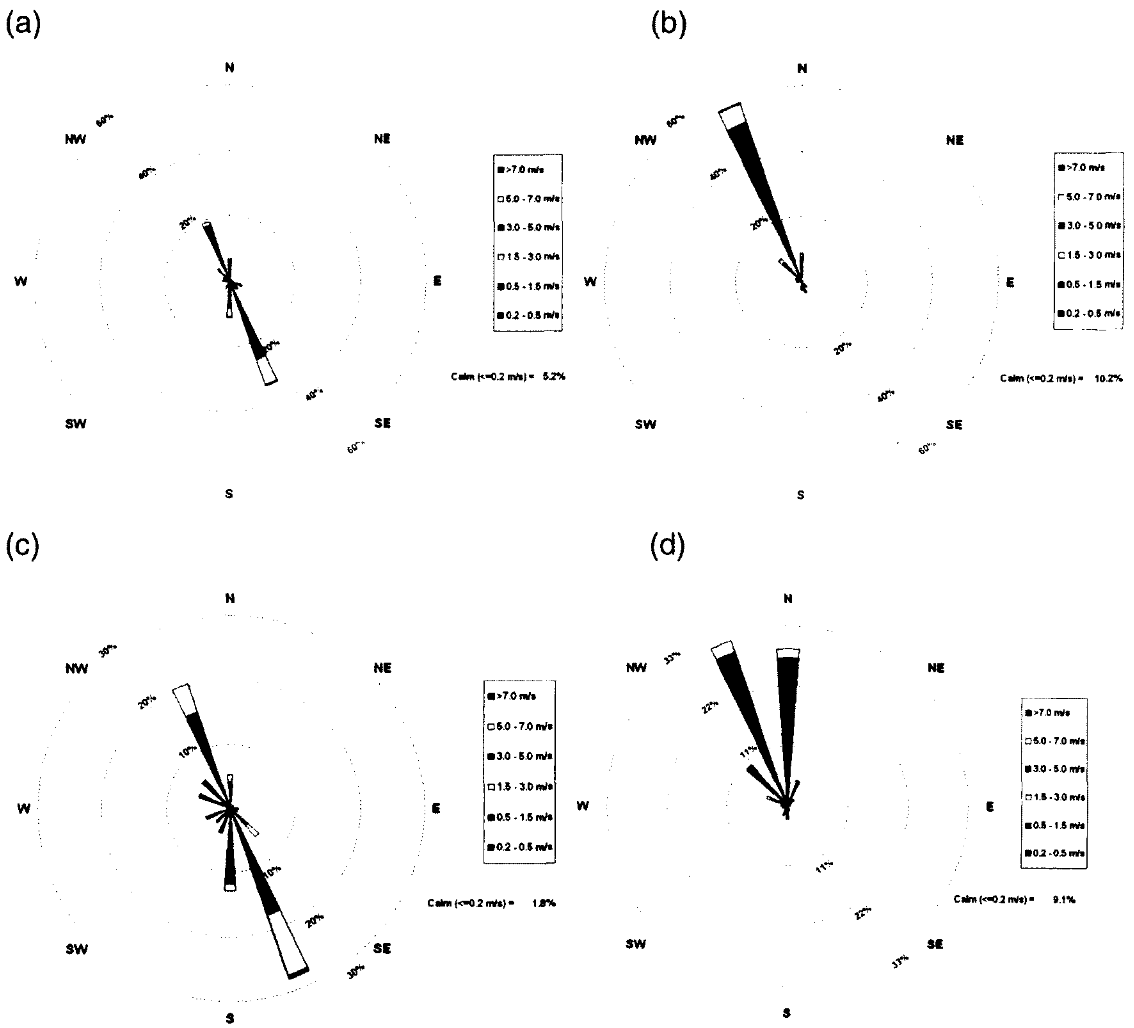

Figure 5-9 **Predicted wind rose at the extracted point for (a) episode 1, and (b) episode 2, (c) TOWN station Episode 1 and (d) GOLF station Episode 2.**

During both episodes, the extracted point has predicted temperatures that are consistent with the observed values at the three surface stations (Figure 5-10).

(a) (b)

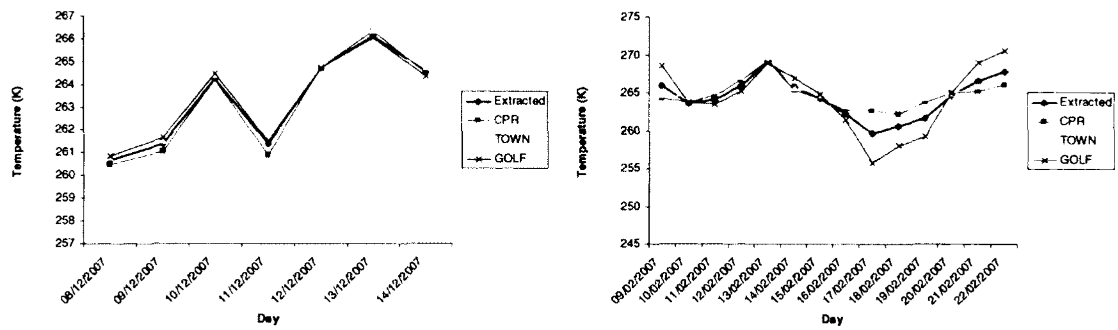

Figure 5-10 **24-hour mean temperatures for the three surface stations and the extracted point for (a) Episode 1, (b) Episode 2.**

CALMET uses the Turner method to calculate Pasquil Gifford stability classes. The CALMET stability classes are defined in Table 5-14.

Table 5-14 **Pasquil Gifford Stability Classes**

Stability Class	Atmospheric Conditions
A	Very Unstable
B	Unstable
C	Slightly Unstable
D	Neutral
E	Slightly Stable
F	Stable

Figure 5-11 shows the frequency distribution of the predicted stability classes at each station and the extracted point. The extracted point and the three stations predict nearly the same frequency of each stability class during both episodes.

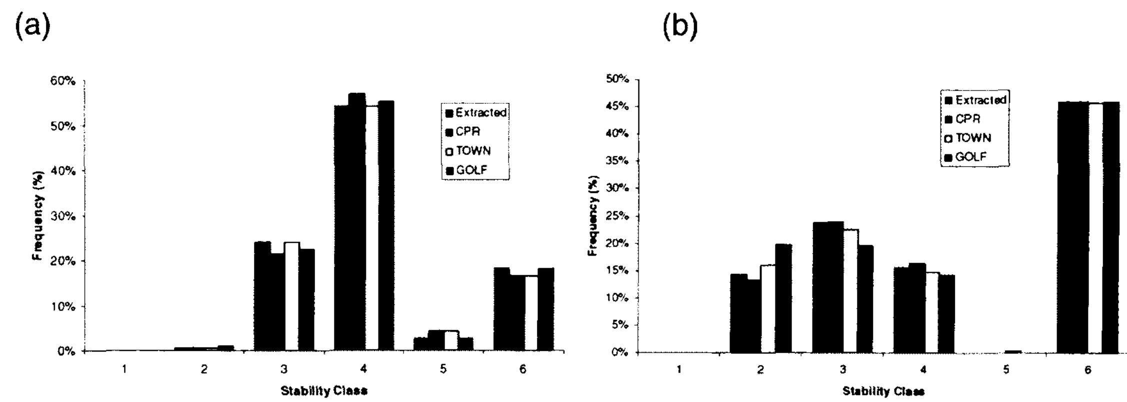

Figure 5-11 **Frequency distribution of predicted stability class at the three surface stations and extracted point for (a) Episode 1, (b) Episode 2. Stability Class 1 = very unstable; Stability Class 2 = unstable; Stability Class 3 = slightly unstable; Stability Class 4 = neutral; Stability Class 5 = slightly stable; Stability Class 6 = stable**

5.3 CALMET DISCUSSION

CALMET was able to reproduce the observed surface station input data very accurately during the full CALMET run. This evaluation was simply a check to make sure the input data were being reasonably maintained by the model following the interpolation scheme. Surface observations are used in CALMET as an initial guess field. The initial guess field is adjusted for kinematic effects of terrain, slope flows and three dimensional divergence minimization to produce a Step 1 wind field (Scire et al. 2000). The second step in the CALMET procedure re-introduces observational data through an inverse-distance squared interpolation scheme which weighs observational data heavily in the vicinity of the observational station and the Step 1 wind field more heavily away from the surface stations. The resulting wind field is then subject to smoothing and divergence minimization to produce the final wind field (Scire et al. 2000)

The evaluation here compares well with a test of CALMET by Cox et al. (2005) and with tests of other diagnostic wind field models in complex terrain reported by Ratto et al. (1994) and Ross et al. (1988). The mean absolute errors for wind speeds in those tests ranged from approximately 0.2 – 0.4 m/s when using the full complement of surface station data. The mean absolute errors for both episodes in the "full" CALMET run are lower than these values, partly an artifact of low mean wind speed. Cox et al. (2005) reported absolute wind speed errors of less than 10% of the mean wind speed, values that are comparable to this study. Wind direction errors were less than 10 degrees 87% of the time (Cox et al. 2005), in comparison with an average of over 90% of predictions within 10 degrees in this study.

Cox et al. (2005) and Ross et al. (1988) provide a comparison to the leave one out method. In these studies a larger number of stations were used in a full run and a smaller number of input stations were used to evaluate diagnostic wind field model performance. Mean wind speed errors in these studies range from 0.4 to 1.4 m/s. CALMET shows mean errors of less than 0.1 m/s in Golden that is well within this range. The mean wind speed errors, which measures the difference between observations and predictions regardless of whether it is positive or negative, indicates a slight over-prediction of the observed values at the surface stations. Cox et al. (2005) reported a mean absolute wind speed error that accounts for approximately 32% of the mean observed wind speed. In Golden, the CALMET mean absolute wind speed error represents 41% of the mean wind speed during episode 1 and 77% of the mean wind speed in episode 2. As mentioned previously, diagnostic wind field models can have difficulty predicting low wind speeds that can be attributed to the model interpolation techniques and the threshold of the anemometer used to measure wind speed (i.e. wind speeds less than 0.5 m/s are recorded as zero are compared to predicted wind speeds that are above 0.5 m/s, thus adding 0.5 m/s to the absolute error, which at low wind speeds accounts for a greater percentage of the mean wind speed).

Predicted wind direction is reported as within 20 degrees of observed values 42% of the time by Cox et al. (2005). In Golden, Episode 1 shows 40% percent of predicted winds within 20 degrees, while Episode 2 shows only 24%. CALMET's prediction of wind direction is not as good in Golden compared with the complex terrain modelling exercise by Cox et al. (2005) during episode 2.

Previous studies by Cox et al. (1998, 2000, and 2005) showed that diagnostic wind models typically predict both wind speed and direction more accurately during non-stable atmospheric conditions. This was not the case in Golden. In comparison to the periods modeled by Cox, the entire episodes modeled here would be considered to have very low wind speeds. Perhaps because winds are relatively light throughout the episodes, there is no real difference in the model accuracy depending on stability. Examination of the stability classes shows that indeed there is never a "very unstable" atmosphere reached during Episode 1. Almost 76% of the time winds are being predicted under neutral or stable conditions during the episode 1 and 62% during Episode 2 which could explain the model's poorer performance. Therefore, it is more appropriate to compare the results in Golden with those during stable periods in Cox et al. (2005).

Cox et al. (2005) reported wind speed mean absolute errors of 1.8 m/s or 45% of the observed wind speed during stable conditions. This is more comparable to the mean absolute errors reported for episode 1. Cox et (2005) also saw a wind direction mean absolute error of 39 degrees during stable periods, which is comparable to the errors reported in Episode 1. Even in comparison with the times of stability, Episode 2 does not compare well with the Cox study.

The CPR and TOWN stations do not perform as well in the "leave one-out method" because they are influenced by each other's observed wind data used in determining the final wind fields in CALMET. They are also influenced by the observed data at the AIRPORT station. As mentioned before, R1 was maximized between the CPR and TOWN station so that each stations radius of influence is nearly overlapping. (The AIRPORT station could not be tested in the leave one out method because it was the only station with observed measurements for RH, pressure, cloud cover, ceiling height and precipitation categories.) The GOLF station, which is further away from the radius of influence of the TOWN, CPR and AIRPORT stations, performs better in the leave one-out method. It appears that CALMET is performing well at the GOLF station, despite its location nearer to the mountainside which would be considered more complex terrain given the influence of the slope flows at this location.

R1 was chosen as 1.3 km because CALPUFF predictions (Chapter 6) improve with higher values of R1. Higher R1 maintains the along-valley flow around Golden because it increases the influence of CPR and TOWN measurements and decreases the influence of the model computed terrain effects and slope flows.

However, this results in the CPR and TOWN stations performing poorly in the leave one out method. There appears to be a trade-off between improving statistically the performance of stations in the CALMET evaluation and improving predicted PM concentrations in CALPUFF. The performance of CALMET is hampered by defining R1 universally for all stations in CALMET. The option to specify R and Rmax values on a station by station basis could possibly improve the wind fields.

With large values for R1 and Rmax the modeled winds, especially those near the Town of Golden are being influenced mainly by the surface station data and therefore winds in and surrounding Golden typically follow the valley alignment as expected (Figure 5-2). The exception is wind channelled through the Kicking Horse pass to the east of Golden.

When CALPUFF was run the CALMET wind fields were calculated using data from all stations. When using all stations in the CALMET run, it is obvious that the winds will be accurate in the grid cell containing the station as we saw in the statistics from "full" CALMET runs. However, what is not clear is how accurate the winds are in other grid cells. Thus, the extracted point comparison and leave one out analysis were performed. It is assumed that the winds do not change much between the extracted point and the input stations. This assumption is based on observed values at all stations that typically show flows are along valley from the northeast or southwest. When compared to the input stations, Figures 5-6 – 5-10 reveal that CALMET is predicting wind speed and direction, temperature, and stability class nearly as well at the extracted point as it does nearer to the input stations. This is also confirmed by a visual assessment of wind vectors in Figures 5-3 – 5-5.

It was hypothesized that the late afternoon and evening high PM concentrations occurring during the episodes may be caused by an along-valley wind flow slowing and reversing. It was suggested that this transition, along with downslope flows and increased emissions, could lead to the build-up of PM during this time of day. CALMET does capture along-valley flow slowing and a slight reversal at times of high PM concentrations. During the day, winds are typically from the south. In the evening, the winds slow and, in some cases, show a reversal and come from the north. This is consistent with winter daytime and night-time wind rose for Golden (Burkholder 2005). The variation in wind direction is best captured by observing the CALPUFF plumes shown in Chapter 6. The diurnal variation can also be observed in the modeled wind speeds (Figure 5-7).

Although the performance of CALMET was poorer than other comparable studies using the leave one out method, visually the surface wind fields look to be as expected when viewed as hourly vectors as in Figure 5-3. In addition the extracted point shows reasonable agreement with observed and predicted values during the "full" CALMET run. CALMET also seems to be capturing some of the important valley wind flows (i.e. slope flows and along-valley flows) that have been hypothesized to lead to increased PM concentrations. Even though these model options and parameters produce poor results during the leave one out method, it is the best performance of the model for the Golden modeling study using the data provided. The model's ability to predict final PM concentrations using the predicted CALMET wind fields will now be tested.

6 CALPUFF

PM concentrations in Golden consistently rank among the highest annual averages in the province for both $PM_{2.5}$ and PM_{10} (Figure 2-1). Episodes of high PM occur more frequently during the winter and early spring (Figure 2-2). Following CALMET optimization, the CALPUFF dispersion model was used to investigate ambient air quality during two particulate matter episodes in the winter of 2005-2006 (Section 4-1). Similar studies have been conducted in many locations, including New Zealand (Barna and Gimson 2004), Beijing (Song et al. 2006) and Athens (Assimakopoulos 2005).

Emission sources were modeled individually and CALPUFF's performance in estimating PM concentrations was evaluated. The model was then used to apportion sources contributing to the episodes (Chapter 7). The source apportionment was compared to receptor modeling completed by the BC MOE in Golden. Emission rates were determined based on the Golden Emissions Inventory (Abel et al. 2006) and adjustments were made using the results of receptor modeling conducted by BCMOE (Evans and Jeong 2007).

Winter episodes of high PM in Golden were hypothesized to occur because of increases in emissions due to combustion sources as well as stagnant dispersal conditions. During episode 1, the PM ratio increases significantly in comparison to the winter mean PM ratio (Table 4-1). An increase in PM ratio indicates a rise in the $PM_{2.5}$ portion of PM_{10}, indicating more contribution from combustion sources. Wood-smoke from space heating in Golden is a significant source of PM during the winter months. As residents do not have access to natural gas, many people burn wood to heat their homes. Incomplete combustion from burning wood in a fireplace or woodstove results in $PM_{2.5}$ emissions. Other combustion sources in Golden include, but are not limited to, emissions from boilers at Louisiana Pacific, agricultural burning, back yard burning, and emissions from prescribed burns in the forests surrounding the Town.

Episodes during the early spring may be attributed to increased releases of road dust and crustal materials due to the spring thaw. As the temperature increases and roads dry out, road traction material that has built up over the winter is made airborne by vehicles on the highways and streets in and around Golden. Wind blown fugitive dust sources will also increase as temperatures rise and snow melts from the surface. During episode 2, the PM ratio decreases significantly in comparison to the winter mean and episode 1 PM ratio (Table 4-2). A decrease in the PM ratio indicates a rise in particles greater than 2.5 microns. These particles are largely comprised of crustal material emissions.

The steep valley walls and weak terrain forced local wind flows means dispersion may largely depend on the diurnal mountain wind system (Section 2-4) As previously discussed, low wind speeds, shallow mixing layers, neutral or stable atmospheric conditions and recirculation in this system may result in the build-up of pollutants near the bottom of the Columbia river valley. CALMET captures some aspects of the diurnal mountain wind system and the available emissions information was used in CALPUFF in an attempt to create the best possible model for use in airshed management decisions.

This chapter explains the model setup, an example of CALPUFF output during episode 1, and an evaluation of the model's performance.

6.1 CALPUFF Setup

CALPUFF is a puff dispersion model capable of handling multiple-layers within the atmosphere and multiple pollutant species (Scire et al. 2000). The non-steady state nature of the model allows it to handle time and space varying meteorological and emission conditions.

CALPUFF uses CALMET's final wind field to disperse point, line and area emission sources within the gridded modeling domain. The puff model represents a continuous emission source, such as a plume, as a number of discrete packets of pollutant material. The puffs are released and evolve in size according to Gaussian-like diffusion and dispersion, but the multiple puffs allow changes in meteorological and emission conditions to be captured. The meteorological processes were determined by modeling in CALMET (Chapter 5). CALPUFF depends largely on the emission estimates and dispersion options selected by the modeler. The following sections describe emission source characterization and the model options selected for this study.

6.2 Receptors

The modeling domain contained a 35 by 40 km grid of receptors spaced 250 m apart. Discrete receptors were located at the PM monitoring locations in Golden (Figure 2-3) to allow for comparison between model estimations and observed ambient PM concentrations. Each receptor point represents a location at which model estimated PM concentrations are calculated.

6.3 CALPUFF Model Options

CALPUFF model options used in this study are provided in Table 6-1. Model options follow the USEPA default recommendation unless otherwise stated. Model options were chosen based on recommendations from the BC Dispersion Modeling Guidelines (BC MOE 2008).

Table 6-1 CALPUFF model options selected

Parameter	Option Selected	USEPA Default
Terrain Adjustment Method	Partial Plume Path Penetration	Yes
Transitional Plume Rise	Modeled	Yes
Stack Tip Downwash	Modeled	Yes
Vertical Wind Shear above Stack Top	Not Modeled	Yes
Chemical Mechanism	Not Modeled	No
Wet Removal	Not Modeled	No
Dry Deposition	Modeled	Yes
Method Used to Compute Dispersion Coefficients	internally calculated using micrometeorological variables	No
Partial Plume Penetration of Elevated Inversion	Modeled	Yes
Minimum Wind Speed Allowed for Non-Calm Conditions	0.5 m/s	Yes

Chemical transformation was not calculated using MESOPUFF II, the chemical transformation module included with CALPUFF, because during the winter months secondary particulates would not be a significant source in Golden. The wet removal option was not used because the appropriate precipitation information was not available. The wet removal of PM during the episodes was likely negligible during the episodes modeled as precipitation occurred very infrequently during both episodes. Computation of the dispersion coefficients was performed internally by CALPUFF as recommended in the British Columbia Air Dispersion Modeling Guidelines (BC MOE 2008)

6.4 Estimating Emission Data

Estimation of PM emission rates, along with source characteristics such as emission velocity, temperature and height, combined with the meteorology are essential to air dispersion modeling. Emissions from point, area, volume and line sources are reported in airshed emission inventories. An emissions inventory (EI) for Golden provided the basis for the emissions input into CALPUFF (Abel et al. 2006). It was not the focus of this study to reiterate the methods used to develop that inventory. The EI contained estimates of annual emissions from all known significant sources in the modeling domain. Unfortunately, the EI did not provide spatial information beyond the point source estimations and small area sources such as mill and rail yards. Most area and line sources are simply an estimate based on a provincial emission inventory database, Air Contaminant Emissions (ACE) Project (MWLAP 2001). This GIS database allows for extraction of local airshed emission estimates based on a variety of factors such as landuse, area and population density. Details on this database can be found in Glen and Wakelin (1998), Gibson (1998), and Fam (1998). Inherent uncertainties in the EI are discussed by Abel et al. (2006).

From the EI, PM emissions data were compiled for point, line and area sources in the Golden Airshed. Point sources include those that can be attributed to a single, fixed emission point such as a smokestack. Line sources, such as railway or vehicle traffic, emit along a fixed line. Area sources include groups of point sources that cannot be assessed on an individual basis, such as backyard burning and residential space heating. For most of the modeled sources, the EI contained the best available emissions data. Updated emissions information gathered is described below. It was not the intention of this study to build an entirely new EI, but rather attempt to model using the emission estimates in the completed EI.

It was necessary to transform the estimates from the EI into specific emission rates and identify or estimate the key source characteristics. An emission inventory catalogs the total emission from each source for the entire airshed. Point source locations are easily identified and source characteristics are measurable making model input straightforward. However, in the EI area sources are not given spatial boundaries and source characteristics need to be estimated. With a lack of information on area source characteristics and spatial bounds it becomes necessary to estimate polygon areas that would be emitting the PM identified in the EI. As the EI was not temporally resolved, annual emission estimates for each source from the EI were applied as emission rates using the specific methods outlined below.

6.4.1 Point Sources

Point sources are emission sources that are released from a stack or specific point. Emissions from point sources are modeled as puffs of pollutant released from a stack at a specified height, speed and temperature. The emission rate determines the rate at which the puffs are released. CALPUFF requires detailed source characteristics such as the location of the emitting stack, the base elevation, stack height, stack diameter, and the exit velocity/temperature of the discharge containing PM. The only point sources modeled in Golden were from the operations at Lousiana Pacific Engineered Wood Products Ltd (LP) (Figure 3-2).

6.4.1a Louisiana Pacific Engineered Wood Products Ltd.

Site Description

LP is located immediately north of the downtown core of Golden. The UTM locations of the point sources as well as building locations and dimensions were provided by LP's environmental engineer, Mike Brygger. Sixteen separate point sources were identified as emitting from the LP site north of the town centre in Golden. These include a hog boiler, cyclones, plywood dryer emissions and plywood press emissions. Stack information was compiled for each source including the location of the emitting stack, the base elevation, stack height, stack diameter, exit velocity of the discharge containing PM and exit temperature (Table 6-2).

The option for CALPUFF to calculate the effects of building downwash at LP was selected. Since buildings and structures can affect the dispersion of plumes due to wake effects, the objects within close proximity to the stacks at LP were incorporated into the modelling. Any buildings and structures with the potential to cause downwash effects were selected based on the criteria in the US EPA Building Profile Input Program (BPIP). Building dimensions and locations were provided by LP (Figure 6-1). This information was processed using BPIP to produce the necessary array of 36 direction-specific building widths and heights for flow vectors from 10 degrees to 360 degrees in 10 degree increments. CALPUFF uses this estimate of building dimensions to model the building downwash effects from each stack emitting at the LP site depending on the wind direction at the time of the emitted puffs.

Emission Rates

Emission rates were also provided by LP and were estimated using published emission factors and production totals as an estimate of operations during each episode. The emission rates for PM_{10} and $PM_{2.5}$ specified for Episode 1 and 2 are listed in Table 6-2. LP operations typically run 24 hours a day therefore, emissions were assumed constant for each episode and the option to vary emissions in CALPUFF was not used.

Figure 6-1 Aerial photo showing source (SRC) locations and building (BLD) dimensions at Louisiana Engineered Wood Products Ltd. Site in Golden BC.

Table 6-2 Summary table of LP point emissions. E1 = episode 1, E2 = episode 2, ER = emission rate

Source	Stack Height (m)	Stack Temp (K)	Stack Exit Velocity (m/s)	Stack Diameter (m)	Emission Rates (g/s) E1 PM_{10}	Emission Rates (g/s) E1 $PM_{2.5}$	Emission Rates (g/s) E2 PM_{10}	Emission Rates (g/s) E2 $PM_{2.5}$
Hog Boiler (SRC1)	21.34	446.15	11.90	1.63	1.76E-01	1.15E-01	1.82E-01	1.19E-01
Plywood Waste Cyclone (SRC2)	15.54	293.15	5.10	1.83	4.58E-01	2.29E-01	4.04E-01	2.02E-01
Chipper Fines Cyclone (SRC3)	14.33	283.15	5.10	1.22	1.61E-01	8.06E-02	1.61E-01	8.06E-02
Powerhouse Dust Cyclone (SRC4)	9.75	278.15	6.10	0.76	7.56E-02	3.76E-02	7.56E-02	3.76E-02
LVL Baghouse (SRC5)	3.05	293.15	39.70	0.76	8.19E-01	0.00E+00	8.19E-01	0.00E+00
Sanderdust Baghouse (SRC6)	2.44	293.15	35.94	0.91	1.08E+00	0.00E+00	1.08E+00	0.00E+00
Dryer 3 Cooling (SRC7)	9.75	306.85	21.75	0.37	8.04E-02	2.63E-02	8.04E-02	5.01E-02
Dryer 3 Heating (SRC8)	9.75	438.15	16.50	0.17	1.53E-01	5.01E-02	1.53E-01	2.63E-02
Plywood Trim Cycline (SRC9)	15.85	293.15	6.09	0.91	1.07E-01	5.38E-02	1.07E-01	5.38E-02
Dryer 4 Bypass North (SRC10)	13.41	369.65	13.58	0.81	9.83E-02	3.22E-02	9.83E-02	3.22E-02
Dryer 4 Bypass Mid (SRC10)	13.41	448.65	3.10	0.81	9.83E-02	3.22E-02	9.83E-02	3.22E-02
Dryer 4 Bypass South	13.41	448.65	10.04	0.81	2.01E-01	6.60E-02	2.01E-01	6.60E-02

(SRC10)								
Dryer 4 Cooling (SRC13)	12.8	306.85	0.19	1.25	8.06E-03	2.64E-03	8.06E-03	2.64E-03
Dryer 4 Cooling (SRC14)	12.8	306.85	0.19	1.25	8.06E-03	2.64E-03	8.06E-03	2.64E-03
Plywood Press Vent (SRC15)	9.75	298.15	0.27	3.05	1.13E-02	0.00E+00	1.13E-02	0.00E+00
LVL Press Vent (SRC16)	6.1	298.15	8.14	2.44	4.54E-02	0.00E+00	4.91E-02	0.00E+00

6.4.2 Line Sources

Line sources are those sources that emit along a fixed line. Emissions are modeled as puffs of pollutant released at equally distributed points along the line segment. Traffic emissions from Highway 95 and the Transcanada Highway, as well as railway locomotive emissions were mapped as line sources for CALPUFF modeling. The highway segments followed closely Highway 1 and Highway 95 indicated in Figure 4.2. The railway segments run alongside the highways.

6.4.2a Highway Traffic Emissions

Highway 95 and the Transcanada Highway were mapped as line sources from the BCMOE's air emissions map (accessed electronically at: http://srmapps.gov.bc.ca/apps/aei/). The emissions from the emissions inventory are derived from the US EPA model MOBILE6. Motor vehicle emissions in MOBILE6 are estimated as the product of the number of vehicle kilometers traveled (VkmT) in the airshed distributed into vehicle categories and a corresponding categorical emission factor determined by the model. Highway VkmTs were estimated from National Parks traffic data near Golden. The annual emissions from highway vehicle sources from the emissions inventory were apportioned to each line segment based upon the length of the road. Each highway line source segment (following paths of Highway 95 and Highway 1 in Figure 5-1) was assigned an emission rate in metric tons per year (Table 6-3). The emission rates were adjusted diurnally in the same manner as local traffic and road dust. (Section 6.3.3b) Local roads were not considered as line sources as they are generally confined to the residential/commercial areas of the Town of Golden. It was determined that given the emissions information available local traffic emissions would be modelled as an area source.

Table 6-3 **Summary of highway segment emissions. The curved road path was closely followed using multiple straight line segments. Note: the southern most segment starts at the southern most point of Highway 95 in the modeling domain and the northern most point ends at the Town of Golden where it intersects with Highway 1. The eastern most point of Highway 1 starts at the eastern edge of the domain and the western most point ends at the western edge of the domain.**

Road (Segments)		**Yearly Emissions (tons)**	
Highway 95	**Distance (m)**	**PM_{10}**	**$PM_{2.5}$**
1 (Southern Most)	1416	0.28	0.24
2	1192	0.24	0.20
3	3479	0.70	0.59
4	1064	0.21	0.18
5	2330	0.47	0.39
6	1926	0.39	0.33
7	2432	0.49	0.41
8	1797	0.36	0.30
9	705	0.14	0.12
10	835	0.17	0.14
11 (Northern Most)	1097	0.22	0.19
Highway 1			
12 (Eastern Most)	1959	0.39	0.33
13	2791	0.56	0.47
14	608	0.12	0.10
15	452	0.09	0.08
16	513	0.10	0.09
17	450	0.09	0.08
18	770	0.16	0.13
19	627	0.13	0.11
20	2239	0.45	0.38
21	1390	0.28	0.23
22	2636	0.53	0.45
23	2224	0.45	0.38
24	1537	0.31	0.26
25	1468	0.30	0.25
26	1052	0.21	0.18
27	384	0.08	0.06
28	302	0.06	0.05
29	899	0.18	0.15
30	1090	0.22	0.18
31	1423	0.29	0.24
32	5174	1.04	0.87
33	514	0.10	0.09
34	2102	0.42	0.36
35	4094	0.82	0.69
36	7459	1.50	1.26
37	2447	0.49	0.41
38	1295	0.26	0.22
39 (Western Most)	2546	0.51	0.43

6.4.2b Railway Locomotive Emissions

Railway lines in the modeling domain were mapped as line sources from BC MOE's air emissions map. The annual emissions from railway locomotive sources were apportioned to each line segment based upon the length of the track, assigning each rail line source segment an emissions rate in metric tons per year (Table 6-4). Emissions from the rail switching yard in Golden were estimated as an area source (Section 6.4.3f)

Table 6-4 **Summary of rail line emissions. The curved railway path was followed as closely as possible using multiple straight-line segments. The southern, northern, eastern and western most points refer to the point where the railway meets the respective edge of the modeling domain.**

		Yearly Emissions (tons)	
Railway (Segments)	Distance (m)	PM_{10}	$PM_{2.5}$
1 (Southern Most)	1620	0.23	0.21
2	8448	1.18	1.08
3	1229	0.17	0.16
4	2110	0.29	0.27
5	712	0.10	0.09
6	924	0.13	0.12
7	1195	0.17	0.15
8	621	0.09	0.08
9	1328	0.19	0.17
10	1315	0.18	0.17
11	1907	0.27	0.24
12	2816	0.39	0.36
13	944	0.13	0.12
14	3582	0.50	0.46
15	2935	0.41	0.38
16	495	0.07	0.06
17	1613	0.23	0.21
18	4397	0.61	0.56
19	2977	0.42	0.38
20	497	0.07	0.06
21	5690	0.80	0.73
22	2089	0.29	0.27
23 (Northern Most)	1165	0.16	0.15
24 (Eastern Most)	3063	0.43	0.39
25	3956	0.55	0.51
26	1053	0.15	0.13
27	2042	0.29	0.26
28	3901	0.55	0.50
29	3589	0.50	0.46
30	1104	0.15	0.14
31	1536	0.21	0.20
32 (Western Most)	2973	0.42	0.38

6.4.3 Area Sources

Area sources emit from an area rather than a distinct point or line. Generally, they are a compilation of point sources too numerous to characterize individually. In CALPUFF, area sources are represented by puffs released from multiple, equidistant points within a defined polygon area. Each area is assigned an emission rate.

From a local landuse map provided by the Town of Golden areas of the town were appropriately chosen that represented the populated areas of the Town that would emit each area source. The Town was divided into four polygons of the major populated areas: South Town; North Town; Kicking Horse; Transcanada. These areas were assigned emission rates for each of the area sources described below (Figure 6-2, Table 6-5).

Modeling during short episodes requires that diurnal variations in emission rates be characterized to achieve an accurate picture of the emission scheme. Initial modeling of area sources without diurnal variation resulted in area source estimates that far exceeded observed PM levels. It is difficult, however, to estimate the diurnal variation of PM. Certainly, PM_{10} and $PM_{2.5}$ ambient levels have distinct patterns corresponding to the time of the day (Figure 4-1 and 4-2). It is difficult to characterize whether meteorology or changes in emissions cause the consistent rise and fall of PM levels. Emission from vehicles rise during the times immediately before and after the "workday" and space heating emissions would also be higher in the morning and evenings when residents are more likely to be at home. Conversely, wind speeds and mixing heights are generally higher during the day and this may account for the drop in PM concentrations during the day. Likely, it is a mix of the two, emission changes and changes in meteorology, which leads to the distinct diurnal pattern seen in Golden. With CALPUFF it is possible to model diurnal variation in emission rates and the methods below describe the scaling factors used for the appropriate area sources.

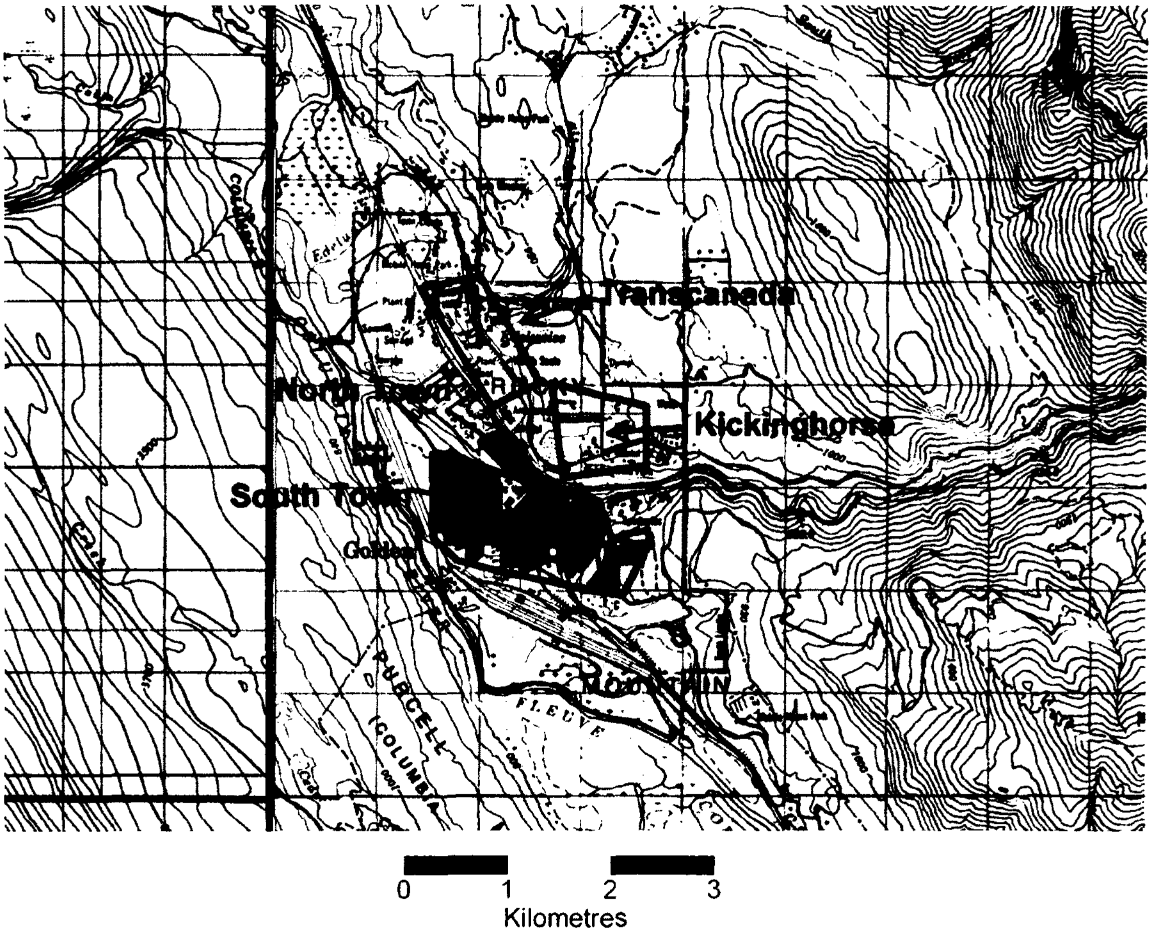

Figure 6-2 Location of four areas defined for area source emissions in CALPUFF.

Table 6-5 Area source emission rates for Episodes 1 and 2. All areas were assumed to emit at the same rate.

	Emission Rates (tons/m^2/year)			
Source	**E1 PM10**	**E1 PM2.5**	**E2 PM10**	**E2 PM2.5**
SPCHT	9.74E-06	9.74E-06	2.25E-06	2.25E-06
LTRFC	1.26E-06	9.93E-07	1.26E-06	9.93E-07
CONS	2.55E-06	1.31E-06	2.55E-06	1.31E-06
BURN	1.00E-06	9.10E-07	1.00E-06	9.10E-07
RDUST	4.90E-06	1.04E-06	3.92E-06	8.32E-07

Note: SPCHT = Space Heating, LTRFC = Local Traffic, CONS = Construction, BURN =Burning, RDUST = Road Dust

6.4.3a Space heating emissions (SPCHT)

Space heating emissions encompass PM emitted from appliances used to heat homes and businesses. This includes emissions from appliances burning all types of fuels. Most space heating PM emissions in Golden come from wood-burning appliances. Space heating emission rates were originally estimated using the data provided in the EI. The EI estimates were determined through a woodstove survey conducted by BC MOE (2004). Initial model runs showed the emission rate estimates to be much too high. Rates were adjusted based upon receptor modeling conducted in Golden (see Section 6-3 for details on rate adjustments). Final space heating emission rates are provided in Table 6-5.

Space heating has a distinct diurnal pattern. Typically, homes are heated in the mornings and evenings when residents are more likely to be at home. During the province-wide woodstove survey, residents were asked when they add wood to their woodstoves. Figure 6-4 displays the data specific to Golden.

Since space heating PM emissions in Golden are almost solely based on woodstove emissions, rates were diurnally adjusted according to the results of the survey question (Table 6-6).

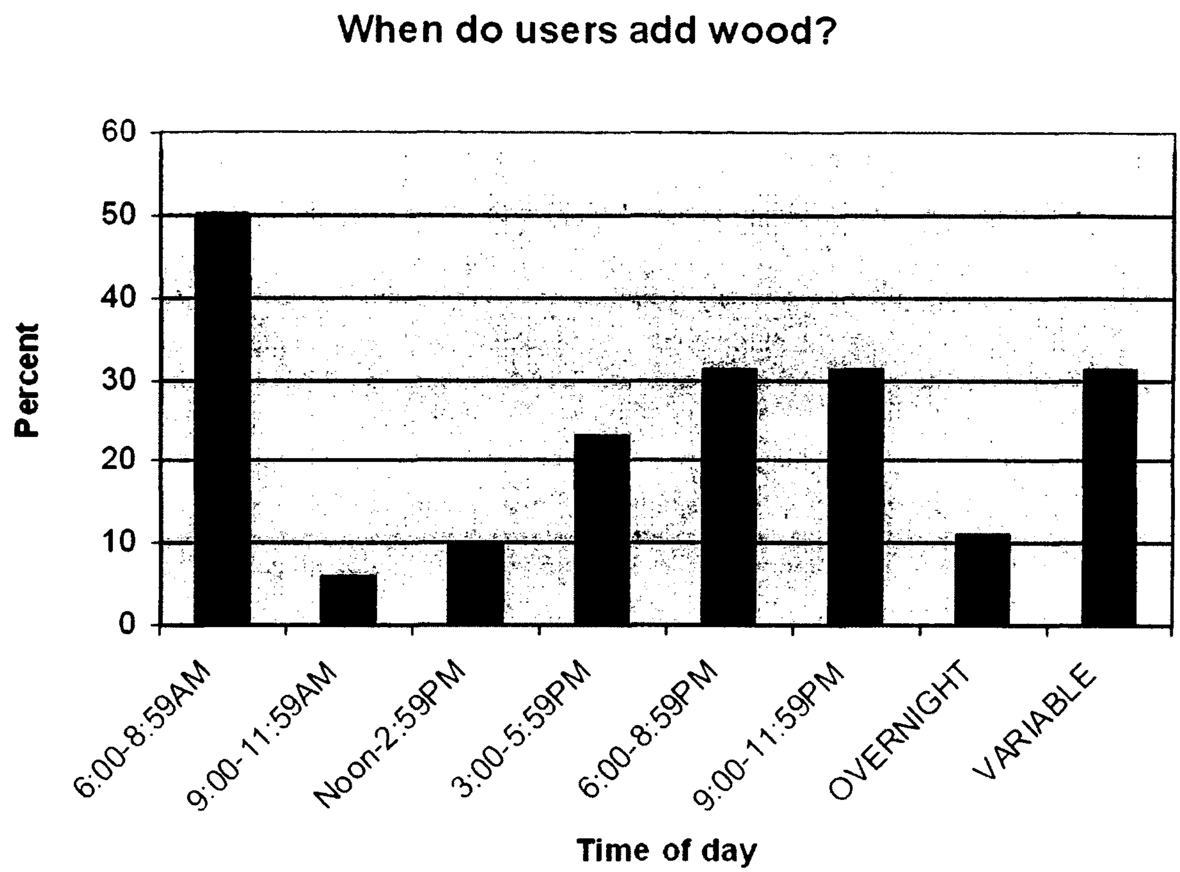

Figure 6-3 **Summary of Golden resident's answers to the question "when do you add wood?" to their woodstoves asked in the BCMOE woodstove survey (BCMOE 2004).**

Table 6-6 Diurnal variation of space heating emissions by hour of day.

Hour of the Day	Diurnal Scaling Factor
0	0.536
1	0.536
2	0.536
3	0.536
4	0.536
5	0.536
6	2.238
7	2.238
8	2.238
9	0.318
10	0.318
11	0.318
12	0.493
13	0.493
14	0.493
15	1.060
16	1.060
17	1.060
18	1.409
19	1.409
20	1.409
21	1.409
22	1.409
23	1.409

6.4.3b Road dust emissions (RDUST)

The EI estimated road dust as a major source of PM. Road dust results from the grinding of granular material deposited on road surfaces, usually from road traction material, road construction activities and material trackout from gravel side roads. It is made airborne by passing vehicles and wind.

As mentioned in the EI, accurate estimates of road dust emissions in inventories are quite difficult to achieve and have a high potential to be erroneous. It was determined that differences in road characteristics and the absence of local silt-testing of dirt, dust and other debris on local highways and roads would severely limit the accuracy of modeling road dust emissions as line sources. Instead, road dust emissions were modelled as a source emitting from the local polygon area sources defined above (Figure 6-2). Road dust emissions are not constant and will generally be suppressed by rainfall and even further limited by snow and ice on roadways. However, since the proper precipitation input information for CALPUFF was not available and precipitation occurred briefly on only 3 days during the episodes, wet removal was not modeled.

A SENES consultant study (SENES 2000) stated that fugitive dust sources would likely not travel large distances from the roadway under most atmospheric conditions. Therefore road dust emissions from highway sources outside Golden were not captured in the EI emission estimates and were subsequently not modeled during this study.

Road dust emission rates (Table 6-5) were varied by diurnal scaling factors (Table 6-7). Since there were no traffic data available from Golden, data from a Prince George air quality project (personal comm. John Spagnol) was used as an estimate. Prince George is a community in the interior of BC that is largely supported by the wood products industry and work traffic likely follows the shift work used in this industry. Golden and Prince George also have a large, busy highway running through their respective communities. Although the populations are different it was assumed for modeling purposes that the diurnal traffic patterns in Golden were similar to those quantified for Prince George.

Table 6-7 Diurnal variation of road dust emissions by hour of day.

Hour of the Day	Diurnal Scaling Factor
0	0.22
1	0.17
2	0.14
3	0.17
4	0.29
5	0.55
6	0.86
7	1.06
8	1.27
9	1.27
10	1.42
11	1.61
12	1.68
13	1.73
14	1.80
15	1.92
16	1.85
17	1.58
18	1.20
19	0.98
20	0.79
21	0.62
22	0.48
23	0.34

6.4.3c Local traffic emissions (LTRFC)

Local traffic emissions are from local vehicles of all sizes traveling within the Town of Golden. The EI separated the local traffic emissions from the highway traffic emissions. Emission estimates in the EI were determined by using the US EPA MOBILE 6 program for mobile source emissions. In CALPUFF, local traffic emissions were modeled as an area source in the populated areas of Golden rather than multiple line sources mapping the entire town road system. Specific information on traffic counts, speed and vehicle types would be necessary to provide more detailed modeling of local traffic emissions on a specific street-by-street basis. The area source emission rates based on the estimates provided in the emissions inventory for local traffic are described in Table 6-5. The emission rates from the emissions inventory are derived from the US EPA model MOBILE6 in the same manner as described for highway line emissions (Section 6.3.2a). Local traffic emissions were varied diurnally using the same emission rate scaling factors as the road dust emissions (Table 6-7).

6.4.3d Construction emissions

Emissions from construction operations in Golden are based on estimates in the emissions inventory related to residential building permits and commercial project valuation. Emission rates for this source were determined based on the annual PM emissions in the emission inventory (Table 6-5). Construction emissions were not modeled during the night-time, non-working hours (6 p.m – 6 a.m).

6.4.3e Burning emissions

Burning emissions include estimated emissions from backyard burning. A major concern of residents in Golden is the effect of prescribed burning operations in the Columbia River Valley. These operations are not included in the CALPUFF modeling because during the episodes the BC Ministry of Forests permitted no prescribed burns. Miscellaneous burning emission rates were determined from the emissions inventory (Table 6-5).

6.4.3f Railway yard emissions

In addition to the railway line emissions, the EI estimated yard emissions specific to the large CPR switching yard to the south of Golden. These emissions were modeled as an area source emitting from the area of the CPR switching yard. EI estimated emissions were apportioned equally based on the area (m^2) of the switching yard. It was assumed that each area of the switching yard emits at the same rate. The area dimensions and emission rates are described in Table 6-8.

Table 6-8 Summary of railway yard area and emission rates.

	Polygon Dimensions							
	Northwest		Southwest		Northeast		Southeast	
	X	Y	X	Y	X	Y	X	Y
Railway Yard	501.92	5681.98	503.47	5681.27	502.25	5682.04	503.27	5681.52
PM10 Emission Rate (tons/m^2/year)	9.25E-06							
PM2.5 Emission Rate (tons/m^2/year)	8.55E-06							

6.4.3g LP Yard Emissions

Yard emissions from LP result from the operation of heavy duty machinery and trucks. PM emissions from this source would largely be fugitive dust emissions. LP yard emission estimates were provided by the plant environmental manager, Mike Brygger. They were modeled as an area source emitting from the area covered by LP operations in Golden. The area dimensions and emission rates are described in Table 6-9.

Table 6-9 **Summary of LP yard area and emission rates. Split into north and south to define more accurate area source polygon.**

	Polygon Dimensions							
	Northwest		Southwest		Northeast		Southeast	
LP Yard	X	Y	X	Y	X	Y	X	Y
North	500.93	5685.26	500.77	5684.70	501.16	5685.32	501.34	5684.98
South	500.77	5684.67	501.18	5683.96	501.36	5684.95	501.70	5684.27

PM10 Emission Rate (tons/m^2/year)	9.40E-05
PM2.5 Emission Rate (tons/m2/year)	1.54E-05

6.5 Emission Rate Adjustments

Preliminary model runs indicated that the model was drastically over-predicting PM concentrations. However, the model was reasonable at predicting the timing of highs and lows in the observed PM concentrations. This suggested that meteorological parameters set by CALMET captured a reasonable dispersal pattern. Indeed, sensitivity tests of CALMET parameters yielded little improvement in the predicted concentrations. It was hypothesized that the emission rate estimates used in the original run, based upon the EI, were inaccurate. New estimates of emission rates were necessary to improve the model accuracy.

There are several reasons why the EI may not be accurate or adequate for modeling purposes. EI's are estimates of emissions usually derived from emissions factors and some measure of the source's emitting activity. In many cases the emission factors may not be applicable to the conditions in the area or there may not be an accurate way of measuring the source's activity. Therefore, emission inventories have inherent uncertainty based on the methods used to obtain estimates, which is further explained in the EI.

Other information was available to attempt to create more accurate emission rates for the model. Postive Matrix Factorization (PMF) analysis, a type of receptor modeling was performed on $PM_{2.5}$ samples collected during the period of November 11, 2005 through August 15, 2006 in Golden. The analysis was performed by the Southern Ontario Centre for Atmospheric Aerosol Research at the University of Toronto. Receptor modeling uses collected samples from a monitoring site to distinguish relative contributions of different emission sources. This method uses temporal variation in the speciation of $PM_{2.5}$, marker elements and meteorological data to identify specific emission sources (Evans and Jeong 2007).

The solution from the receptor modeling in Golden revealed seven factors contributing to PM. The factors identified were: Road Salt, Sulphate, Residential Wood Burning, Wood Processing, Crustal Material, Traffic and Residential Winter Heating. Additionally, the analysis provided a factor breakdown of the average $PM_{2.5}$ concentrations in each season (Figure 6-4).

The preliminary CALPUFF runs determined that two area sources, space heating and road dust were unreasonably high, severely inflating overall predicted PM concentrations. The receptor modeling provided much lower averages for the daily contributions from road dust and space heating. To achieve more accurate emission rates, the information in Figure 6-4 regarding daily contributions to the average $PM_{2.5}$ concentrations was used to reduce the original emission rates. It was assumed that the winter heating factor and the residential wood burning factor would represent the space heating emissions and that the road dust would be represented by the crustal factor as suggested by Evans and Jeong (2007). Predicted daily average concentrations were determined from the modeled TOWN receptor that represented the location used to collect the receptor modeling data. The original emission rates were then reduced based on the percent reduction between the predicted daily average concentrations from preliminary model runs and those determined from the receptor modeling. The receptor modeling data were taken from the episode specific days where data were collected for PMF analysis. Road dust emission rates were reduced by 91% and 93% for episode 1 and 2, respectively. Space heating emission rates were reduced by 65% and 92% for episode 1 and 2, respectively. These seemingly large reductions reflect the uncertainty and lack of seasonality in the EI estimates for these sources.

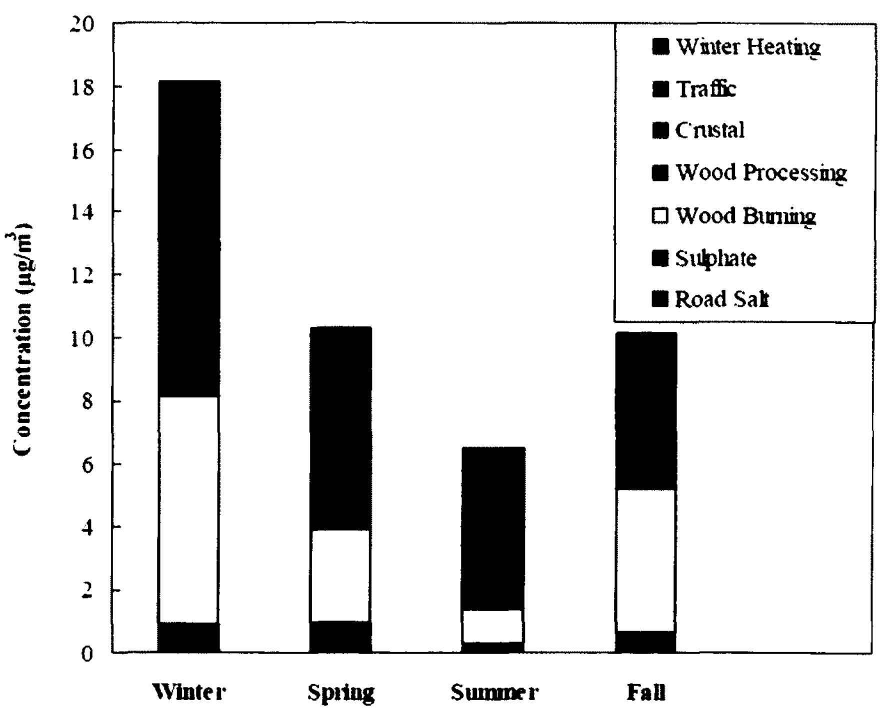

Figure 6-4 **Factor breakdown of PMF analysis for $PM_{2.5}$ in Golden (Evans and Jeong 2007).**

Table 6-10 shows that in general the results of CALPUFF with the two new emission rates were better than the results with the original emission rates derived from the EI, when compared to the receptor modeling.

Table 6-10 **Emission inventory (EI), receptor modeling and CALPUFF model predicted percentages (based on the adjusted EI emission rates) of total estimated PM in each case is provided for (a) episode 1, and (b) episode 2. Emission inventory results are from those at the TOWN station. LP is used as a comparison because the emission estimates were the most reliable and complete. CALPUFF results have been adjusted by comparison with the receptor modeling.**

(a)

Emission Source	EI	Receptor	CALPUFF
Space heating	45.1	75.0	62.5
Road dust	20.1	8.3	7.2
LP	9.6	2.8	1.5

(b)

Emission Source	EI	Receptor	CALPUFF
Space heating	45.1	48.0	35.9
Road dust	20.1	17.0	12.6
LP	9.6	19.0	3.3

6.6 Example of CALPUFF Evening Wind Flow and High PM event

Modeled meteorological conditions that typically lead to high PM concentrations in the evening are displayed in Figure 6-5. In addition to wind vectors and PM concentrations other modeled meteorological conditions are provided (Table 6-11) to show the major factors affecting dispersion in this CALPUFF model run. In the diagrams, Golden is located at the convergence of the valley to the east and the main river valley. The wind vectors are proportional in size to the wind speed. Note the increase in PM as the wind speed across the grid slows, the air stagnates and the flow reverses. The wind speed modeled at the TOWN station (Table 6-11 remains quite low, but it is evident that winds are slowing across the modeling domain. As the wind speed slows, the wind direction changes from southerly to northerly at the TOWN station (Table 6-11). During this time, the PM_{10} levels rise. Following the rise in PM, the mixing height remains low and the winds come from the north throughout the night maintaining the high PM concentrations until the morning.

(a)
Dec 10, 2005
18:00 LST(UTC-0700)

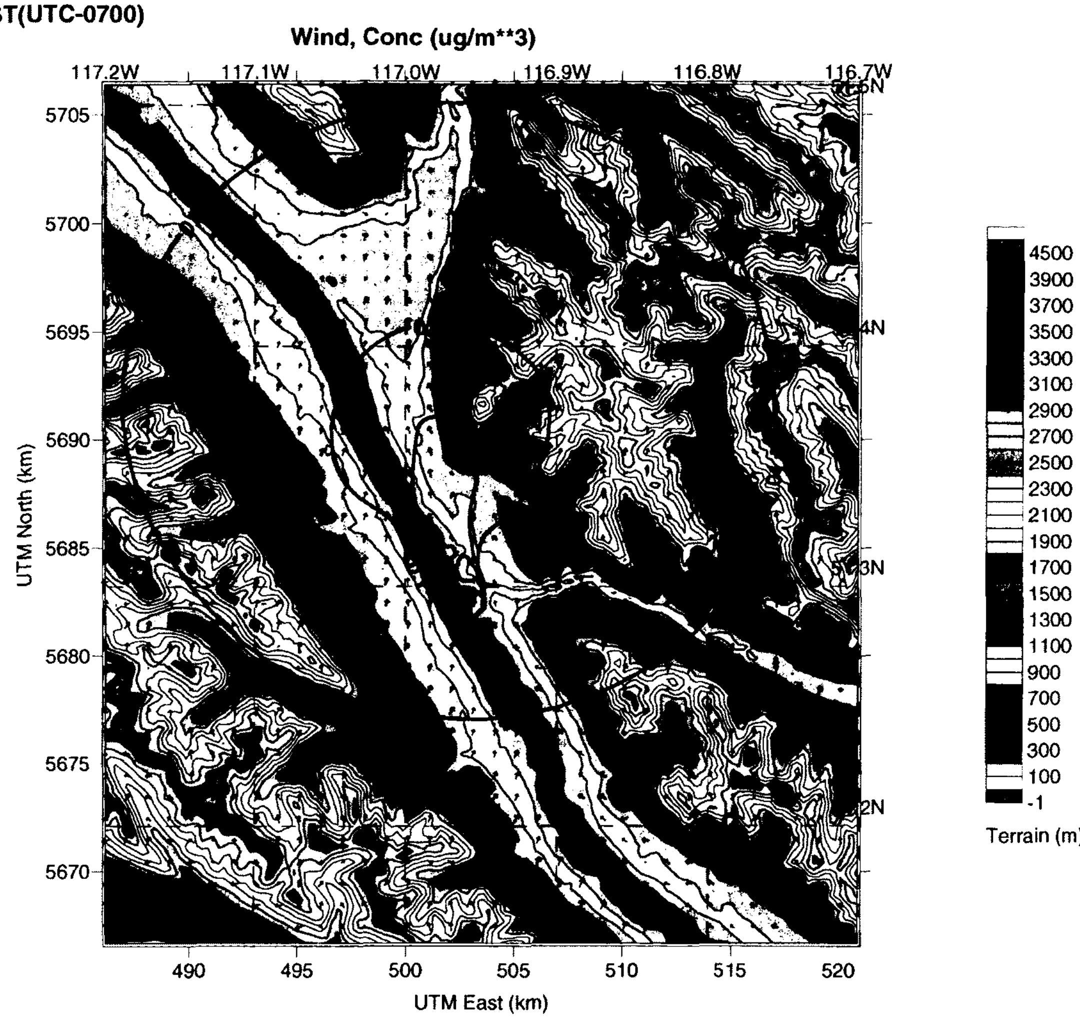

(b)
Dec 10, 2005
19:00 LST(UTC-0700)

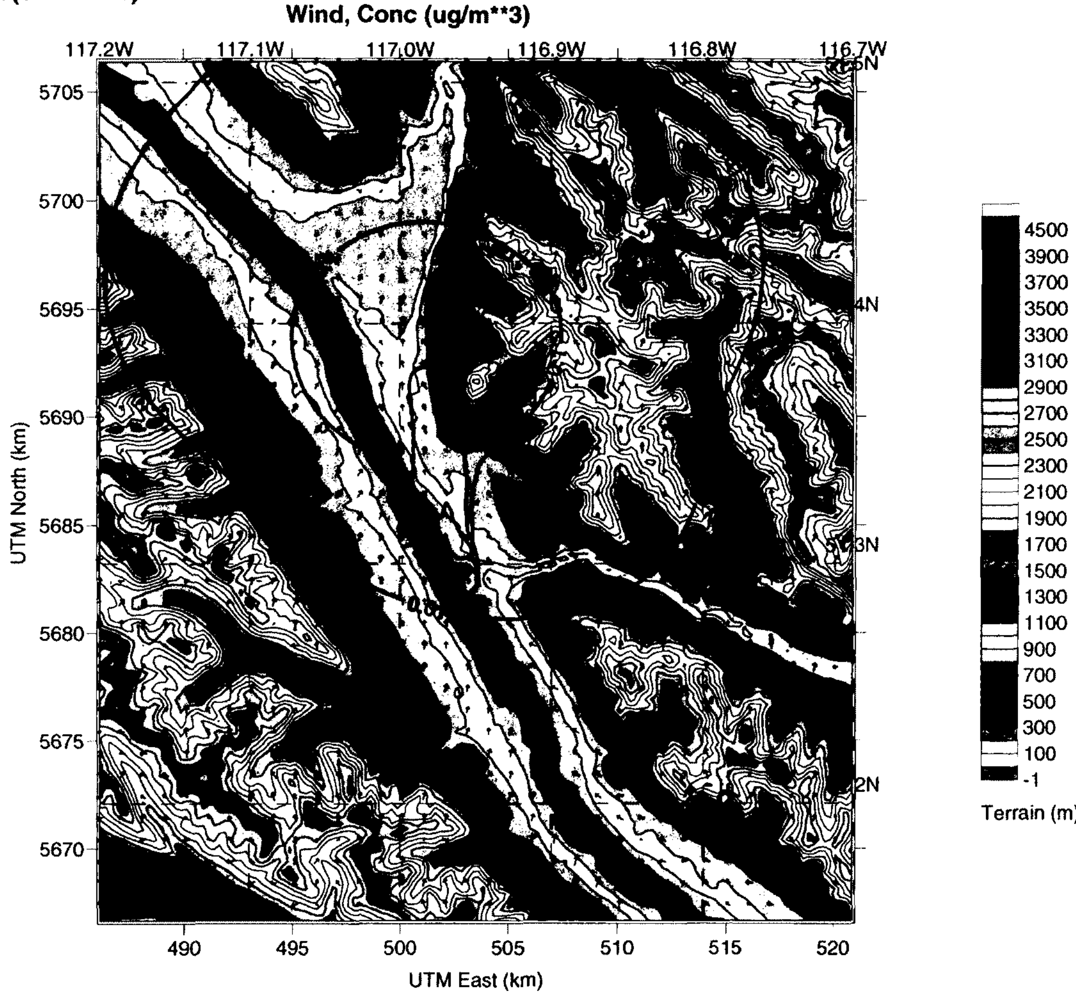

(c)
Dec 10, 2005
20:00 LST(UTC-0700)

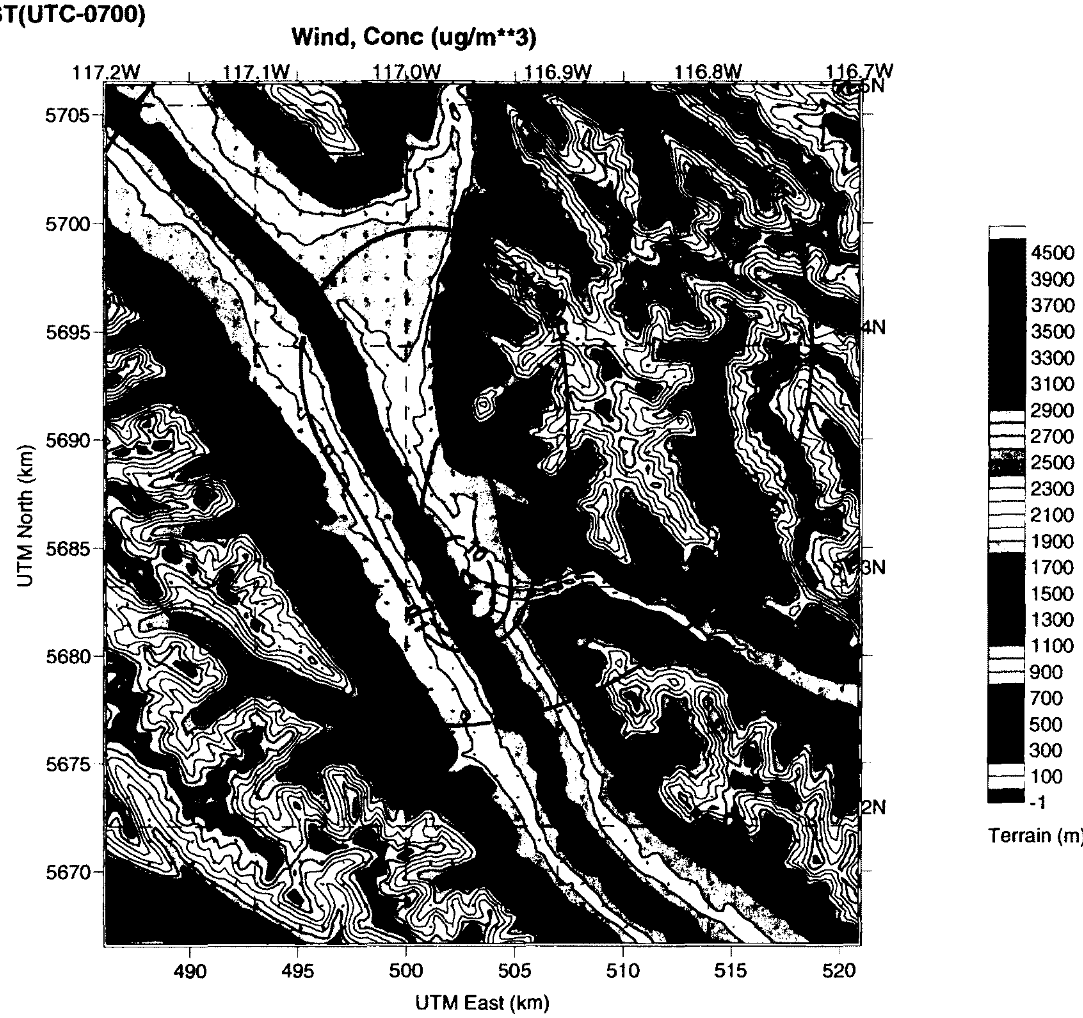

(d)
Dec 10, 2005
21:00 LST(UTC-0700)

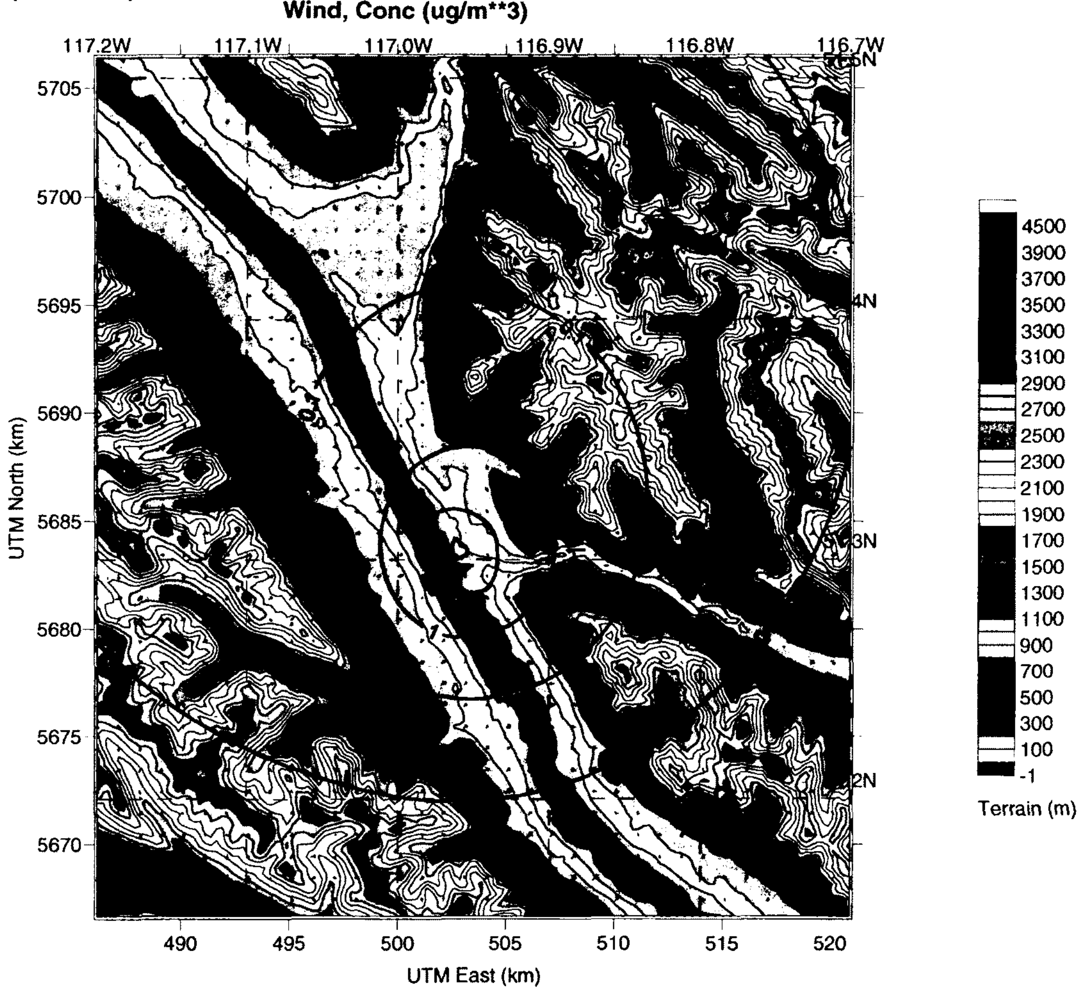

(e)
Dec 10, 2005
22:00 LST(UTC-0700)

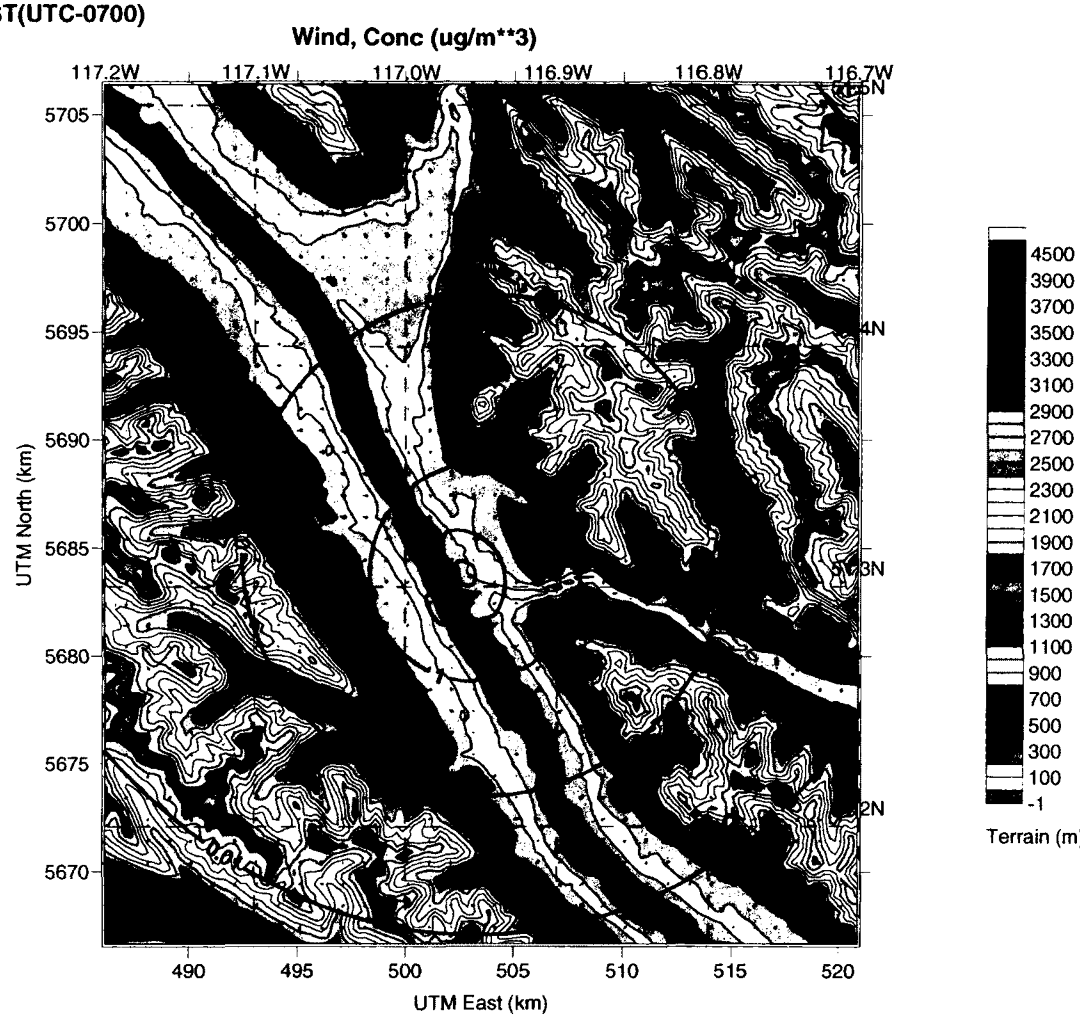

Figure 6-5 **(a-e) Hourly CALPUFF ground level PM_{10} concentrations ($\mu g/m^3$) from 18:00 to 22:00 on December 10, 2005, representing the entire modeling domain, showing wind vectors and PM_{10} concentrations for 5 consecutive hours. Note the increase in PM as the wind speed slows and the air stagnates around the Town of Golden located at the convergence of the valley to the east and the main river valley.**

Table 6-11 **PM levels, mixing heights, wind speed and wind direction at the TOWN station surrounding the high PM event described in Figure 6-5.**

Time	PM_{10} (µg/m³)	$PM_{2.5}$ (µg/m³)	Mix hgt (m)	Wspd (m/s)	Wdir
12/10/05 12:00	3.7	1.7	500	0.85	168
12/10/05 13:00	10.2	5.3	353	0.49	185
12/10/05 14:00	17.7	8.26	378	0.58	229
12/10/05 15:00	24.6	14.6	358	0.48	172
12/10/05 16:00	38.8	23.4	29	0.65	168
12/10/05 17:00	10.8	9.7	40	0.95	161
12/10/05 18:00	8.2	6.9	47	1.25	159
12/10/05 19:00	42.2	40.0	27	0.51	338
12/10/05 20:00	70.0	59.4	27	0.46	346
12/10/05 21:00	97.8	78.7	26	0.36	282
12/10/05 22:00	90.6	74.8	27	0.48	127
12/10/05 23:00	45.9	42.3	31	0.68	309
12/11/05 0:00	68.2	54.6	27	0.56	338
12/11/05 1:00	38.1	27.5	40	0.77	341
12/11/05 2:00	33.6	26.9	27	0.49	146
12/11/05 3:00	43.1	33.9	27	0.49	341
12/11/05 4:00	41.6	27.3	33	0.66	339
12/11/05 5:00	37.3	26.6	26	0.29	298
12/11/05 6:00	19.0	19.3	31	0.68	156

6.7 CALPUFF Evaluation Procedures

This section provides a statistical comparison of the model predicted PM with the observed PM data collected at all three monitoring locations in Golden. It is important to test the model's ability to predict PM concentrations to assess the validity of the model as a tool for airshed management. The ability of the model to predict the highest levels of PM concentrations is given special consideration.

In order to assess the performance of the model during each episode the predicted PM concentrations were compared with the observed ambient concentrations in Golden using a variety of approaches. Chang and Hanna (2004) suggested that there is no single best method of assessing air quality model performance. They recommended that a suite of different performance measures be used.

The suite of performance measures used in our evaluation were used in a recent evaluation of CALPUFF by Song et al. (2006) as suggested by Willmott (1982) and Seigneur et al. (2000). These were applied in Barna and Gimson (2002), Zhang et al. (2004) and Assimakopoulos (2005). Our evaluation also contains methods used in another BC modeling study by Levelton Consultants Ltd. in Williams Lake (Schutte et al. 2005)

First, a direct comparison of the hourly and daily averages was performed. Scatter plots were also created to gauge initial model performance and to visually indicate when the modeled predictions are within a factor of two of the observed PM values (Ross 1991).

Next, as a primary indicator of model performance the dimensionless Normalized Root Mean Square Error (NRMSE) was calculated at each monitor for the entire episode:

$$NRMSE = \sqrt{}(AVG(PR)-AVG(OB))^2/(MAX(OBS)-MIN(PR))^2$$

In addition, NRMSE was used to evaluate the top 10 predicted concentrations in an effort to evaluate how the model predicted the peak PM concentrations during the episode. A low NRMSE value indicates good model performance.

The fractional bias (Fb) was calculated for each monitoring station:

$$Fb = 2(OB-PR)/(OB+PR).$$

Fb is a performance measure used to determine if a model meets the minimum performance standards of the USEPA (USEPA 1992). As mentioned previously there is no standard measure of "good" model performance. Fb was chosen in this study as it is an accepted and often performed statistical evaluation of a model with procedures outlined and endorsed by the USEPA.

In contrast to the application of the Fb statistic in the CALMET evaluation (Section 5-2), the USEPA provides a procedure where Fb is calculated twice at each monitoring station. First, Fb was calculated for the average, where OB and PR represent the hourly concentrations of PM. Secondly, Fb was calculated for the standard deviations, where OB and PR represent the standard deviations of the hourly concentrations of PM. The number of hourly concentrations included in the test determines the stringency. It can be performed on all paired values during the entire episode (most stringent), can assess only the higher values (top 25) of the episode pair-wise (less stringent) and can also compare the highest 25 values un-paired (least stringent). All levels of stringency were tested, however the results from only the most stringent Fb test are provided.

The two Fb statistics were plotted with bias of average on the x-axis and bias of standard deviation on the y-axis. The closer the fractional bias is to the centre of the plot (zero), the fewer tendencies it has towards bias. An acceptable model (USEPA 1992) has Fb statistics within +/- 0.67 representing an over/under prediction within a factor of two.

To compare model performance with other CALPUFF and dispersion modeling studies a number of additional statistical performance measures were applied. This included:

Fractional gross error (FGE) = (OB-PR) / 0.5(OB +PR)

Statistical measure of perfect model	0.0
Range of this statistic from other studies	0.29 – 0.99

Geometric mean bias (MG) = exp(ln OB – ln PR)

Statistical measure of perfect model	1.0
Range of this statistic from other studies	1.01 – 1.83

Correlation coefficient (CORR) = (OB-AVG(OB))(PR-AVG(PR) / σOB * σPR

Statistical measure of perfect model	1.0
Range of this statistic from other studies	0.40 – 0.82

Willmott's index of agreement (D) =

$1.0 - (OB\text{-}PR)^2/((OB\text{-}AVG(OB))+(PRAVG(OB)))^2$

Statistical measure of perfect model	1.0
Range of this statistic from other studies	0.08 – 0.89

Fraction of predictions within factor of 2 of observations (FAC2)

Statistical measure of perfect model	100%
Range of this statistic from other studies	52% - 98%

Statistical tests were performed to test both hourly and daily (24-hour) model predictions.

6.8 EPISODE 1 MODEL PERFORMANCE

The time series plots (Figure 6-6) show the detailed model output, however investigation of the model performance measures is needed. Averaged over the entire first episode, the model under-predicted at the CPR and GOLF stations and over-predicted at the TOWN station for both PM_{10} and $PM_{2.5}$ (Table 6-12). The CPR station shows the best agreement averaged over the entire episode for both PM_{10} and $PM_{2.5}$.

Table 6-12 Average observed and predicted values at all three monitoring stations during Episode 1.

Pollutant	Value	Concentration ($\mu g/m^3$)		
		CPR	Town	Golf
$PM_{2.5}$	Observed	10.90	14.23	6.96
	Predicted	10.71	21.64	2.46
PM_{10}	Observed	16.78	21.10	11.79
	Predicted	14.87	30.61	3.68

The average over the entire episode does not show how the model is capturing the daily or hourly observed concentrations. Since this study is interested in short periods of elevated levels of PM, the focus is on the ability of CALPUFF to predict hourly concentrations.

Scatterplots of predicted and observed PM concentrations are provided (Figure 6-7 – 6-9). The CPR station has a more balanced scatter, with some grossly over- and under-estimated hourly concentrations. The TOWN station shows much fewer under-predictions, but has many more over-estimated hourly concentrations, while the GOLF station shows the opposite.

(a)

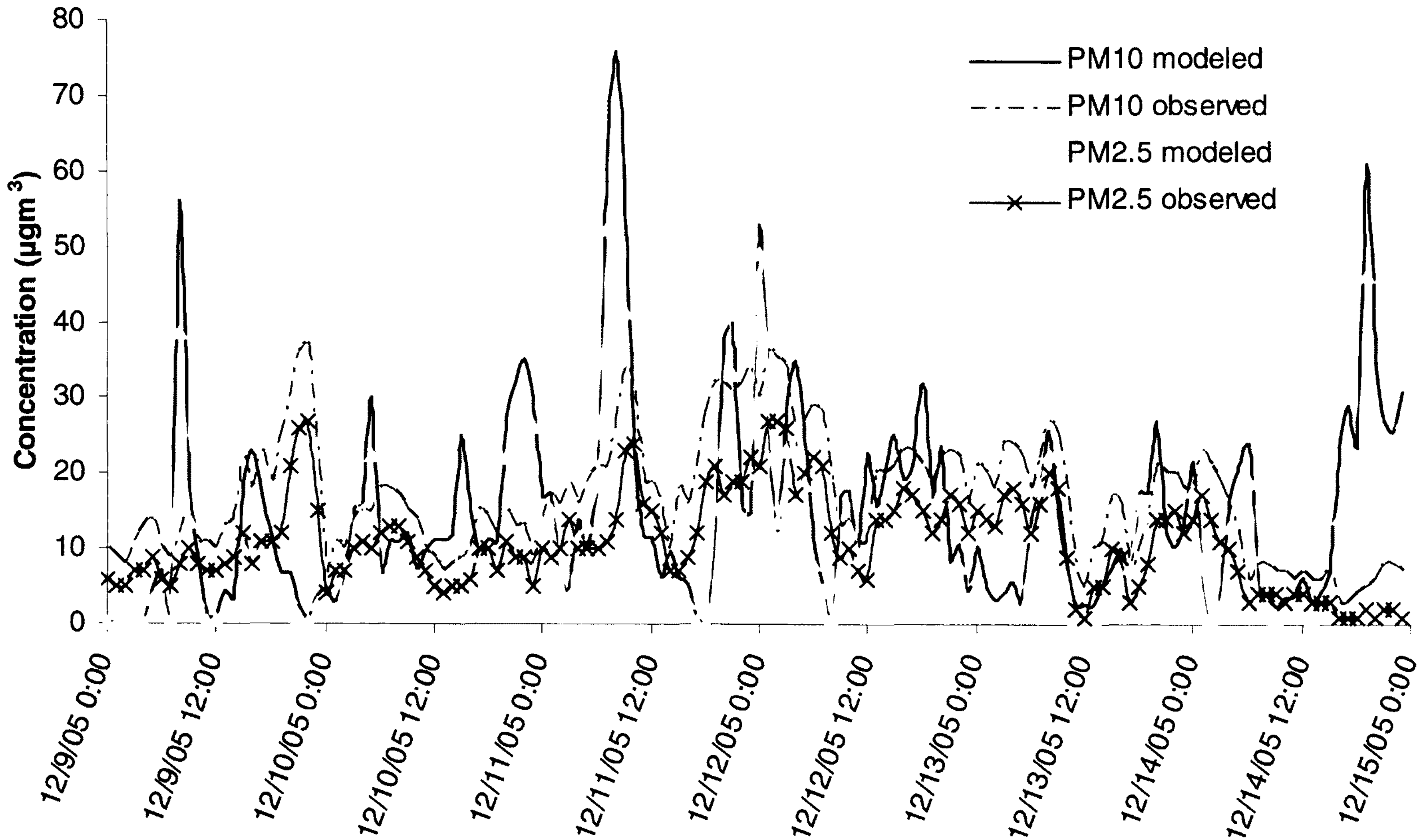

80
70
60
50
40
30
20
10
0
Concentration (μgm³)
PM10 modeled
PM10 observed
PM2.5 modeled
PM2.5 observed
12/9/05 0:00
12/9/05 12:00
12/10/05 0:00
12/10/05 12:00
12/11/05 0:00
12/11/05 12:00
12/12/05 0:00
12/12/05 12:00
12/13/05 0:00
12/13/05 12:00
12/14/05 0:00
12/14/05 12:00
12/15/05 0:00

(b)

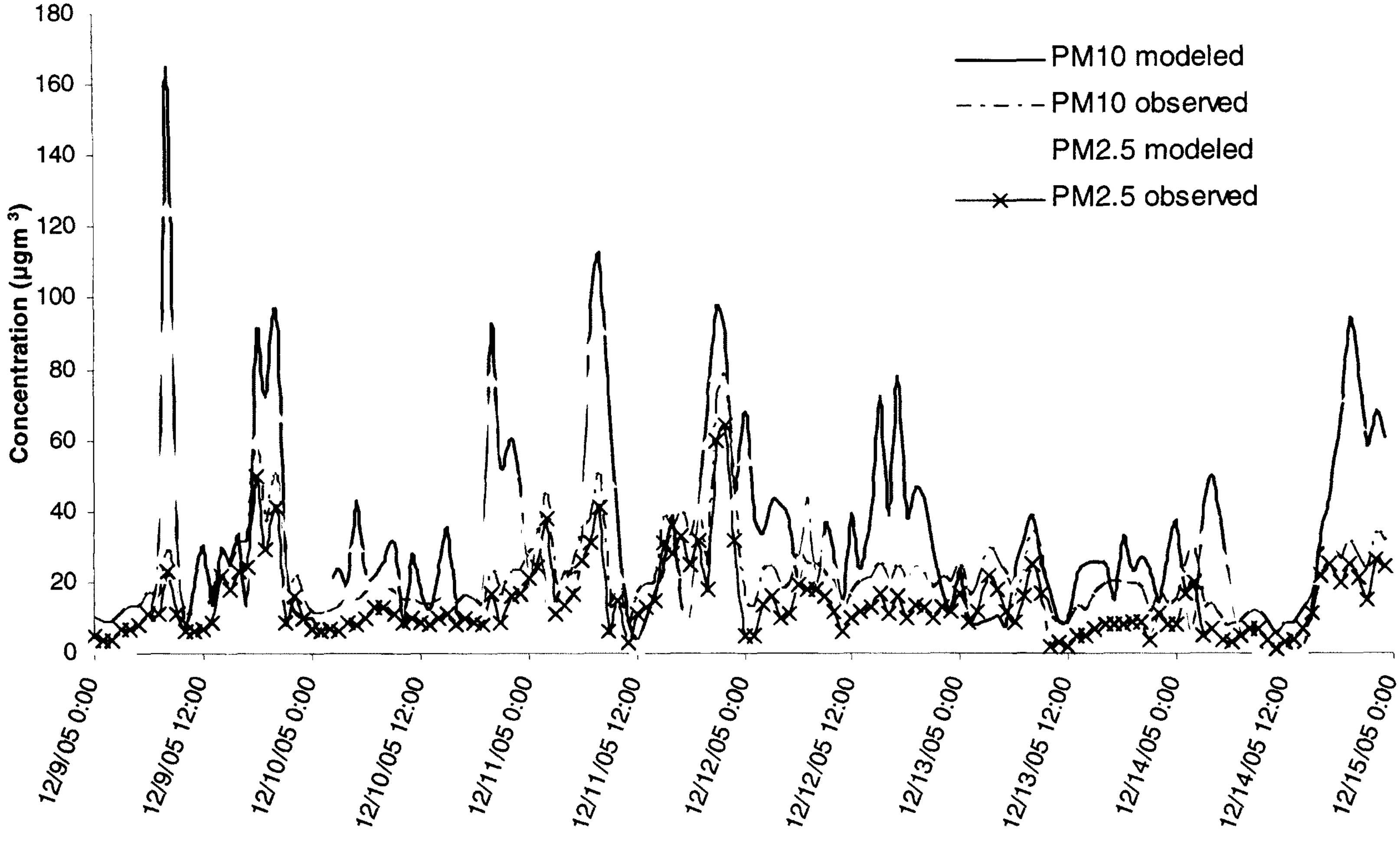

PM10 modeled
PM10 observed
PM2.5 modeled
PM2.5 observed
Concentration (μgm⁻³)
180
160
140
120
100
80
60
40
20
0
12/9/05 0:00
12/9/05 12:00
12/10/05 0:00
12/10/05 12:00
12/11/05 0:00
12/11/05 12:00
12/12/05 0:00
12/12/05 12:00
12/13/05 0:00
12/13/05 12:00
12/14/05 0:00
12/14/05 12:00
12/15/05 0:00

(c)

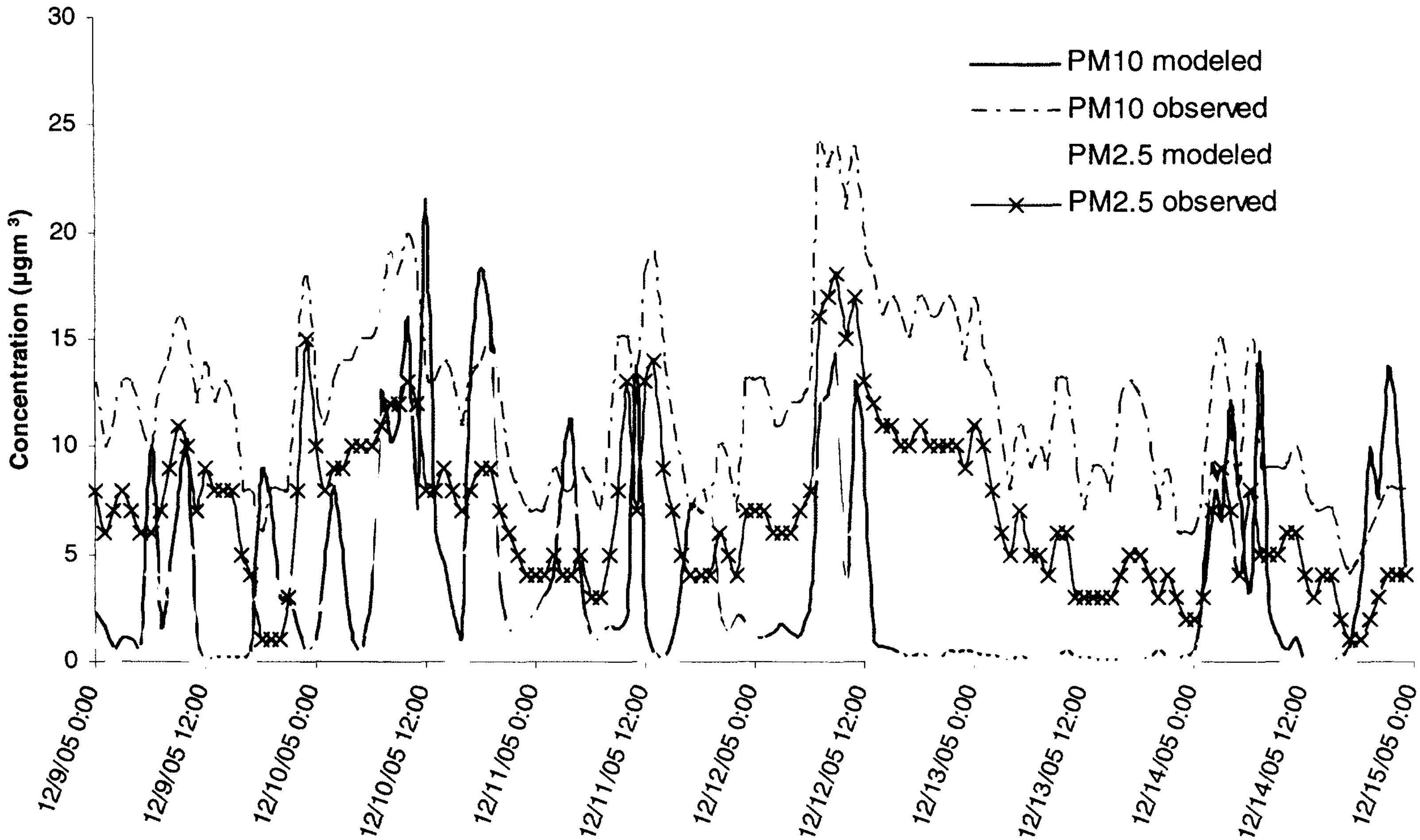
30
25
20
15
10
5
0
Concentration (µgm⁻³)
PM10 modeled
PM10 observed
PM2.5 modeled
PM2.5 observed
12/9/05 0:00
12/9/05 12:00
12/10/05 0:00
12/10/05 12:00
12/11/05 0:00
12/11/05 12:00
12/12/05 0:00
12/12/05 12:00
12/13/05 0:00
12/13/05 12:00
12/14/05 0:00
12/14/05 12:00
12/15/05 0:00

(d)

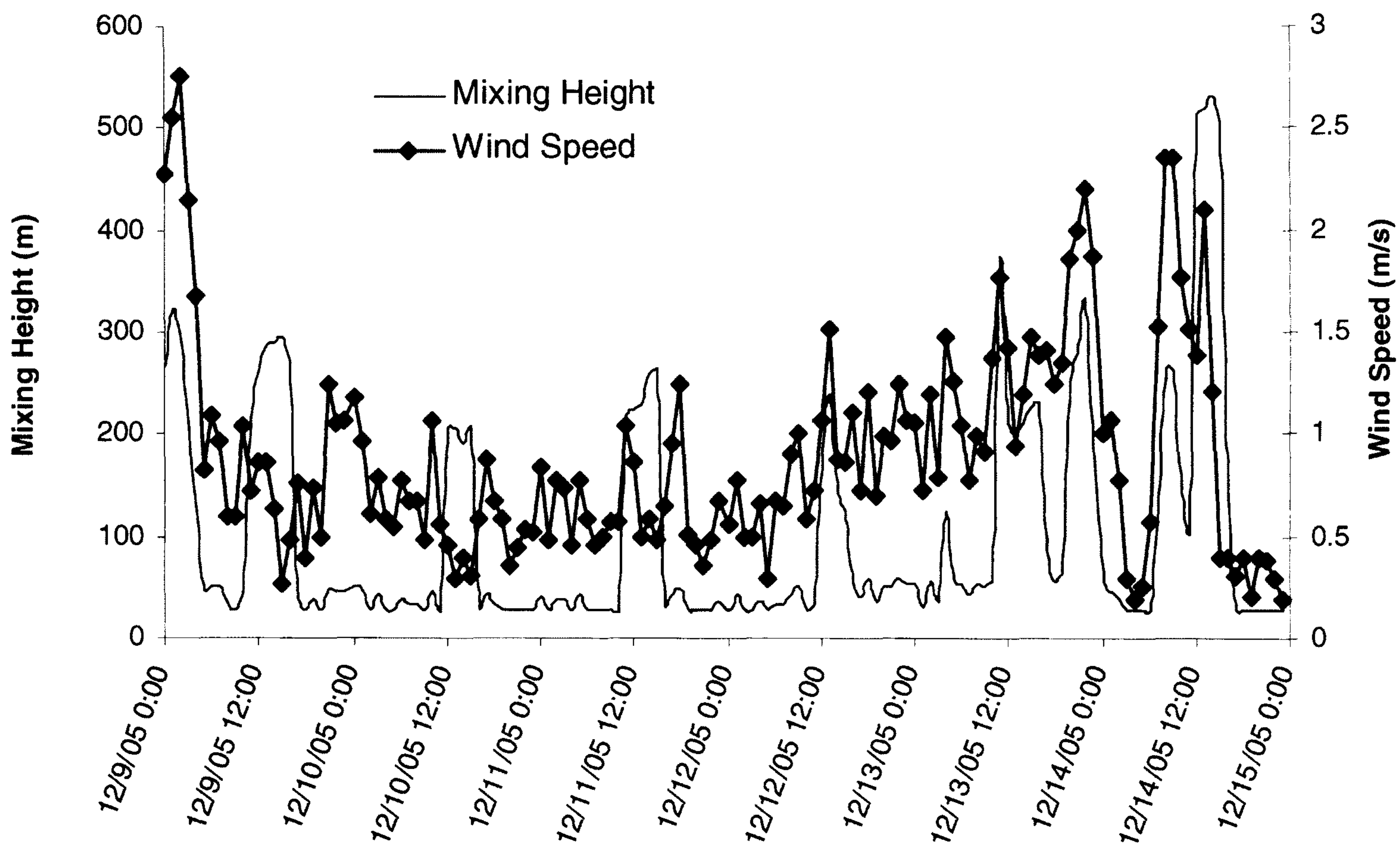

Figure 6-6 **Time series plots showing model predicted and observed PM_{10} and $PM_{2.5}$ for episode 1 at (a) CPR station, (b) Town station, (c) Golf station. Also included is (d) a time series of mixing height and wind speeds at the Town station.**

(a) (b)

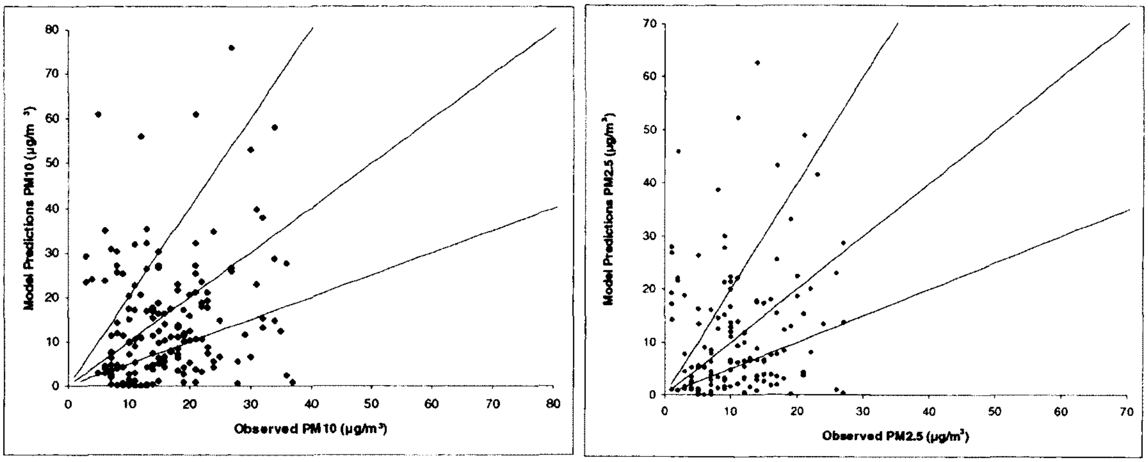

Figure 6-7 **Scatterplots of predicted versus observed concentrations, paired in location and time at the CPR station for (a) PM_{10}, and (b) $PM_{2.5}$ for Episode 1. The outer black lines bound predicted concentrations within a factor of 2 of observed values.**

(a) (b)

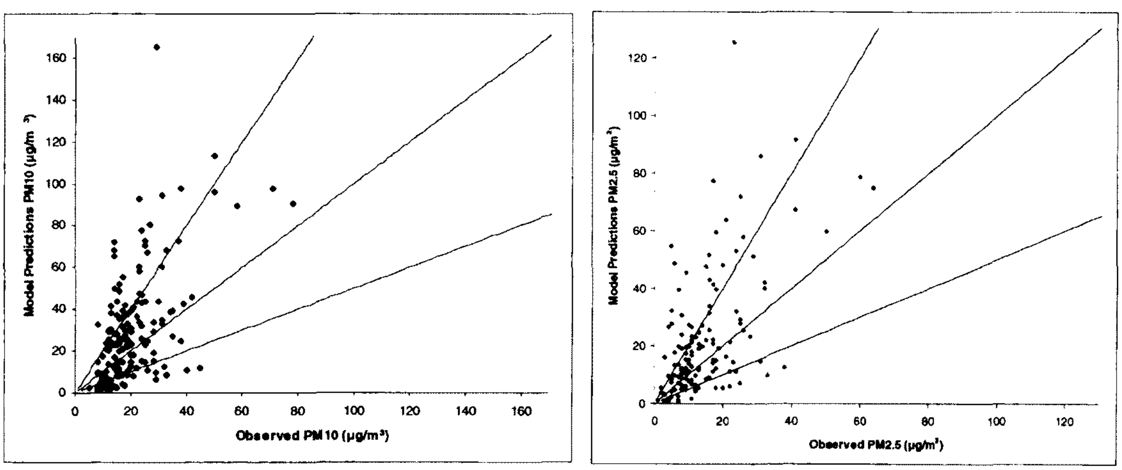

Figure 6-8 **Scatterplots of predicted versus observed concentrations, paired in location and time at the TOWN station for (a) PM_{10}, and (b) $PM_{2.5}$ for Episode 1. The outer black bound predicted concentrations within a factor of 2 of observed values.**

(a) (b)

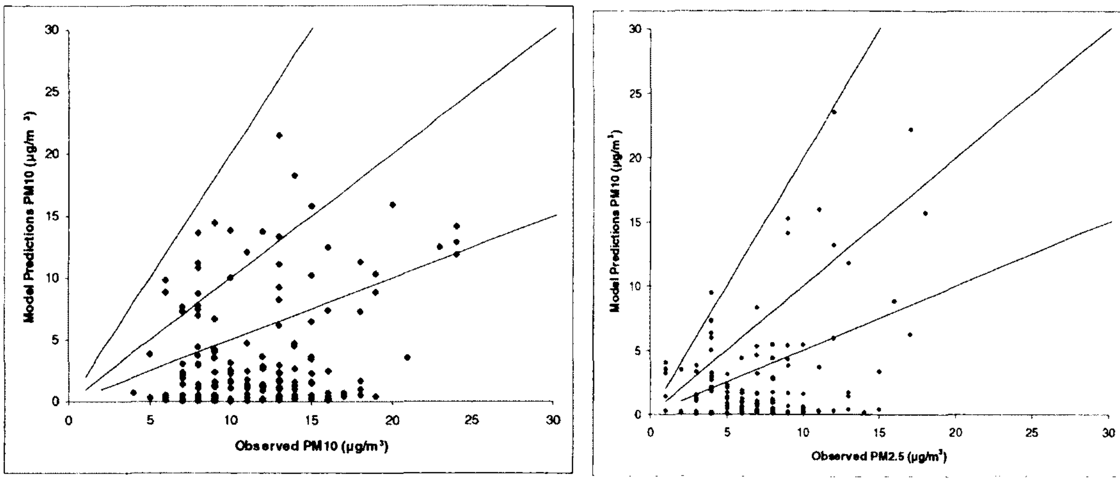

Figure 6-9 **Scatterplots of predicted versus observed concentrations, paired in location and time at the GOLF station for (a) PM_{10}, and (b) $PM_{2.5}$ for Episode 1. The outer black lines bound predicted concentrations within a factor of 2 of observed values.**

The NRMSE ranges between stations with the lowest values occurring at the TOWN station for both PM_{10} and $PM_{2.5}$ (Table 6-13). PM_{10} errors are larger at the TOWN and GOLF stations and slightly less at the CPR station. In general, errors increase when the daily averages are compared. The NRMSE increases when only the top ten observed concentrations are considered (Table 6-14).

Table 6-13 **Normalised Root Mean Square Error (NRMSE) values for the entire first episode.**

Pollutant	Averaging Period	NRMSE		
		CPR	Town	Golf
$PM_{2.5}$	1-hour	0.474	0.298	0.368
	24-hour	0.404	0.549	0.756
PM_{10}	1-hour	0.415	0.321	0.486
	24-hour	0.424	0.634	1.061

Table 6-14 **Normalised Root Mean Square Error (NRMSE) values for the top ten observed values during the first episode.**

Pollutant	Averaging Period	NRMSE		
		CPR	Town	GOLF
$PM_{2.5}$	1-hour	0.572	0.459	0.590
PM_{10}	1-hour	0.636	0.434	0.586

Fractional Bias is a performance measure used to determine if a model meets the minimum performance standard by the USEPA (USEPA 1992). By USEPA standards the model was performing adequately at the CPR station for all measures (PM_{10}-1hr, $PM_{2.5}$-1hr, PM_{10}-24hr, $PM_{2.5}$-24hr) and the TOWN station for two measures (PM_{10}-24hr, $PM_{2.5}$-24hr) (Figure 6-10). The model did not perform adequately for any measures at the GOLF station.

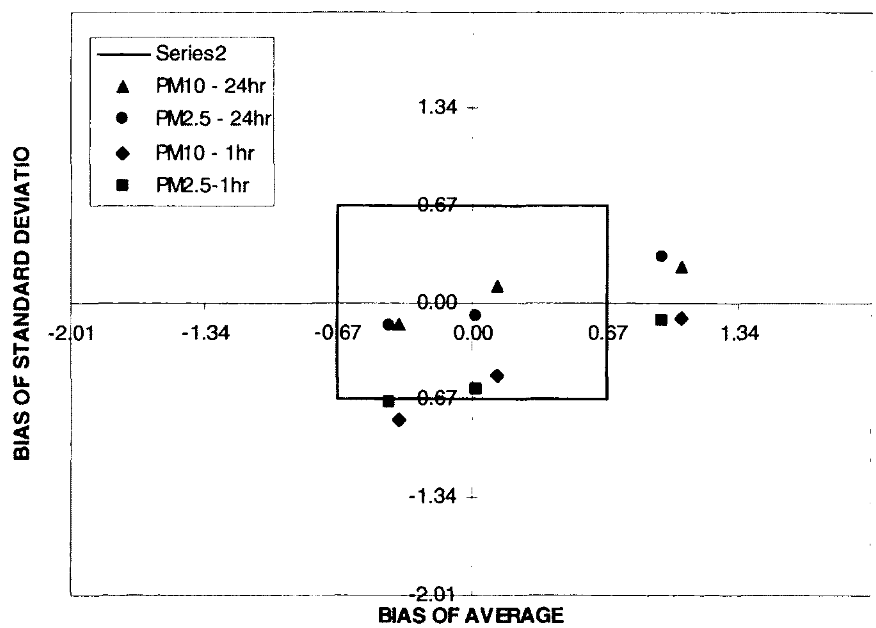

Figure 6-10 **Fractional bias: Episode 1 using entire episode (most stringent) US EPA method. The inner box represents acceptable model performance measures (US EPA 1992).**

Additional performance measures described in section 6.7 are provided (Table 6-15, 6-16). These will be evaluated comparatively with other studies (Section 6.10).

Table 6-15 CALPUFF model performance measures for PM_{10} during Episode 1.

1-hour	CPR	TOWN	GOLF
FGE	0.12	0.37	1.05
MG	1.13	0.69	3.20
R	0.21	0.59	0.24
D	0.87	0.87	0.75
FAC2	46	56	21

24-hour	CPR	TOWN	GOLF
R	0.34	0.69	0.20
D	0.98	0.96	0.77
FAC2	83	100	33

Table 6-16 CALPUFF model performance measures for $PM_{2.5}$ during Episode 1.

1-hour	CPR	TOWN	GOLF
FGE	0.02	0.41	0.96
MG	1.02	0.66	2.83
R	0.15	0.60	0.36
D	0.84	0.86	0.81
FAC2	40	59	22

24-hour	CPR	TOWN	GOLF
R	0.31	0.77	0.60
D	0.97	0.96	0.82
FAC2	67	83	17

6.9 EPISODE 2 MODEL PERFORMANCE

The time series plots (Figure 6-11) show the detailed model output, however investigation of the model performance measures during episode 2 is needed. Averaged over the entire second episode, the model over-predicted at the CPR and TOWN stations and under-predicted at the GOLF station for $PM_{2.5}$ (Table 6-17). PM_{10} concentrations were under-estimated at all three stations. The CPR station and the TOWN station shows the best agreement averaged over the entire episode for PM_{10} and $PM_{2.5}$, respectively.

Scatterplots of predicted and observed PM concentrations are provided (Figure 6-12 – 6-14). The results reconfirm the predictions shown in the overall episode averages. There are still many times when the model is grossly over- or under-estimating the observed values.

Table 6-17 Average observed and predicted values at all three monitoring stations during Episode 2.

Pollutant	Value	Concentration ($\mu g/m^3$)		
		CPR	Town	Golf
$PM_{2.5}$	Monitor	6.91	9.96	1.76
	Predicted	8.09	13.87	0.28
PM_{10}	Monitor	23.95	35.36	7.31
	Predicted	16.00	28.10	1.05

(a)

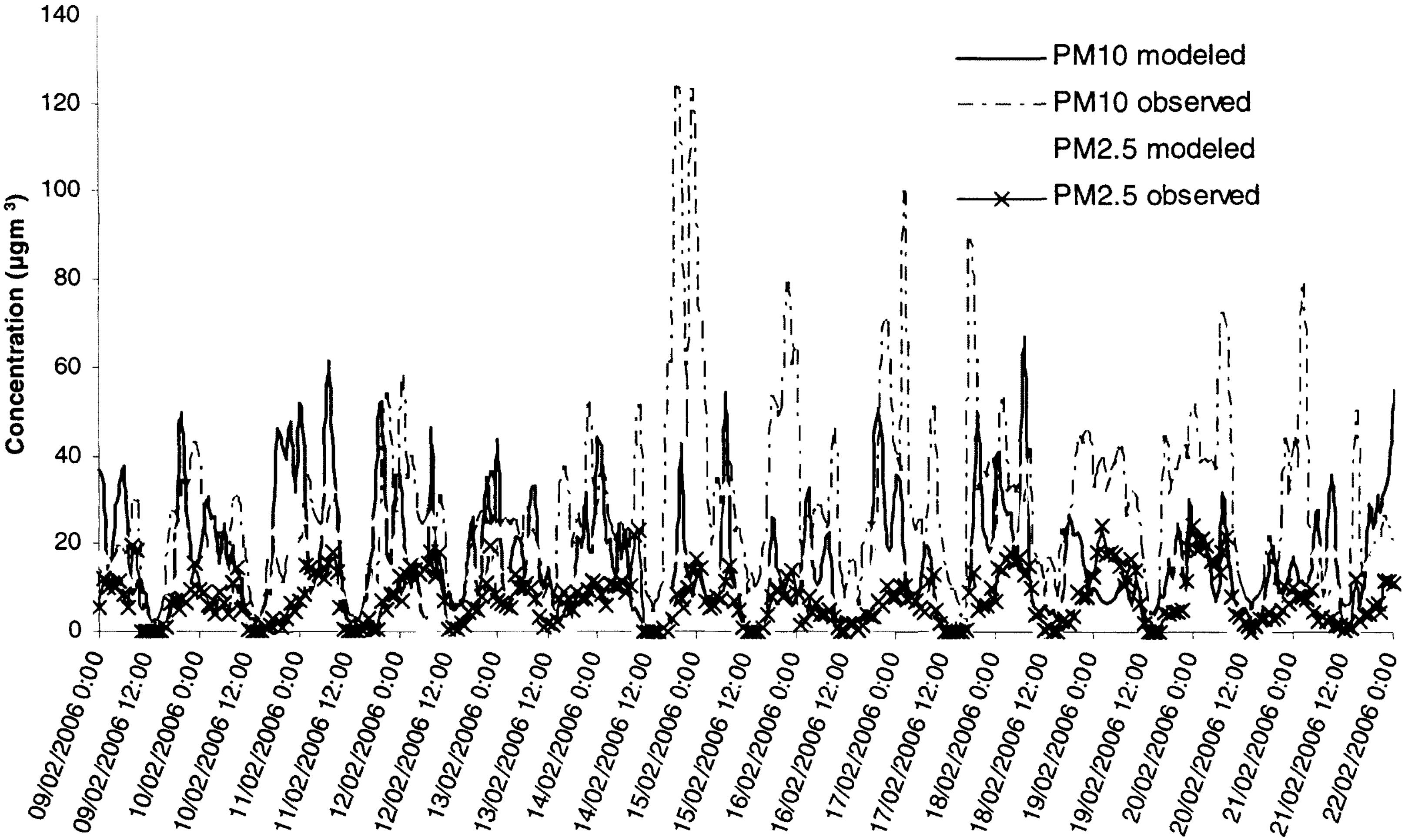

140
120
100
80
60
40
20
0
Concentration (µgm⁻³)
PM10 modeled
PM10 observed
PM2.5 modeled
PM2.5 observed
09/02/2006 0:00
09/02/2006 12:00
10/02/2006 0:00
10/02/2006 12:00
11/02/2006 0:00
11/02/2006 12:00
12/02/2006 0:00
12/02/2006 12:00
13/02/2006 0:00
13/02/2006 12:00
14/02/2006 0:00
14/02/2006 12:00
15/02/2006 0:00
15/02/2006 12:00
16/02/2006 0:00
16/02/2006 12:00
17/02/2006 0:00
17/02/2006 12:00
18/02/2006 0:00
18/02/2006 12:00
19/02/2006 0:00
19/02/2006 12:00
20/02/2006 0:00
20/02/2006 12:00
21/02/2006 0:00
21/02/2006 12:00
22/02/2006 0:00

(b)

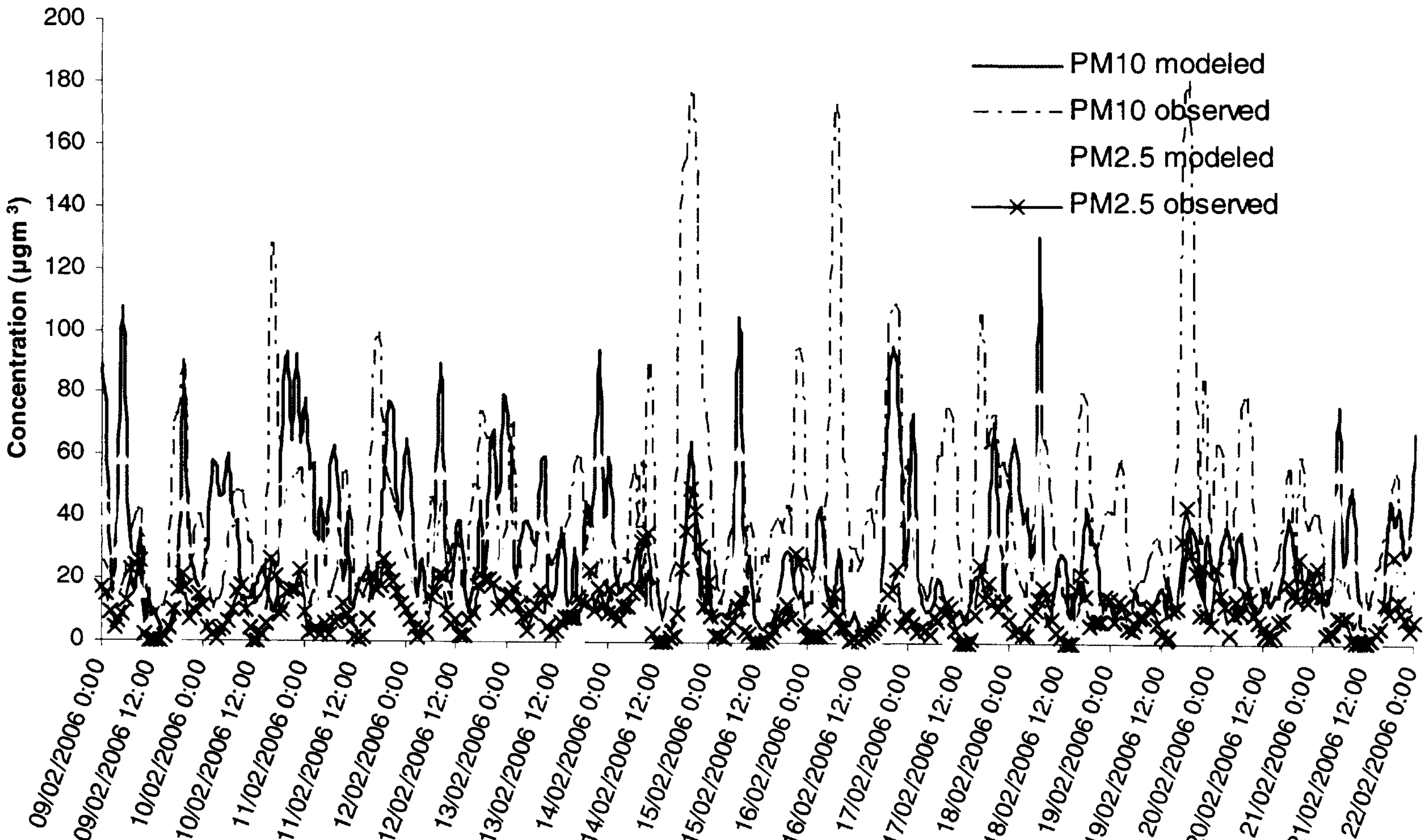

200
180
160
140
120
100
80
60
40
20
0
Concentration (µgm⁻³)
PM10 modeled
PM10 observed
PM2.5 modeled
PM2.5 observed
09/02/2006 0:00
09/02/2006 12:00
10/02/2006 0:00
10/02/2006 12:00
11/02/2006 0:00
11/02/2006 12:00
12/02/2006 0:00
12/02/2006 12:00
13/02/2006 0:00
13/02/2006 12:00
14/02/2006 0:00
14/02/2006 12:00
15/02/2006 0:00
15/02/2006 12:00
16/02/2006 0:00
16/02/2006 12:00
17/02/2006 0:00
17/02/2006 12:00
18/02/2006 0:00
18/02/2006 12:00
19/02/2006 0:00
19/02/2006 12:00
20/02/2006 0:00
20/02/2006 12:00
21/02/2006 0:00
21/02/2006 12:00
22/02/2006 0:00

(c)

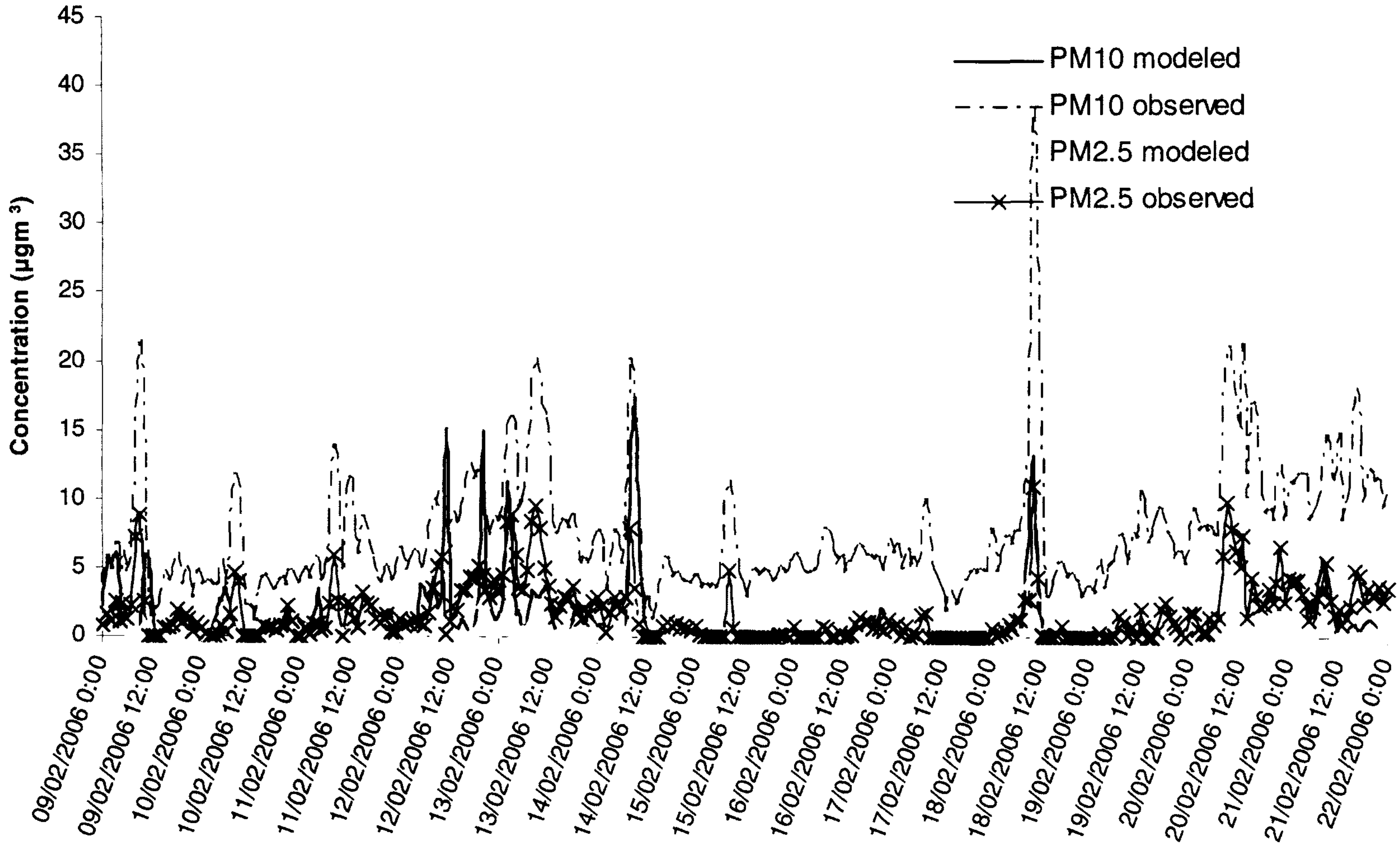
PM10 modeled
PM10 observed
PM2.5 modeled
PM2.5 observed
Concentration (μgm⁻³)
45
40
35
30
25
20
15
10
5
0
09/02/2006 0:00
09/02/2006 12:00
10/02/2006 0:00
10/02/2006 12:00
11/02/2006 0:00
11/02/2006 12:00
12/02/2006 0:00
12/02/2006 12:00
13/02/2006 0:00
13/02/2006 12:00
14/02/2006 0:00
14/02/2006 12:00
15/02/2006 0:00
15/02/2006 12:00
16/02/2006 0:00
16/02/2006 12:00
17/02/2006 0:00
17/02/2006 12:00
18/02/2006 0:00
18/02/2006 12:00
19/02/2006 0:00
19/02/2006 12:00
20/02/2006 0:00
20/02/2006 12:00
21/02/2006 0:00
21/02/2006 12:00
22/02/2006 0:00

(d)

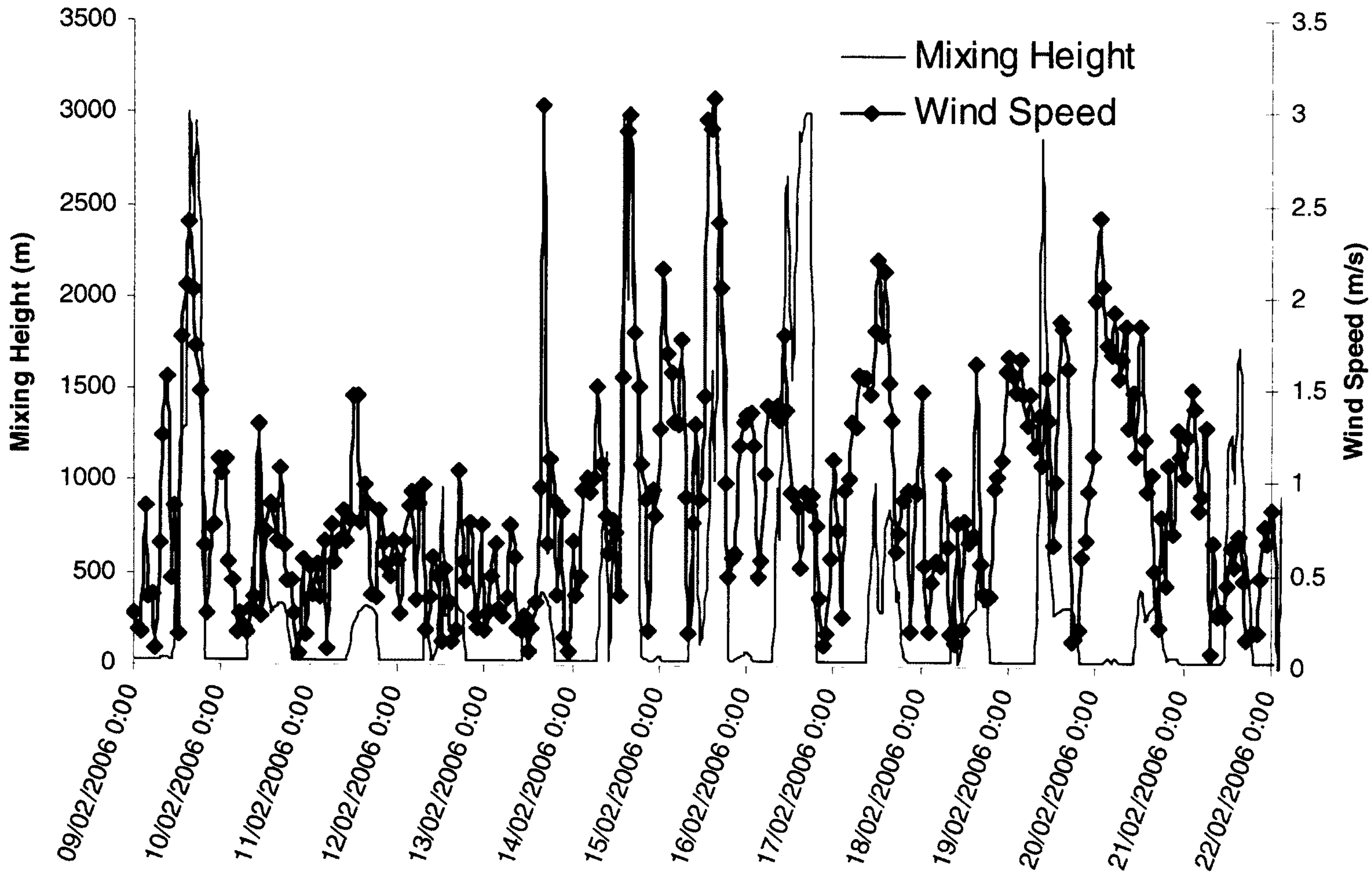

Figure 6-11 **Time series plots showing model predicted and observed PM_{10} and $PM_{2.5}$ for episode 2 at (a) CPR station, (b) Town station, (c) Golf station. Also included is (d) a time series of mixing height and wind speeds at the Town station during episode 2.**

(a) (b)

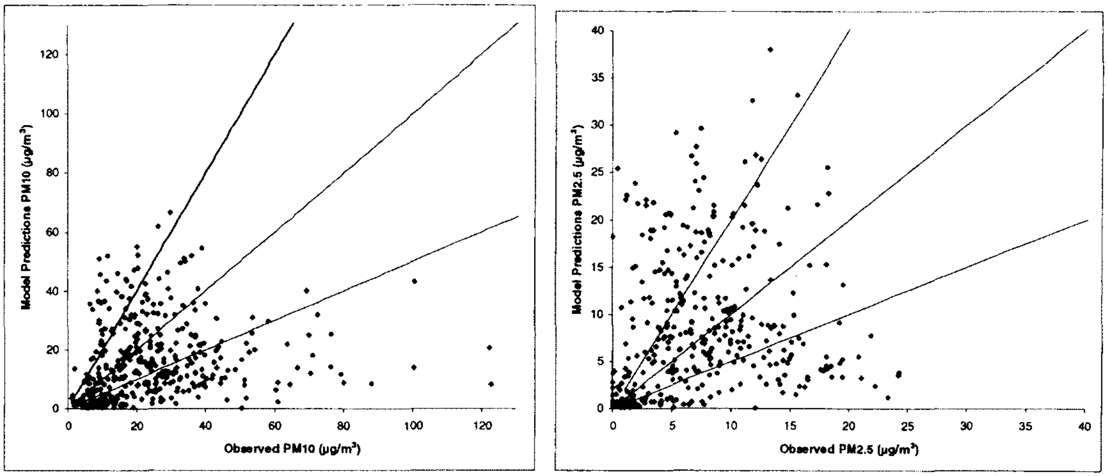

Figure 6-12 Scatterplots of predicted versus observed concentrations, paired in location and time at the CPR station for (a) PM_{10}, and (b) $PM_{2.5}$ for Episode 2. The outer black bound predicted concentrations within a factor of 2 of observed values.

(a) (b)

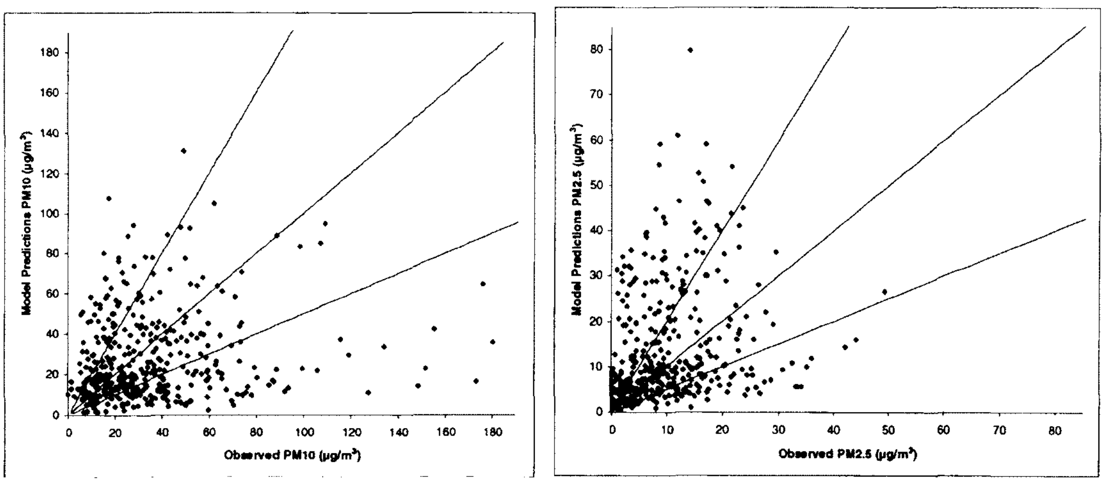

Figure 6-13 Scatterplots of predicted versus observed concentrations, paired in location and time at the TOWN station for (a) PM_{10}, and (b) $PM_{2.5}$ for Episode 2. The outer black bound predicted concentrations within a factor of 2 of observed values.

(a) (b)

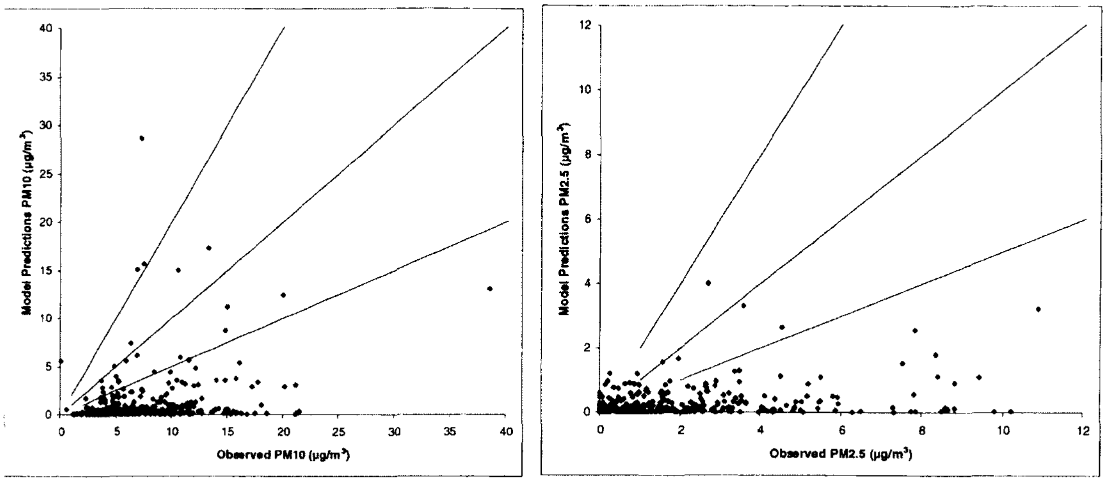

Figure 6-14 Scatterplots of predicted versus observed concentrations, paired in location and time at the GOLF station for (a) PM_{10}, and (b) $PM_{2.5}$ for Episode 2. The outer black bound predicted concentrations within a factor of 2 of observed values.

The NRMSE shows a range between stations with the lowest values occurring at the TOWN station for $PM_{2.5}$ and at the CPR station for PM_{10} (Table 6-18). In general, errors are higher for $PM_{2.5}$ in the hourly comparison. Errors also increase when the daily averages are compared. The NRMSE increases when only the top ten observed concentrations are considered (Table 6-19).

Table 6-18 Normalised Root Mean Square Error (NRMSE) values for the entire second episode.

Pollutant	Averaging Period	NRMSE		
		CPR	Town	Golf
$PM_{2.5}$	1-hour	0.340	0.285	0.239
	24-hour	0.576	0.820	1.677
PM_{10}	1-hour	0.181	0.187	0.198
	24-hour	0.454	0.303	2.282

Table 6-19 **Normalised Root Mean Square Error (NRMSE) values for the top ten observed values during the second episode.**

Pollutant	Averaging Period	NRMSE		
		CPR	Town	Golf
$PM_{2.5}$	1-hour	0.713	0.521	0.799
PM_{10}	1-hour	0.627	0.664	0.488

By USEPA standards regarding Fb the model was performing adequately at the TOWN station for all measures (PM_{10}-1hr, $PM_{2.5}$-1hr, PM_{10}-24hr, $PM_{2.5}$-24hr) and the CPR station for three measures (PM_{10}-1hr, $PM_{2.5}$-1hr, $PM_{2.5}$-24hr) (Figure 6-15). The model did not perform adequately for any measures at the GOLF station.

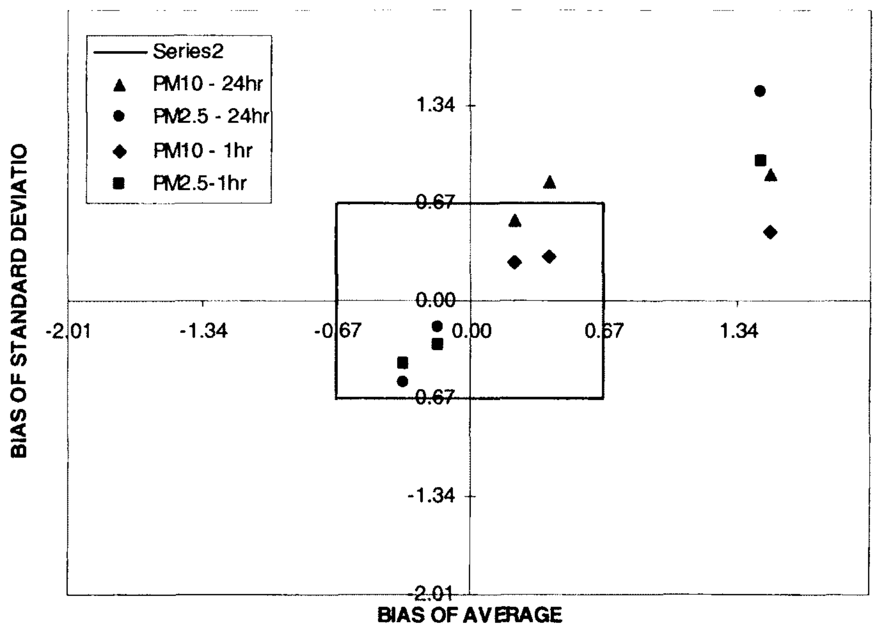

Figure 6-15 **Fractional bias: Episode 2 using entire episode (most stringent) USEPA method. The inner box represents acceptable model performance measures (USEPA 1992).**

Additional performance measures described in section 6.7 are provided (Table 6-20, 6-21). These will be evaluated comparatively with other studies (Section 6.10).

Table 6-20 CALPUFF model performance measures for PM_{10} during Episode 2.

1-hour	CPR	TOWN	GOLF
FGE	0.40	0.23	1.50
MG	1.50	1.26	6.98
R	0.18	0.15	0.27
D	0.84	0.86	0.61
FAC2	44	50	5

24-hour	CPR	TOWN	GOLF
R	-0.56	-0.20	0.31
D	0.92	0.97	-1.62
FAC2	69	75	0

Table 6-21 CALPUFF model performance measures for $PM_{2.5}$ during Episode 2.

1-hour	CPR	TOWN	GOLF
FGE	-0.16	0.33	1.45
MG	0.85	0.72	6.28
R	0.25	0.24	0.21
D	0.84	0.82	0.58
FAC2	45	45	15

24-hour	CPR	TOWN	GOLF
CORR	-0.41	-0.11	0.63
D	0.95	0.89	-3.21
FAC2	75	88	0

6.10 Overall Model Performance

Before examining the CALPUFF results it was necessary to evaluate the model's performance. Assessing the validity of the model predictions helps put into context the following chapters analyzing CALPUFF's characterization of PM episodes in Golden.

As mentioned in Section 4.8, the Fractional Bias (Fb) is a performance measure used to determine if a model meets the minimum performance standard by the US EPA (US EPA 1992). By US EPA standards the model is performing adequately during both episodes in estimating hourly PM_{10} and $PM_{2.5}$, as well as daily $PM_{2.5}$, concentrations at the CPR station. At the TOWN station the model performs adequately for only the daily estimations of PM_{10} and $PM_{2.5}$ concentrations. The model is far below acceptable standards for all estimations at the GOLF station.

The other performance measures are presented as a means to compare with other studies. Song et al. (2006) reported FGE values between 0.29 and 0.59, stating that these values indicated an acceptable degree of model agreement with daily average observational data. FGE values for hourly predicted concentrations in our study compared favorably with these values at the CPR and TOWN stations, but high FGE values are recorded at the GOLF station. MG values for Song et al. (2006) ranged from 1.01 to 1.83 comparing well with values at the CPR and TOWN stations that ranged from 0.66 to 1.50. Song et al. (2006) reported high correlation coefficients ranging from 0.74 to 0.82. CALPUFF predictions in Golden do not show nearly as high correlation coefficients ranging from 0.15 to 0.60. Song et al. (2006) reported Willmott's index of agreement (D) values ranging from 0.83 to 0.89. Our study compared well at the CPR and TOWN stations with values ranging from 0.82 to 0.87. Finally, Song et al. (2006) reported percentage of predictions within a factor of 2 between 68% and 98%. Based on hourly concentrations our model predicted within a factor of 2 of observations only 40% to 59% of the time.

The comparison with Song et al. (2006), although the most complete in the literature, is a very strict test for our model as we are attempting to predict hourly average concentrations rather than daily average concentrations as in the Song et al. study. Typically, as the averaging period increases the performance of a dispersion model will improve (Schutte et al. 2005). In general, our performance measures improve when daily average concentrations are considered. The exception to this is still the correlation coefficient.

Our performance measures compare more favourably with some other studies. Chang et al. (2003) reported a CALPUFF FAC2 of 52% and MG of 1.069. Barna and Gimson (2002) saw higher FGE values ranging from 0.69 to 0.99, lower index of agreement values ranging from 0.67 to 0.87, and correlation coefficients ranging from 0.49 to 0.77 during their evaluation of hourly predicted PM concentrations during PM episodes in New Zealand. It appears that CALPUFF in Golden is performing better during our episodes than those modeled by Barna and Gimson (2002), at least at the CPR and TOWN stations. Assimakopoulos (2005) reported index of agreement values ranging from 0.08 to 0.73 and correlation coefficients ranging from 0.4 to 0.61 depending on the characteristics of the modeling environment. CALPUFF in Golden compares well with this study.

Since air quality health problems are most severe during peak PM concentration hours, comparison of NRMSE during the top 10 observed concentrations for each episode was performed. CALPUFF tends to show larger errors when only the top 10 observed concentrations are considered indicating poorer performance at characterizing higher levels of PM.

The suite of performance measures used here indicates that the model is not performing at an optimal level at all stations. However, based on comparison with some similar studies the model performance is adequate at the CPR and TOWN station. The GOLF station's poor performance in predicting PM concentrations was not expected as the station performed well in the CALMET evaluation (Chapter 3). It is evident in both episodes that there are periods of time when the model predictions at the GOLF station are extremely low for a period of several hours or even days (Figures 6-6 and 6-11). An analysis of the wind direction during these times indicates that both the observed and predicted winds are from the northwest. Northwest winds would disperse pollutants released from the point and area sources near town down valley to the Southeast. None of the pollutants sources would be carried towards the GOLF receptor.

During the hours where modelled PM concentrations at the GOLF stations are extremely low, there were PM concentrations observed at the station. This would suggest that although most of the sources modelled were in the Town of Golden and south of the GOLF station, there exists an unknown source or background level of PM that affects the GOLF station even when winds are from the northwest. Holmes and Morawska (2006) noted that CALPUFF typically shows reasonable agreement with pollutant concentrations with discrepancies usually accounted for by failure to model an unknown source. Based on our study, it would be reasonable to assume that the GOLF station's poor model performance is due to a failure to identify all sources of PM in the modeling domain. A PM emission source to the north of Golden could have been left out of the model. Or, the area sources already included in the model could have been characterized improperly. The area sources were only modeled as releasing from the more populated areas of the Town and this left the GOLF station as the only station outside the area source boundaries. The low levels at the GOLF stations could also be attributable to not including a background PM level due to natural sources (i.e forest fires and windblown fugitive dust) in the model.

An additional analysis of the modelled PM concentrations versus wind direction was performed (Figure 6-16, 6-17) and compared to the observed PM concentrations versus wind direction presented previously in Figures 4-7 and 4-8. The analysis lends further support to the hypothesis that there is a missing source unaccounted for to the north-northeast of the GOLF station, with a lower occurrence of elevated levels of PM concentrations modelled with north or northwest winds, when compared with the observations (Figure 6-16c, Figure 6-17c). In contrast, the observed and modelled wind directions that result in the highest PM concentrations compare well at the other two stations.

Analysis of the PM modeling results is presented in the following chapter. The results of the model performance evaluation at the three stations must be taken into account when interpreting the PM results, especially given the GOLF station's poor performance.

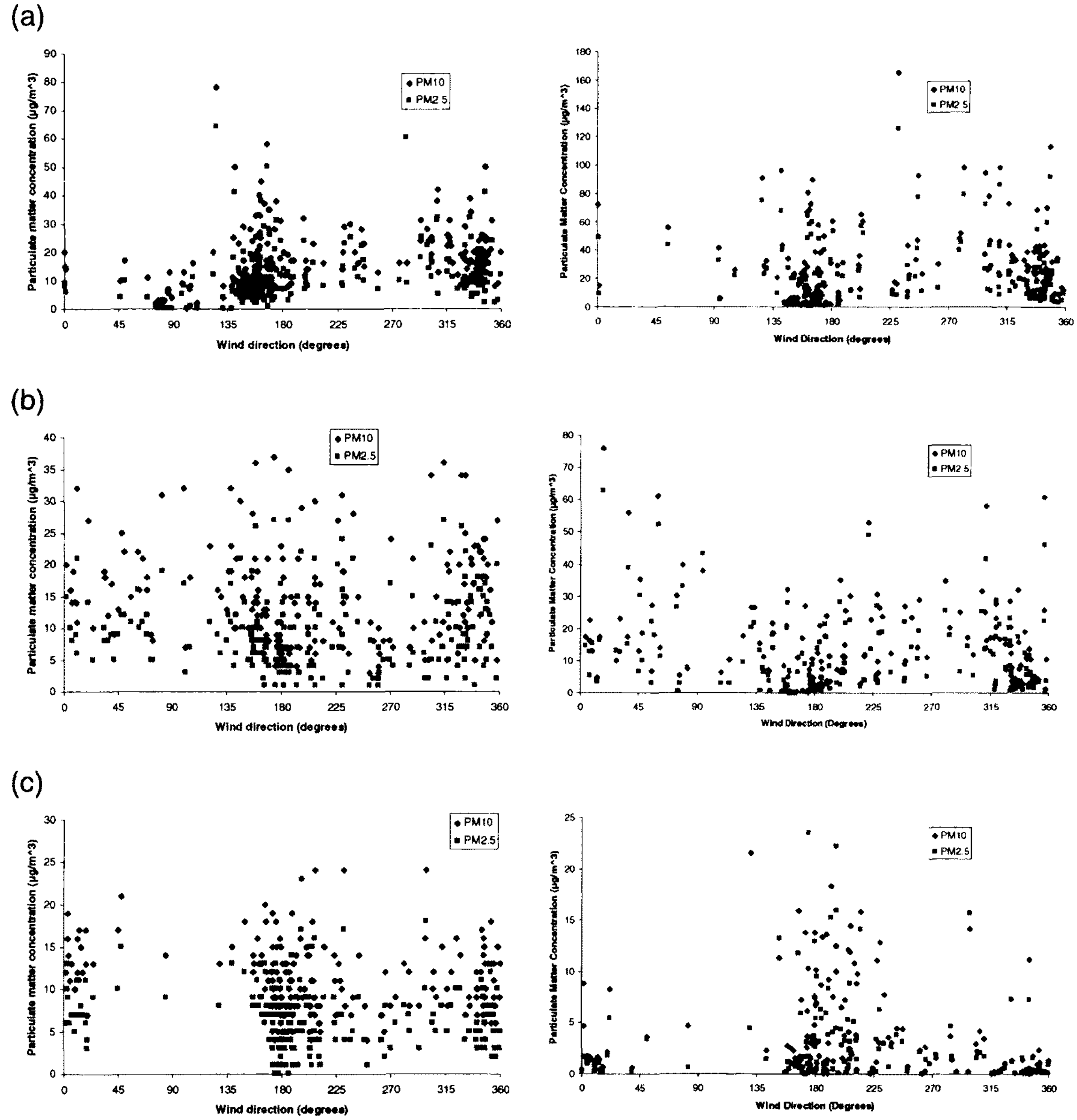

Figure 6-16 **Hourly PM concentrations and wind direction for Episode 1 at (a) Town station; (b) CPR station; (c) Golf station. Graphs to the left shows the measurements observed during each Episode 1 and the graph on the right shows the model predicted concentrations by wind direction.**

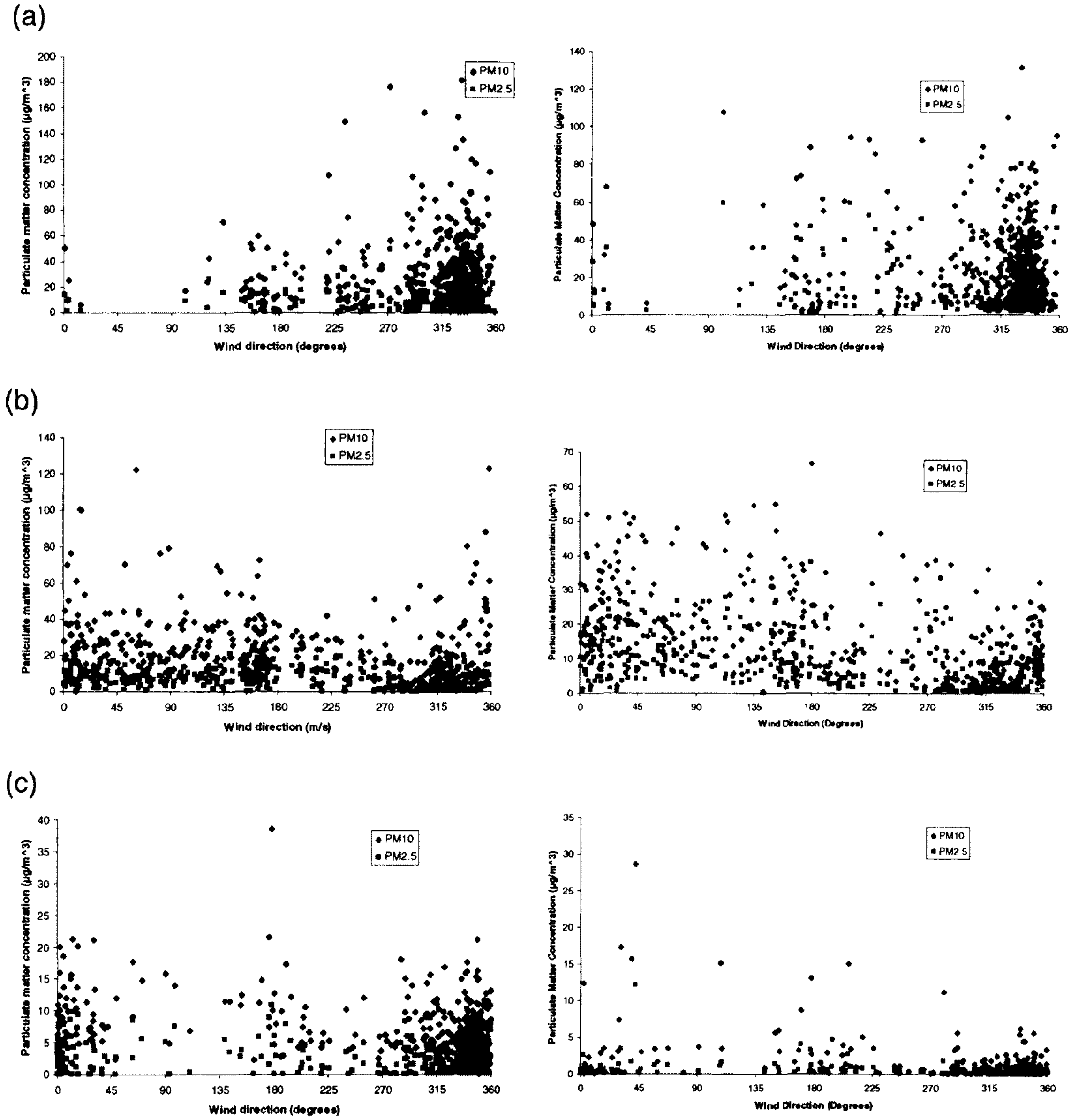

Figure 6-17 Hourly PM concentrations and wind direction for Episode 2 at (a) Town station; (b) CPR station; (c) Golf station. Graphs to the left shows the measurements observed during each Episode 2 and the graph on the right shows the model predicted concentrations by wind direction.

7 PARTICULATE MATTER ANALYSIS AND SOURCE APPORTIONMENT

The CALPUFF model was evaluated and the model found adequate at estimating PM concentrations at the CPR and TOWN stations. PM concentrations are not accurately estimated at the GOLF station. Following model evaluation, an analysis of the overall PM concentration predictions was performed, along with an analysis of the sources contributing to the two episodes under investigation.

A goal of this study was to determine the meteorological conditions that prevail during the episodes of PM under investigation. Most importantly the conditions during the hours with the highest PM concentrations can indicate specific meteorological parameters that lead to spikes in PM that may affect community health in Golden.

Source apportionment allows for analysis of what sources contribute to the high PM concentrations at each station. Diurnal variation in emissions and hourly meteorological conditions will determine the percent contribution of each source at the three monitors. This will allow for the investigation of any spatial variability in emission impacts.

7.1 Particulate Matter and Meteorological Analysis

A comparison of basic meteorological parameters routinely recorded at weather stations with particulate matter levels during both episodes has been performed (Chapter 4). The analysis determined that high PM levels occur most often at low wind speeds. High PM levels occurred during both northwesterly and southeasterly winds along the valley alignment. During both episodes, the highest PM concentrations occur in the late afternoon and into the evening (Figure 4-1 and

4-2). This was hypothesized to occur because of a combination of meteorological and emissions related processes. Downslope flows during this part of the day could bring emissions toward the valley floor, where PM monitors in Golden are located. In addition, the along-valley flow is typically slowing (Figure 7-1) and reversing at this time.

The mixing height typically lowers during this time as well (Figure 7-2). Coinciding with the shift in wind and collapse of the mixing height, emission generating activities are increased at this time of the day. During the late afternoon and early evening, traffic increases as residents drive home from work or school and space heating emissions increase as residents burn wood, oil or gas to heat their homes upon arrival.

Meteorological parameters (wind speed, mixing height, temperature, and Monin-Obukhov Length) estimated by CALMET were compared to the predicted particulate matter levels during both episodes. The comparison can show the influence of the predicted parameters on particulate matter concentrations. Time series of predicted meteorological parameters were compared to time series of PM levels to investigate correlation (Table 7-1). High correlation values, either negative or positive, would indicate that there is a possible effect of the parameter on predicted PM concentrations. A multiple regression analysis was also performed (Table 7-2).

Negative correlations between wind speed and PM levels, as well as mixing height and PM levels, are moderate for both episodes, especially at the CPR and

TOWN stations. This is expected with lower wind speeds or mixing height hindering dispersion of particulate matter as it is emitted.

(a)

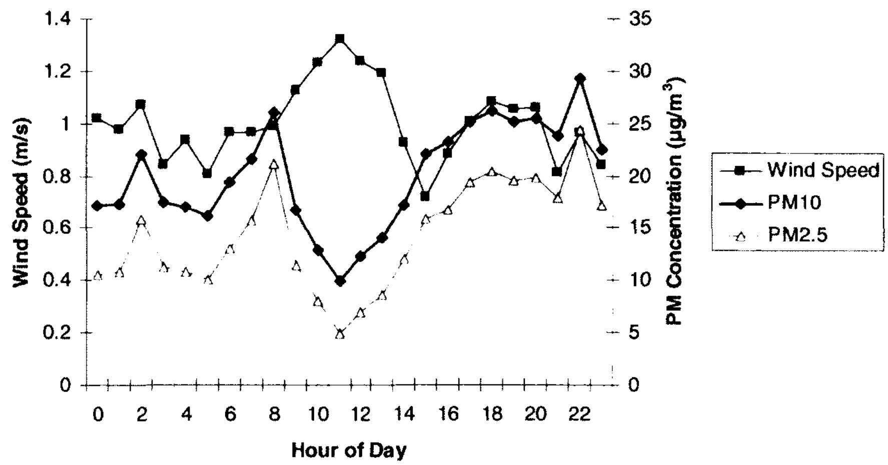

(b)

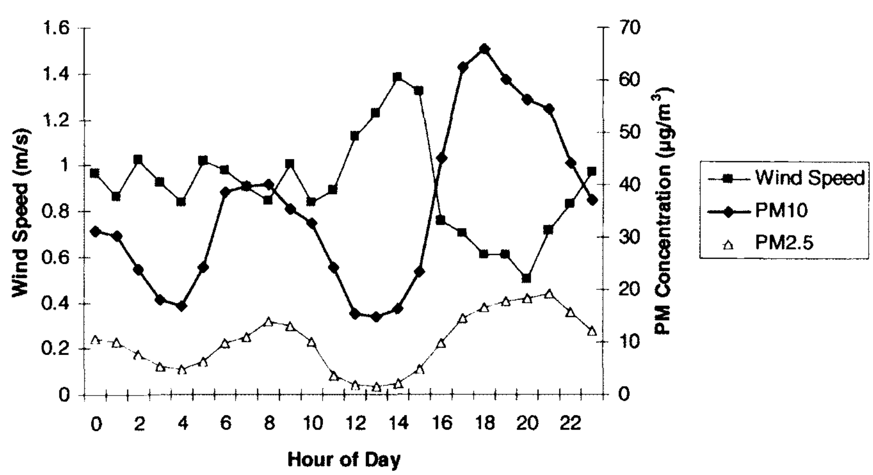

Figure 7-1 Modeled wind speed and observed particulate matter concentrations at the TOWN station for (a) Episode 1; (b) Episode 2. The wind speed and PM averages are from all days in each episode.

(a)

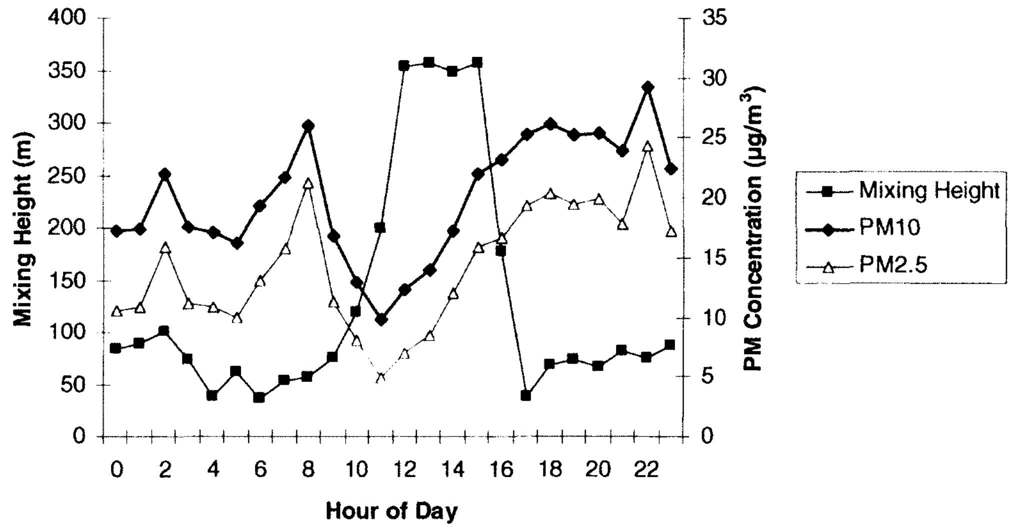

(b)

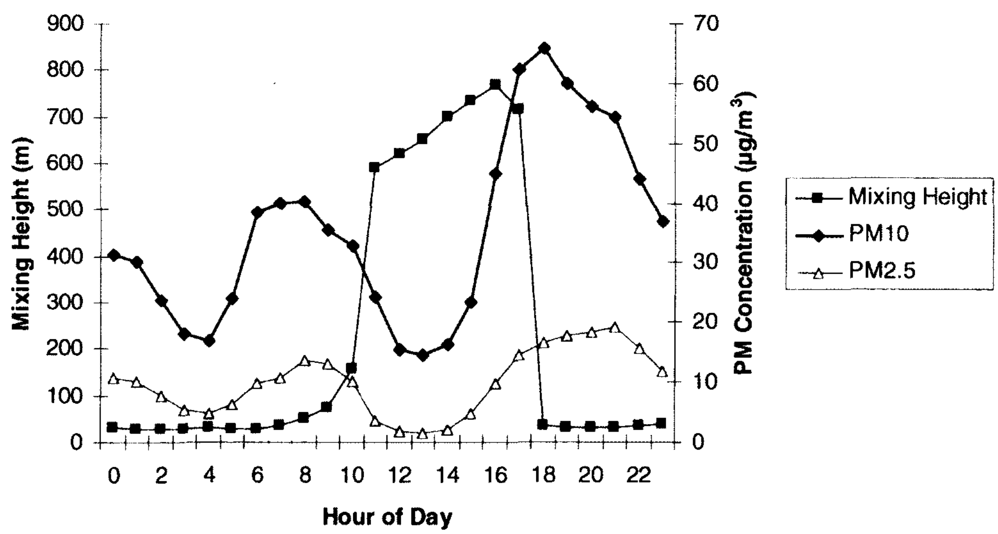

Figure 7-2 **Modeled mixing height and observed particulate matter concentrations at the TOWN station for (a) Episode 1; (b) Episode 2, The mixing height and PM averages are from all days in each episode.**

Temperature is also moderately, negatively correlated with observed values meaning that lower temperatures correspond to higher PM concentrations. This lends support to the hypothesis that at lower temperatures emissions from sources such as space heating would increase. It should also be recognized that other factors, such as mixing height and wind speed, tend to co-vary with temperature, so a negative correlation with temperature may also be related to dispersion. However, under this hypothesis stronger correlation coefficients should be calculated for $PM_{2.5}$, the main pollutant emitted by space heating. This occurs at the TOWN station but not at the CPR station. Emissions from space heating were varied diurnally, but were not adjusted to reflect temperature fluctuations. However, by coincidence, the diurnal fluctuations calculated from the woodstove survey would follow typical daily temperature patterns.

Multiple regression analysis was used to investigate the significance of wind speed, mixing height and temperature on PM concentrations. Table 7-2 summarizes the individual p-values (representing the significance of each parameter in predicting the corresponding PM concentration) as well as the multiple regression r-squared (representing the amount of variability in PM accounted for by the variables wind speed, temperature and mixing height) and p-values of the F variable (representing the significance of the multiple parameters included in the regression; values <0.05 indicate that the multiple regression results are significant).

Episode 1: Wind speed is a significant variable only at the TOWN station. Mixing height is significant in determining PM concentrations in all scenarios except PM_{10} at the TOWN station. Temperature is a significant factor at both the CPR and

TOWN stations. Overall, the three variables tested account for 30-40% of the PM concentration variability

Table 7-1 Correlation coefficients between predicted meteorological parameters and predicted PM levels during both episodes. Wspd = wind speed, Mix hgt = mixing height, Temp = temperature, Mon-obu = Monin-Obukhov length.

	CPR		TOWN		GOLF	
Episode 1	PM_{10}	$PM_{2.5}$	PM_{10}	$PM_{2.5}$	PM_{10}	$PM_{2.5}$
Wspd	-0.48	-0.46	-0.54	-0.56	-0.14	-0.11
Mix hgt	-0.34	-0.38	-0.42	-0.48	-0.29	-0.27
Temp	-0.56	-0.51	-0.23	-0.35	-0.08	-0.11
Mon-obu	0.02	0.01	-0.05	0.05	0.09	0.15
Episode 2						
Wspd	-0.51	-0.50	-0.56	-0.58	-0.22	-0.22
Mix hgt	-0.52	-0.51	-0.40	-0.42	-0.13	-0.16
Temp	-0.40	-0.38	-0.23	-0.25	0.04	-0.01
Mon-obu	0.62	0.65	0.26	0.25	0.13	0.22

Table 7-2 Multiple regression results for wind speed (WS), temperature (T) and mixing height (Mix Hgt) as compared to predicted PM_{10} and $PM_{2.5}$ levels during each episode.

	Individual p-value			Multiple Regression	
E1 PM10	WS	T	Mix Hgt	R-squared	Significance F
CPR	0.111	0.000	0.001	0.409	0.000
TOWN	0.000	0.016	0.146	0.325	0.000
GOLF	0.641	0.687	0.002	0.068	0.002
E1 PM2.5					
CPR	0.068	0.000	0.012	0.325	0.000
TOWN	0.000	0.000	0.026	0.406	0.000
GOLF	0.864	0.425	0.003	0.059	0.005
E2 PM10					
CPR	0.000	0.694	0.000	0.325	0.000
TOWN	0.000	0.131	0.000	0.399	0.000
GOLF	0.000	0.006	0.019	0.063	0.000
E2 PM2.5					
CPR	0.000	0.501	0.000	0.317	0.000
TOWN	0.000	0.073	0.000	0.436	0.000
GOLF	0.000	0.074	0.012	0.057	0.000

Episode 2: Wind speed and mixing height are significant variables at all stations. Temperature is not a significant factor except at the GOLF station for PM_{10}. Once again, the variables account for 30-40% of the PM variation.

During both episodes it appears that high PM concentrations are largely affected by low wind speeds and low mixing height. This would also be supported by the time series plots presented in Chapter 6 (Figure 6-6Figure 6-6d and Figure 6-11d). Temperature can also be significant, however it is likely an indicator of the "built-in" diurnal variation of the area sources modeled. Low wind speeds and mixing height are crucial to pollutant dispersion, especially during the night. CALMET uses the vertical temperature profile above the height of the previous hour's mixing height from the HOBO/upper air data as well as the calculated surface heat fluxes, and calculates the daytime convective mixing height. It then calculates the mechanical mixing height based on Venkatram (1980) and the surface wind speed and surface roughness. The daytime mixing height is the maximum of the calculated convective or mechanical mixing height. In the absence of surface convective mixing, surface wind speeds and surface roughness are used to estimate only the mechanical mixing height at night, resulting in lower mixing height predictions. In this study, the daytime mixing heights seem reasonable, but the night-time mixing heights are extremely low, especially during episode 2, which may contribute to the over-prediction of PM concentrations.

Variability in PM concentrations is caused by differing dispersal (meteorological) conditions and emission processes. PM variability not characterized by meteorological factors is likely due to changes in emissions not captured by the level of detail in the emission scenarios.

7.2 Source Apportionment

Source apportionment determines the types and amounts of PM that come from specific emission sources. As demonstrated in Golden by the Evans and Jeong (2007), source apportionment analysis can be accomplished through receptor modeling. Receptor modelling is typically expensive as it involves laboratory time to chemically analyze air filter samples. In this section, CALPUFF results are used to apportion the sources contributing to the PM concentrations recorded at all three monitoring station.

The CALPUFF setup described and evaluated in Chapter 6 was used to model individual source contributions. Sources were combined to produce an overall PM_{10} and $PM_{2.5}$ concentration. By modeling individual sources, the contribution of each source to the total can be estimated. The GOLF station is analyzed in this section, however the analysis should be taken in the context of the poor model performance at this location. It should be noted that there is likely an unknown source (background or otherwise) that was not included in the model that affects PM levels at the GOLF station. Inclusion of this unknown source would significantly reduce the impacts of other sources at the GOLF station.

7.2.1 Episode 1 Source Apportionment

Source contributions over the entire first episode (Figure 7-3) show that space heating, road dust , LP operations and construction operations account for the majority of PM_{10} at all three monitors. Space heating emissions impact the CPR and

TOWN stations the most, while LP emissions contribute the most to the GOLF station.

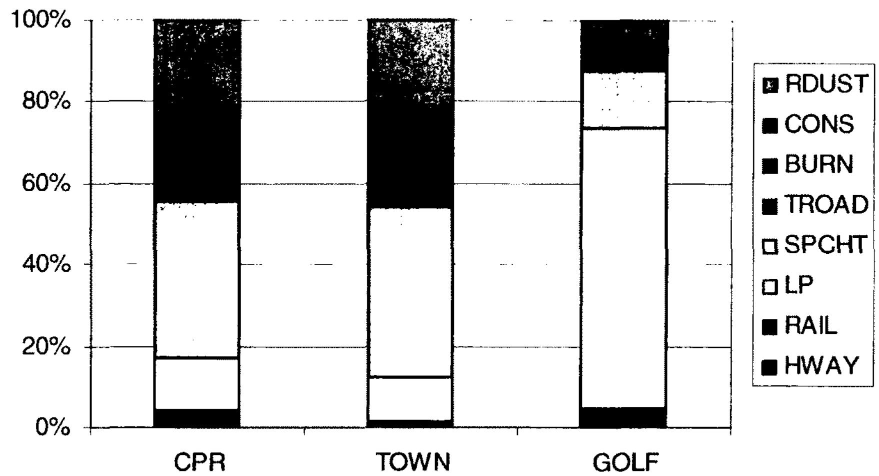

Figure 7-3 **PM_{10} source contribution to the entire first episode. RDUST = road dust; CONS = construction; BURN = burning; TROAD = town road traffic; SPCHT = space heating; LP = Lousiana Pacific Wood Products Ltd.; Rail = railway; HWAY = highway**

During the top 25 hourly concentrations, the impact of space heating is higher at the CPR and TOWN stations, while the GOLF station record over 75% of its ambient concentration from emissions at LP (Figure 7-4).

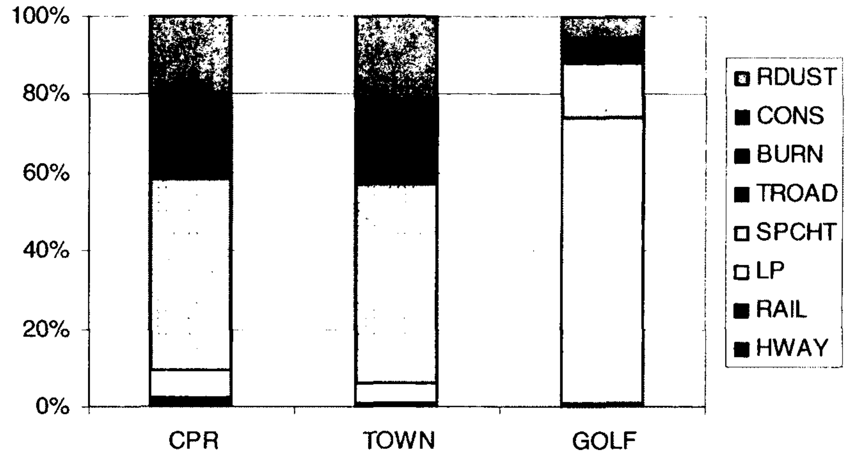

Figure 7-4 **PM_{10} source contribution to the top 25 hourly PM concentrations during the first episode**

Source contributions to $PM_{2.5}$ concentrations over the entire first episode show that space heating emissions are the largest constituent at all three stations (Figure 7-5). When only the top 25 concentrations are considered the impact of the space heating emissions is further heightened (Figure 7-6).

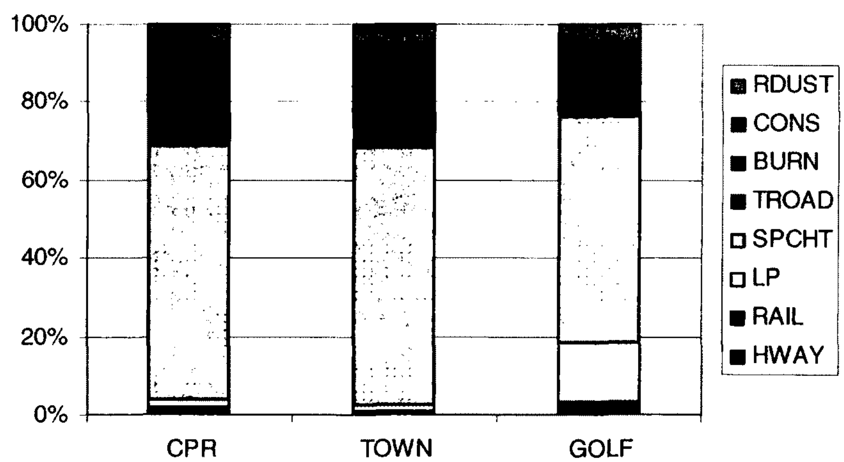

Figure 7-5 **$PM_{2.5}$ source contribution to the entire first episode**

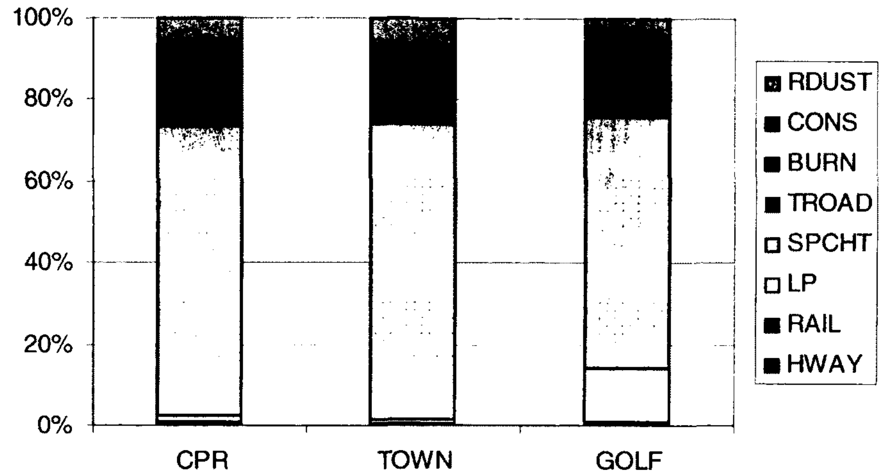

Figure 7-6 **$PM_{2.5}$ source contribution top 25 hourly PM concentrations during the first episode**

7.2.2 Episode 2 Source Apportionment

Source contributions over the entire second episode (Figure 7-7) show that road dust, LP operations, space heating and construction operations account for the majority of PM_{10} at all three monitors. Road dust and LP emissions impact the CPR and TOWN stations the most, while LP emissions contribute the most to the GOLF station. When the top 25 hourly concentrations are isolated (Figure 7-8), the emissions from road dust contribute a larger proportion to the overall PM concentrations.

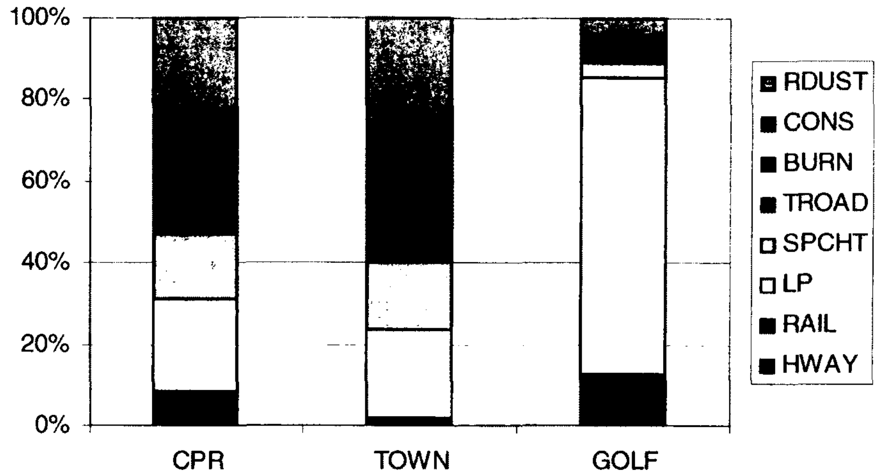

Figure 7-7 PM_{10} **source contributions to the entire second episode.**

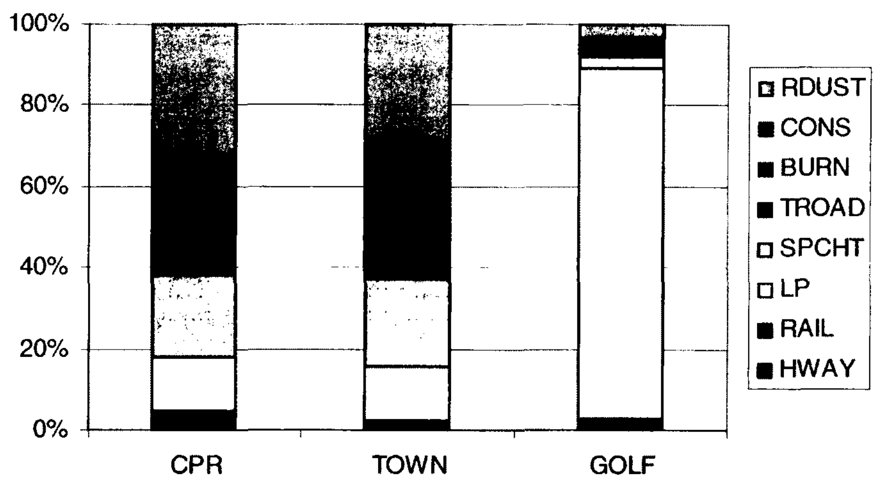

Figure 7-8 PM_{10} **source contribution to the top 25 hourly PM concentrations during the second episode.**

Source contributions to $PM_{2.5}$ over the entire second episode (Figure 7-9) showed that space heating emissions impact all three monitors the most. Other area sources made up the majority of the remaining emissions. The contribution of space heating emissions was also emphasized when the top 25 hourly concentrations are isolated (Figure 7-10).

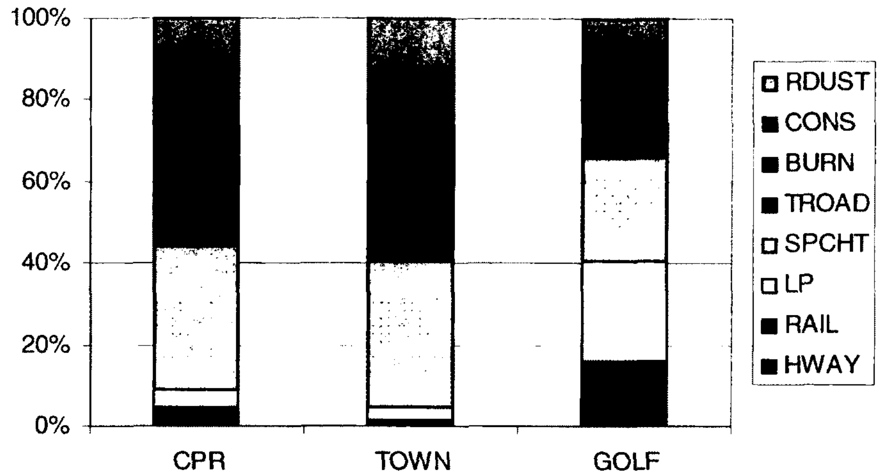

Figure 7-9 $PM_{2.5}$ source contributions to the entire second episode.

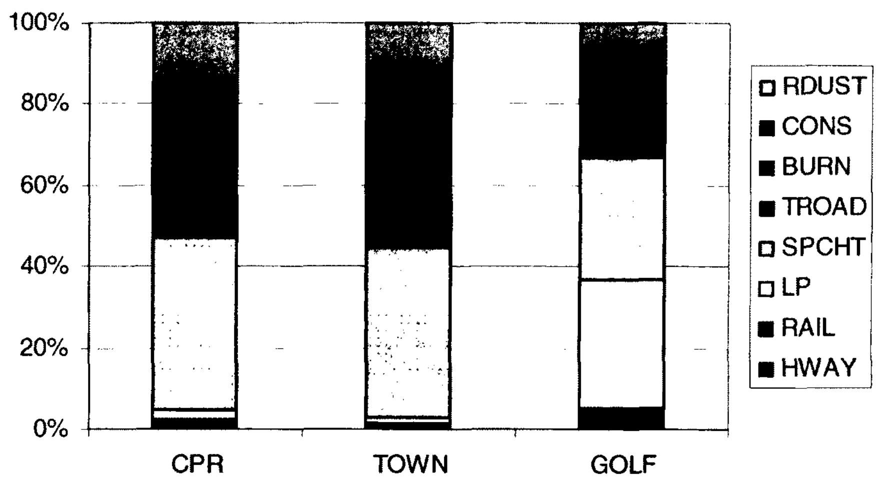

Figure 7-10 $PM_{2.5}$ source contribution to top 25 hourly PM concentrations during the second episode.

The source apportionment showed similar source contributions to both the CPR and TOWN stations, with quite different emissions contributing to the PM concentrations at the GOLF station. Overall, space heating emissions contributed the most to both episodes at the CPR and TOWN stations. LP emissions were the main contributor at the GOLF station.

7.3 Individual Source Results

This section describes each individual modeled source's contribution to the predicted PM levels at the CPR, TOWN and GOLF receptors.

7.3.1 LP Emissions

The contributions from LP operations were 13%, 11% and 69% for PM_{10} during episode 1 at CPR, TOWN and GOLF respectively. LP operations contributed 2%, 2% and 15% of $PM_{2.5}$ during episode one at CPR, TOWN and GOLF respectively. During episode two, LP operations contributed 23%, 22% and 72% to PM_{10} at CPR, TOWN and GOLF respectively. LP operations contributed 4%, 3% and 24% of $PM_{2.5}$ during episode two at CPR, TOWN and GOLF respectively (Table 7-3).

Table 7-3 LP emission source contributions to predicted PM levels at the CPR, TOWN and GOLF receptors. For comparative purposes the total PM loading for all sources during the episode (μg/m^3) is also included.

		Percent Contribution to PM			Total PM Loading All Sources (μg/m^3)		
Episode	Pollutant	CPR	TOWN	GOLF	CPR	TOWN	GOLF
1	PM_{10}	13	11	69	2,318	4,772	589
	$PM_{2.5}$	2	2	15	6,128	10,763	401
2	PM_{10}	23	22	72	1,676	3,414	389
	$PM_{2.5}$	4	3	24	3,098	5,311	107

7.3.2 Highway Emissions

The contributions from highway emissions were 2%, 0.5% and 3% for PM_{10} during episode 1 at CPR, TOWN and GOLF respectively. Highway emissions contributed 1%, 0.3% and 2% of $PM_{2.5}$ during episode one at CPR, TOWN and GOLF respectively. During episode two, highway emissions contributed 4%, 1% and 1% to PM_{10} at CPR, TOWN and GOLF respectively. Highway emissions contributed 2%, 0.5% and 2% of $PM_{2.5}$ during episode two at CPR, TOWN and GOLF respectively (Table 7-4).

Table 7-4 Highway emission source contributions to predicted PM levels at the CPR, TOWN and GOLF receptors. For comparative purposes the total PM loading for all sources during the episode (μg/m³) is also included.

		Percent Contribution to PM			Total PM Loading All Sources (μg/m³)		
Episode	Pollutant	CPR	TOWN	GOLF	CPR	TOWN	GOLF
1	PM_{10}	2	0.5	3	2,318	4,772	589
	$PM_{2.5}$	1	0.3	2	6,128	10,763	401
2	PM_{10}	4	1	1	1,676	3,414	389
	$PM_{2.5}$	2	0.5	2	3,098	5,311	107

7.3.3 Railway Emissions

To investigate the effects of the rail operations in the Golden airshed this analysis combines the PM outputs for both railway line and yard emissions. The contributions from railway emissions were 3%, 1% and 2% for PM_{10} during episode 1 at CPR, TOWN and GOLF respectively. Railway emissions contributed 1%, 0.4% and 1% of $PM_{2.5}$ during episode one at CPR, TOWN and GOLF respectively. During episode two, railway emissions contributed 5%, 1% and 12% to PM_{10} at CPR, TOWN and GOLF respectively. Railway emissions contributed 3%, 1% and 14% of $PM_{2.5}$ during episode two at CPR, TOWN and GOLF respectively (Table 7-5).

Table 7-5 Railway emission source contributions to predicted PM levels at the CPR, TOWN and GOLF receptors. For comparative purposes the total PM loading for all sources during the episode (μg/m³) is also included.

		Percent Contribution to PM			Total PM Loading All Sources (μg/m³)		
Episode	Pollutant	CPR	TOWN	GOLF	CPR	TOWN	GOLF
1	PM_{10}	3	1	2	2,318	4,772	589
	$PM_{2.5}$	1	0.4	1	6,128	10,763	401
2	PM_{10}	5	1	12	1,676	3,414	389
	$PM_{2.5}$	3	1	14	3,098	5,311	107

7.3.4 Space Heating Emissions

The contributions from space heating were 37%, 42% and 14% for PM_{10} during episode 1 at CPR, TOWN and GOLF respectively. Space heating contributed 65%, 66% and 58% of $PM_{2.5}$ during episode one at CPR, TOWN and GOLF respectively. During episode two, space heating contributed 16%, 17% and 4% to PM_{10} at CPR, TOWN and GOLF respectively. Space heating contributed 36%, 36% and 25% of $PM_{2.5}$ during episode two at CPR, TOWN and GOLF respectively (Table 7-6).

Table 7-6 Space heating emission source contributions to predicted PM levels at the CPR, TOWN and GOLF receptors. For comparative purposes the total PM loading for all sources during the episode (µg/m^3) is also included.

		Percent Contribution to PM			Total PM Loading All Sources (µg/m^3)		
Episode	Pollutant	CPR	TOWN	GOLF	CPR	TOWN	GOLF
1	PM_{10}	37	42	14	2,318	4,772	589
	$PM_{2.5}$	65	66	58	6,128	10,763	401
2	PM_{10}	16	17	4	1,676	3,414	389
	$PM_{2.5}$	36	36	25	3,098	5,311	107

7.3.5 Road Dust

The contributions from road dust were 23%, 23% and 6% for PM_{10} during episode 1 at CPR, TOWN and GOLF respectively. Road dust contributed 8%, 8% and 5% of $PM_{2.5}$ during episode one at CPR, TOWN and GOLF respectively. During episode two, road dust contributed 23%, 27% and 4% to PM_{10} at CPR, TOWN and GOLF respectively. Road dust contributed 11%, 13% and 6% of $PM_{2.5}$ during episode two at CPR, TOWN and GOLF respectively (Table 7-7).

Table 7-7 Road dust emission source contributions to predicted PM levels at the CPR, TOWN and GOLF receptors. For comparative purposes the total PM loading for all sources during the episode (μg/m³) is also included.

		Percent Contribution to PM			Total PM Loading All Sources (μg/m³)		
Episode	Pollutant	CPR	TOWN	GOLF	CPR	TOWN	GOLF
1	PM_{10}	23	23	6	2,318	4,772	589
	$PM_{2.5}$	8	8	5	6,128	10,763	401
2	PM_{10}	23	27	4	1,676	3,414	389
	$PM_{2.5}$	11	13	6	3,098	5,311	107

7.3.6 Local Traffic Emissions

The contributions from local traffic emissions were 5%, 6% and 2% for PM_{10} during episode 1 at CPR, TOWN and GOLF respectively. Local traffic emissions contributed 7%, 7% and 6% of $PM_{2.5}$ during episode one at CPR, TOWN and GOLF respectively. During episode two, local traffic emissions contributed 8%, 9% and 2% to PM_{10} at CPR, TOWN and GOLF respectively. Local traffic emissions contributed 14%, 15% and 9% of $PM_{2.5}$ during episode two at CPR, TOWN and GOLF respectively (Table 7-8).

Table 7-8 Local traffic emission source contributions to predicted PM levels at the CPR, TOWN and GOLF receptors. For comparative purposes the total PM loading for all sources during the episode (μg/m³) is also included.

		Percent Contribution to PM			Total PM Loading All Sources (μg/m³)		
Episode	Pollutant	CPR	TOWN	GOLF	CPR	TOWN	GOLF
1	PM_{10}	5	6	2	2,318	4,772	589
	$PM_{2.5}$	7	7	6	6,128	10,763	401
2	PM_{10}	8	9	2	1,676	3,414	389
	$PM_{2.5}$	14	15	9	3,098	5,311	107

7.3.7 Construction Emissions

The contributions from construction operations were 11%, 12% and 4% for PM_{10} during episode 1 at CPR, TOWN and GOLF respectively. Construction operations contributed 10%, 10% and 7% of $PM_{2.5}$ during episode one at CPR, TOWN and GOLF respectively. During episode two, construction operations contributed 16%, 17% and 4% to PM_{10} at CPR, TOWN and GOLF respectively. Construction operations contributed 18%, 19% and 12% of $PM_{2.5}$ during episode two at CPR, TOWN and GOLF respectively. The construction emissions were based on prorated annual estimates. It was not known what actual construction operations were being conducted during the episodes (Table 7-9).

Table 7-9 Construction emission source contributions to predicted PM levels at the CPR, TOWN and GOLF receptors. For comparative purposes the total PM loading for all sources during the episode (µg/m³) is also included.

		Percent Contribution to PM			Total PM Loading All Sources (µg/m³)		
Episode	Pollutant	CPR	TOWN	GOLF	CPR	TOWN	GOLF
1	PM_{10}	11	12	4	2,318	4,772	589
	$PM_{2.5}$	10	10	7	6,128	10,763	401
2	PM_{10}	16	17	4	1,676	3,414	389
	$PM_{2.5}$	18	19	12	3,098	5,311	107

7.3.8 Burning Emissions

The contributions from burning were 4%, 5% and 1% for PM_{10} during episode 1 at CPR, TOWN and GOLF respectively. Burning contributed 7%, 7% and 5% of $PM_{2.5}$ during episode one at CPR, TOWN and GOLF respectively. During episode two, burning contributed 6%, 7% and 1% to PM_{10} at CPR, TOWN and GOLF respectively. Burning contributed 13%, 13% and 8% of $PM_{2.5}$ during episode two at CPR, TOWN and GOLF respectively (Table 7-10).

Table 7-10 **Burning emission source contributions to predicted PM levels at the CPR, TOWN and GOLF receptors. For comparative purposes the total PM loading for all sources during the episode (μg/m³) is also included.**

		Percent Contribution to PM			Total PM Loading All Sources (μg/m³)		
Episode	Pollutant	CPR	TOWN	GOLF	CPR	TOWN	GOLF
1	PM_{10}	4	5	1	2,318	4,772	589
	$PM_{2.5}$	7	7	5	6,128	10,763	401
2	PM_{10}	6	7	1	1,676	3,414	389
	$PM_{2.5}$	13	13	8	3,098	5,311	107

7.4 Comparison with Receptor Modeling

Figure 7-9 provides a comparison of the modeled CALPUFF source apportionment of $PM_{2.5}$ with the receptor modeling of $PM_{2.5}$ conducted by BCMOE (Evans and Jeong 2007) during the speciation project in Golden. PMF analysis data were obtained for the specific days that receptor modeling data were collected during each episode. Only 4 filters were collected during each episode. Due to the small sample size, a seasonal comparison is also provided which compares the modeled data with the larger sample size used to provide the seasonal $PM_{2.5}$ breakdown (Figure 6-5). Since the final emission rates in CALPUFF were adjusted using the results of the receptor modelling it is noted that the comparison here is somewhat circular. However, the comparison can be used to illustrate whether the adjusted emission rates were mirrored in the results at the receptors in CALPUFF.

To review, the solution from the receptor modeling in Golden revealed seven factors contributing to PM. The factors identified were: Road Salt, Sulphate, Residential Wood Burning, Wood Processing, Crustal Material, Traffic and Residential Winter Heating. It was assumed that the winter heating and the residential wood burning factors would be an appropriate comparison with modeled space heating emissions, road dust emissions would be compared to the crustal factor, the wood processing factor would be compared directly with LP emissions and traffic emissions would be compared with traffic emissions as suggested by Evans and Jeong (2007). Filters for receptor modeling were collected at the TOWN station, therefore comparative modeled data was from the TOWN receptor.

During episode 1, the CALPUFF modeled space heating emissions were a smaller contributor to PM levels in comparison to the residential wood burning factor presented in the receptor modeling, but are still the most significant factor. The other sources showed reasonable agreement with the receptor modeling analysis. The modeled data showed the best agreement with the seasonal receptor data. During episode 2, the seasonal receptor modeling and the CALPUFF modeling source apportionment did not show as good agreement. Specifically the receptor modelling indicated a higher contribution from LP and a lower contribution from space heating than was modeled with Calpuff. When compared with the receptor modeling from the episode, the LP contribution was similar, but the space heating contribution was still lower.

(a)

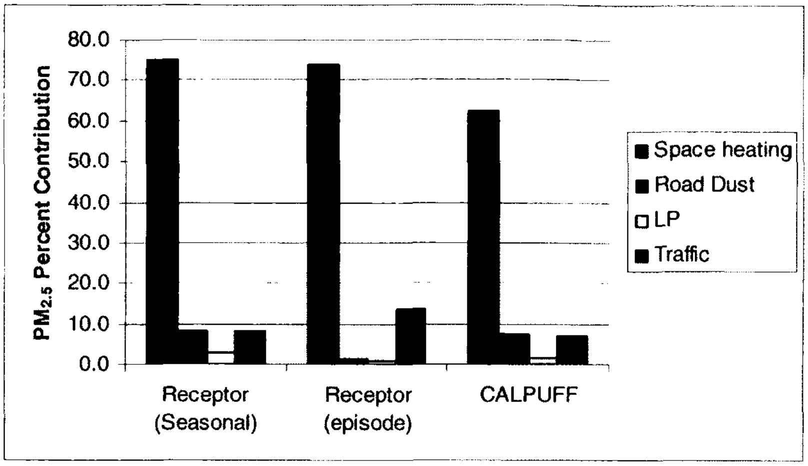

(b)

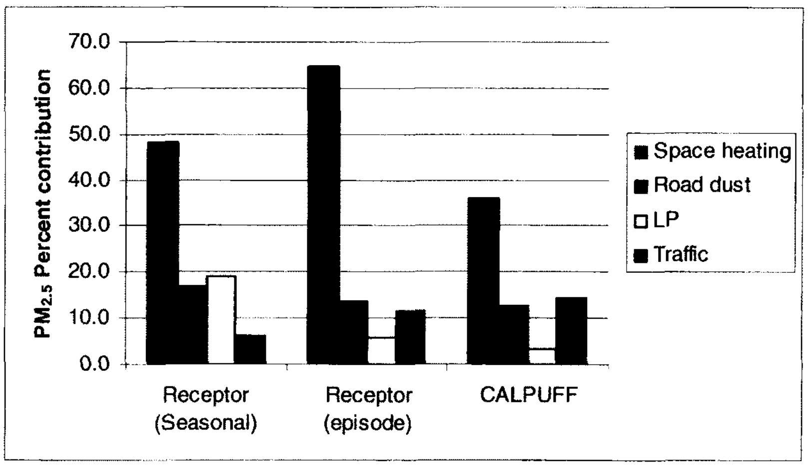

Figure 7-11 **Source apportionment comparison between seasonal receptor modeling, receptor modeling specific to the episode and CALPUFF predicted percentages of total estimated $PM_{2.5}$ is provided for (a) episode 1, and (b) episode 2.**

7.5 Discussion

CALPUFF was used to model eight sources identified as contributors to PM in the EI. CALPUFF results show that, as hypothesized, space heating was the top contributor to both PM_{10} and $PM_{2.5}$ during episode 1. During episode 2, LP and road dust were the top contributors to PM_{10} and space heating is the top contributor to $PM_{2.5}$. Road dust was hypothesized to be a major contributor to this "spring-time" episode and its contribution to the PM_{10} portion supports this hypothesis.

CALMET predicted a typical daily pattern in the boundary layer. Stability increases as the sun goes down and the earth's surface is cooled by emitting infrared radiation. This causes the convective mixing layer to shrink and the cooling continues into the night and morning. Typically, the poor dispersal in the evening is predicted by CALMET to remain through night-time hours and into the morning. This leads to extended periods of high PM as pollutants from all sources remain "trapped" creating a build-up of PM. CALMET predicts neutral or stable atmospheric conditions at these times. PM concentrations rise as both vertical and horizontal dispersion are hindered by the increasing stability and decreasing wind speeds. As the sun rises in the morning, heating of the surface causes the mixing layer to grow. An increase in horizontal wind speeds is accompanied by better vertical dispersion as the atmosphere becomes more unstable. CALMET predicts a fairly repetitive cycle throughout the two episodes. Thus, high PM concentrations typically occur during the morning and evening hours. It is unclear to what extent the upper air profiles input into CALMET (Figure 5-3) contribute to the build-up of pollutants, but the persistence of temperature inversions throughout the episodes would hinder the growth of the mixing layer and the dispersion of the PM. A more accurate vertical temperature and wind profile is essential for accurate modeling within the Columbia River Valley.

The source apportionment of the 25 highest PM concentrations for each episode was used to investigate which sources were contributing to the high hours of PM. These hours are of importance because of the health related consequences of extreme peaks in PM (Section 2-1). Overall, these hours contribute a large portion of the loading during each episode. Isolation of the highest PM concentrations in episode 1 at the CPR and TOWN monitors saw a jump in contributions of space heating emissions for both PM_{10} and $PM_{2.5}$. There are several coinciding factors that contribute to the prevalence of space heating during these times. A spike in the diurnal variation of space heating emissions occurs at the same time that CALMET predicts lower mixing heights, slowing of wind speeds and at times a reversal of flow (see for example, Figure 6-6, Table 6-12). CALMET predicts these poor dispersal conditions during the early morning hours (low mixing heights, low wind speeds) and evening hours (low mixing heights, low wind speeds and at times flow reversal). Typically, the highest concentrations occur during these hours as well (Figure 4-1 and 4-2). This supports the predictions made in Chapter 4 that a slowing of the wind speed combined with a low mixing height and possible reversal of the along-valley flow may contribute to higher PM concentrations. It is also supported by the correlation and multiple regression analysis (Section 7-1). These confirmed that both wind speed and mixing height were significant factors in the prediction of PM concentrations.

The same factors are allowing for road dust to contribute more to PM_{10} and space heating more to $PM_{2.5}$ during episode 2. Spikes in the diurnal variation of road dust emissions corresponds to the timing of the same meteorological factors described during episode 1 making them more prevalent during high hours of PM. Road dust emits mostly in the coarse fraction of PM_{10} and thus does not have as great of an effect on the $PM_{2.5}$ subset. Space heating emissions contribute more to the higher $PM_{2.5}$ concentrations because of similar factors as those described for episode 1.

The largest industrial emitter in Golden is LP. As such, residents are interested in its effects on PM concentrations. As expected, the modeling shows that LP emissions affect all stations in Golden. The effects are largely in the PM_{10} range. Over the past 10 years LP has performed several upgrades designed to reduce $PM_{2.5}$ emissions. The major improvements affecting air emissions from the mill and powerhouse from the LP site include: installing a baghouse on the plywood sander reducing emissions of sander dust significantly; installing a dry electrostatic precipitator on the powerhouse boiler, and; removing two old 1960-era dryers and replacing them with a highly efficient dryer coupled with a new wet electrostatic precipitator. In an effort to control PM_{10}, over the past 7 years has had a more consistent road dust control program for mill haul roads using dust suppressant and a consistent watering program during dry summer days.

A pattern exists in the apportionment of predicted LP emissions to each monitor. Predicted LP emissions account for a higher percentage of the PM at the GOLF station as compared to the other two stations. At first it may seem LP's location to the north of the Town causes increased predicted concentrations at the GOLF station. This pattern, however, is deceiving because the apportionment is displayed on a percentage basis. The overall amount of PM loading from LP modeled at all three stations is similar for episode 1. During episode 2, the total LP emissions at the CPR and TOWN stations are considerably more than those at the GOLF station. LP emissions are accounting for a higher percentage of the modeled PM at the GOLF station because the unknown source(s) or background PM level likely impacting this location is not modelled. Conversely, the CPR and TOWN stations, represented as discrete receptors within the area sources defined boundaries, are impacted much more from area sources. This clarification shows that despite LP's lower percent contribution at the CPR and TOWN stations the potential exposure to residents of Golden is higher at these locations compared to the GOLF station during modeling of episode 2 and similar at all three stations during modeling of episode 1.

The GOLF station results must be taken in context with the poor predictive performance at this station as described in the CALPUFF model performance evaluation (Chapter 6). Although LP emissions are a high percentage of the emissions recorded at this station, it must be considered that the predicted PM values are much too low. It is likely that there are sources not modeled or not modeled properly that contribute to the PM observed at the GOLF station. Other CALPUFF studies have shown that when CALPUFF is not in reasonable agreement with pollutant concentrations it tends to be as a result of an unknown source (Holmes and Morawska 2006). The modeling scenario places the GOLF station as the only monitor outside the boundaries of the area sources. The area sources in the model do not disperse to the GOLF monitor as readily as the elevated stacks producing the LP emissions.

LP emissions are more readily dispersed because of the effective release height of the stacks. When the winds are from the north, the peaks in PM have more contribution from the LP emissions. Northerly winds bring the LP emission towards the residents in the Town area and further south. Southerly winds bring the LP emissions away from the TOWN and towards the GOLF monitor. High PM events at the CPR and TOWN station during southerly wind events are entirely dominated by the area sources modeled.

There is an important limitation to this modeling analysis. Only two short episodes were modeled and different meteorological conditions during other parts of the year will influence emission dispersion. For example, predominantly stagnant conditions or northerly winds could cause more of an influence of LP emissions on the populated areas of Golden.

Line source emissions from highway and railway emission do not have much effect on PM concentrations. Examining outputs of CALPUFF line source dispersion shows that modeled emissions do not disperse far from the roadway or rail line segment. Unless a monitor is located very near to the roadway, the impacts are likely not to be great; the effects are on a micro-scale. Conversely, residents living along highways, busy roadways or rail lines may have quite a different apportionment of PM sources than those living further away.

Figure 7-11 shows the modeled sources and receptor modeling contributions to PM loading during the episode. Episode 1 CALPUFF results show reasonable agreement with the receptor modeling. The wintertime $PM_{2.5}$ emissions from the receptor modeling predicted space heating as the major contributor. CALPUFF modeled a lower contribution, but predicts that space heating is the most significant contributor of $PM_{2.5}$ at 62.5%. The other modeled emission sources show good agreement with the receptor modeling. The CALPUFF modeling supports the seasonal receptor modeling analysis for episode 1, however this is expected given that the emission rates were adjusted based on the receptor modeling. The limited number of receptor modeling samples taken during the episodes agreed reasonably well with the modeled results, but more samples would be needed to attempt any further analysis.

Episode 2 CALPUFF results show less agreement with the receptor modeling (Figure 7-11). Springtime receptor modeling was used for the comparison with the February episode. The wintertime receptor modeling did not compare well with Episode 2 CALPUFF results either. For episode 2 the CALPUFF modeling does not support the results of the receptor modeling. Given that CALPUFF emission rates were adjusted based on the receptor modeling results it is unexpected that the results of the CALPUFF and receptor modeling do not agree. This suggests that the CALMET meteorology modeled or the CALPUFF source characterization incorrectly captured the emissions from source to receptor.

It was observed in initial model runs that CALPUFF modeling using the existing emissions inventory significantly over-predicted PM concentrations.

Sarigiannis et al. (2004) showed that using inaccurate or out-of-date emissions inventories can cause significant error in dispersion modeling. The results of CALPUFF were improved using results from the recent receptor modeling analysis (Evans and Jeong 2007). This highlights the importance of having accurate, detailed emissions information for any modeling project. Certainly it would provide for a more accurate picture of dispersal in Golden if some of the area sources in this study were defined as individual point sources or more detailed emission information regarding the area emissions were known.

The source apportionment from CALPUFF modeling has provided an estimate of the sources contributing to PM during two episodes. Although model performance was not ideal, based on the available emission information and meteorological network CALPUFF predictions generally agree with the results of the receptor modeling indicating that the sources of concern are space heating, road dust and, at times, LP emissions.

8 MODELING SUMMARY

Application of the CALPUFF modeling system allowed for investigation of two episodes of high PM concentrations in Golden. The study set out to answer three questions:

- What are the dispersal mechanisms and emission processes that contribute to episodes of PM in Golden?
- Can these conditions be modeled in CALPUFF with the existing emissions information to accurately represent PM concentrations during these episodes?
- Will CALPUFF predicted PM source apportionment compare well with receptor modeling conducted by BCMOE (Evans and Jeong 2007)?

Examining the dispersion and emissions characteristics within and surrounding the Town of Golden prior to modeling identified that high PM concentrations during the episodes typically occurred during hours with low wind speeds. In addition, high PM levels were usually initiated during the late afternoon or early evening, with high concentrations persisting sometimes all night. It is likely at this time the along-valley wind flows are slowing and reversing, and, combined with escalated emissions from increased traffic and space heating contributed to higher PM levels.

Testing of the CALMET model revealed poor comparative performance of the meteorological model when surface stations were omitted in the "leave one out" method. However, CALMET showed reasonable agreement with observed conditions when run with a full suite of surface stations. Furthermore, CALMET was able to capture along-valley wind speed slowing and reversal in direction during late afternoon and early evening.

The CALPUFF dispersion model was not able to capture the hourly PM concentrations during the episodes with great accuracy. CALPUFF has had varying degrees of success in modeling pollutant concentrations accurately in complex terrain. The accuracy of this modeling exercise was comparable to other CALPUFF studies of similar application. CALPUFF's ability to characterize dispersion in complex terrain depends upon input of meteorological parameters from surface stations and upper air stations. Ideally, these stations would be located within or very close to the modeling domain. The upper air station closest to Golden was more than 400 kilometers away; although site specific temperature and SODAR data were used as well. The upper air profiles may have compromised CALPUFF's ability to capture the PM concentrations accurately.

Wind speed and mixing height are key factors in the dispersion of pollutants in Golden. In the absence of a local upper air station, data from Prince George, combined with local upper air wind data from the SODAR and HOBO temperature transect, were used as a surrogate upper air input file for CALMET. Mixing height is determined based on the vertical temperature profile, surface heat fluxes, horizontal winds, and surface roughness parameters. The upper air data, although partially local, likely does not provide the most accurate picture of the complete vertical temperature profile. CALPUFF over and under predictions are largely attributed to times when the mixing height is extremely low or high, respectively, for consecutive hours. Low mixing height during the night is attributable to the low wind speeds observed during the episodes. The unrealistically low mixing heights predicted during this study can be adjusted by applying an appropriate minimum mixing height. The daytime mixing heights could be better predicted by better defining the vertical temperature profile from the upper air data. Providing more accurate upper air data is a necessary component to any future modeling studies in Golden. Ideally, twice-daily rawisonde upper air data would be collected in Golden to allow for the local vertical temperature and wind profile to be established.

Inaccurate emission rate estimates, broad definition of area sources within the modeling domain and missing PM sources or background PM levels limited CALPUFF modeling accuracy. The emission rates originally tabulated from the emissions inventory and later revised from the receptor modeling did not depict the actual emission rates. Point source emissions are easily characterized because of legislated emissions reporting. Therefore, the accuracy of the LP emissions are likely the highest. However, area source emission estimates are hampered not only by the accuracy of the emission rates, but the definition of the emitting area. Additional information on the spatial variability of area emissions would improve modeling efforts. At the GOLF station, it is likely that a missing PM source or a failure to apply a background level of PM to the modeling, resulted in large periods of under-prediction. Future studies should identify any missing PM source (likely to the North of town) or apply an appropriate background PM level. A background PM level could be captured by establishing an additional monitoring station in an pristine environment near Golden, well away from anthropogenic sources.

The source apportionment of the CALPUFF results identified the major contributors to degraded air quality levels during the two episodes under investigation as space heating, road dust and, intermittently, LP operations. These results compared favourably with receptor modeling conducted during the same period in Golden.

CALPUFF modeling was commissioned in Golden, along with a number of other studies, to provide insight on the sources and relative contributions of PM in Golden. Our study set further goals to accurately model hourly predictions during episodes of high PM. CALPUFF identified PM source contributions in Golden. In addition, the prediction of hourly PM concentrations was comparable to other similar studies despite the identified limitations of meteorological and emissions data.

9 REFERENCES

Abel, T. et al. 2006. *An Air Emissions Inventory for Golden, British Columbia.* British Columbia Ministry of Environment. http://wlapwww.gov.bc.ca/kor/epd/air_emissions_golden/air_emiss_golden

Abdul-Wahab S.A. 2004. Evaluation of the Industrial Source Complex short term model: dispersion over terrain. *Journal of the Air and Waste Management Association* 54: 396-408.

Allwine, J.K et al. Peer Review of the CALMET / CALPUFF Modeling System. The Kevric Company Inc. August 28, 1998. http://www.epa.gov/scram001/7thconf/calpuff/calpeer.pdf

Arena, N., Georgieva E., Ratto, C.F. 1997. Diagnostic wind field modeling for complex terrain: new development and testing. *Physica* Medica 8 (Supplement 1): 373-374.

Arya, S.P. 1999. *Air pollution meteorology and dispersion.* Oxford University Press, New York.

Australian Environment Protection Authority, 2000. *AUSPLUME Gaussian-plume Dispersion Model Technical User Manual.* Victoria, Australia.

Assimakopoulos, V. 2005. Evaluation of CALPUFF modeling system performance: an application over the Greater Athens Area, Greece. *International Journal of Environment and Pollution* 24: 22:32.

Barna, M.G. and N.R. Grimson. 2002. Dispersion modeling of a wintertime particulate pollution episode in Christchurch, New Zealand. *Atmospheric Environment* 36: 3531–3544.

Bellasio, R. 2005. Algorithms to account for topographic shading effects and surface temperature dependence on terrain elevation in diagnostic meteorological models. *Boundary-Layer Meteorology* 114: 595–614.

British Columbia Ministry of Environment. 2008. *Guidelines for Air Quality Dispersion Modelling in British Columbia.* *http://www.env.gov.bc.ca/epd/bcairquality/reports/pdfs/air_disp_model_08.pdf*

British Columbia Ministry of Environment. 2002. *Fine Particulates: What They Are and How They Affect Us.* Water, Air and Climate Branch. Victoria, BC. http://www.env.gov.bc.ca/air/particulates/fpwtaaht.html

British Columbia. Provincial Health Officer. (2003). *Report on the Health of British Columbians. Provincial Health Officer's Annual Report 2002.The health and well-being of people in British Columbia.* Victoria, B.C.: Ministry of Health Planning.

Brechler, J. 2000. Model assessment of air pollution in Prague. *Environmental Monitoring and Assessment* 65: 269-276.

Burkholder, B. 2005. *PM in Golden.* British Columbia Ministry of Environment. Golden BC.

Caton, R.B. and D.V. Bates. 2002. Updating BC Provincial Air Quality Objectives – An Options Discussion Paper. British Columbia Ministry of Environment. http://www.env.gov.bc.ca/air/airquality/pdfs/aqo_paper.pdf

Chang, J.C. and S.R. Hanna. 2004. Air quality model performance evaluation. *Meteorology and Atmospheric Physics* 87: 167-196.

Chang, J.C. et al. 2003. Evaluations of CALPUFF, HPAC, and VLSTRACK with two mesoscale field datasets. *Journal of Applied Meteorology* 42: 453-466.

Cimorelli, A.J. et al. 2005. AERMOD: A dispersion model for industrial source applications. Part I: General model formulation and boundary layer characterization *Journal of Applied Meteorology* 44 (5): 682-693.

Cox, R.M., Sontowski, J. and C. Dougherty. 2005. An Evaluation of three diagnostic wind models (CALMET, MCSCIPUF, and SWIFT) with wind data from the Dipole Pride 25 experiments. *Meteorological Applications* 12:4: 329-341.

Curry, J.A. and P.J. Webster. 1999. Thermodynamics of atmospheres and oceans. Academic Press, San Diego.

Dabberdt, Walter F. and Erik Miller. 2000. Uncertainty, ensembles and air quality dispersion modeling: applications and challenges. *Atmospheric Environment* 34: 4667 – 4673.

Dockery, W.D., Cunningham, J., Damokosh, A.I., Neas, L.M., Spengler, J.D., Koutrakis, P., Ware, J.H., Raizenne, M., Speizer, F.E., 1996. Health effects of acid aerosols on North American children: respiratory symptoms. *Environmental Health Perspectives* 104: 500.

Dosio, A. et al. 2001. Assessing the meteorological conditions of a deep Italian Alpine valley system by means of a measuring campaign and simulations with two models during a summer smog episode. *Atmospheric Environment* 35: 5441–5454.

Enstrom, J.E. 2005. Fine particulate air pollution and total mortality among elderly Californians, 1973-2002. *Inhalation Toxicology* 17 (14): 803-816.

Elbir, Tolga. 2003. Comparison of model predictions with the data of an urban air quality monitoring network in Izmir, Turkey. *Atmospheric Environment* 37: 2149–2157.

EPA. 2003. AERMOD: Latest Features and Evaluation Results. US Environmental Protection Agency. http://www.epa.gov/scram001/7thconf/aermod/eval.pdf.

EPA. *Draft User's Guide for the Industrial Source Complex (ISCST3) Dispersion Models.* EPA-454/ B-95-003a. US Environmental Protection Agency: North Carolina.

Evans, G.J., and Cheol-Heon Jeong. 2007. Data Analysis and Source Apportionment of $PM_{2.5}$ in Golden, BC using Positive Matrix Factorization (PMF). Southern Ontario Centre for Atmospheric Aerosol Research, University of Toronto.

Gera, B.S. et al. 1996. Sodar in Dispersion Modeling. *Journal of Applied Meteorology* 35: 1632-1636.

Ghose, MK, et al. 2005. Assessment of the status of urban air pollution and its impact on human health in the city of Kolkata. *Environmental Monitoring Assessment* 108 (1-3): 151-167.

Irwin, J.S. et al. A comparison of CALPUFF air quality simulation results with monitoring data for Krakow Poland. *7th Int. Conf. on Harmonisation within Atmospheric Dispersion Modeling for Regulatory Purposes.* Belgirate, Italy. May 2001. http://rtmod.jrc.it/~thunis/harmo7/P217.pdf, September 25, 2005.

Isakov, V. et al. 2004. Near-field dispersion modeling for regulatory applications. *Journal of Air and Waste Management Association* 54: 473-482.

Jansen, K.L. et al. 2005. Associations between health effects and PM and black carbon in subjects with respiratory disease. *Environmental Health Perspectives* 113 (12).

Kaur, S. 2005. Pedestrian exposure to air pollution along a major road in Central London, UK. *Atmospheric Environment* 39 (38): 7307-7320.

Levy, JI et al. 2002. Using CALPUFF to evaluate the impacts of power plant emissions in Illinois: model sensitivity and implications. *Atmospheric Environment* 36: 1063-1075.

McEwen, B.A. 2003. Applicatioin of high resolution mesoscale model fields with the CALPUFF dispersion modeling system in Prince George, B.C. *Thesis (M.Sc.) University of Northern Britsh Columbia, Faculty of Natural Resources and Environmental Studies.*

Moraes, Osvaldo L.L. et al. 2005. Surface layer parameters over a complex terrain. *Atmospheric Environment* 39: 3103-3112.

Ministry of Water, Land and Air Protection (MWLAP). 2001. Air Contaminant Emissions (ACE) Model GIS User Manual and Report.

National Institute of Water and Atmospheric Research, NIWA. 2004. Good Practice Guide for Atmospheric Dispersion Modeling. *Ministry for the Environment, New Zealand. www.mfe.govt.nz*

Oettl, D. eta al. 2001. Evaluation of a Gaussian and a Lagrangian model against a roadside data set, with emphasis on low wind speed conditions. *Atmospheric Environment* 35: 2123-2132.

Oke, T.R. *Boundary layer climates.* Methuen, New York. 1987.

Olesen, H.R. 2005. User's Guide to the Model Validation Kit. *Initiative on Harmonisation within Dispersion Modelling for Regulatory Purposes.* www.harmo.org/kit

Ostermann, K., and Alex Schutte. 2004. CALMET Modeling for the Williams Lake Airshed. *Prepared for the Ministry of Environment, Cariboo Region.* http://www.env.gov.bc.ca/epd/bcairquality/reports/pdfs/CALMET_wlmslake.pdf

Ostro, B., 1993. The association of air pollution and mortality: examining the case for inference. *Archives of Environmental Health* 48: 336.

Ovadnevaite, J. et al. 2006. 2002 summer fires in Lithuania: Impacts on the Vilnius city air quality and the inhabitants health. *Science of the Total Environment* 356: 11-21.

Pasquill F. 1961. The estimation of the dispersion of windborne material. *Meteorological Magazine* 90: 33–49.

Ratto, CF et al. (1994) Mass consistent models for wind fields over complex terrain: the state of the art. *Environmental Software* 9: 247-268.

Robe, F.R. and J.S. Scire. 1998. Combining mesoscale prognostic and diagnostic wind models: A practical approach for air quality applications in complex terrain. *10th Joint Conference on the Application of Air Pollution Meteorology.* January 11-16, 1998. Phoenix, Arizona.

Ross, D.G. et al. (1988) Diagnostic wind field modeling for complex terrain: model development and testing. *Journal of Applied Meteorology* 7: 785-796.

Sakiyama, S. et al. 2005. Guidelines for air quality dispersion modeling in British Columbia. *British Columbia Ministry of Environment, Air Protection Section.* Victoria, BC. http://wlapwww.gov.bc.ca/air/airquality/pdfs/airdispmodelguide_july%2005.pdf

Schmitz, R. 2005. Modeling of air pollution dispersion in Santiago de Chile. *Atmospheric Environment* 39: 2035–2047

Schnelle, K.B. and P.R. Dey. 2000. *Atmospheric Dispersion Modeling Compliance Guide.* McGraw-Hill, New York.

Scire, J. and J. Godfrey. 2005. Earth Tech Inc. CALPUFF Training Course. Course Notes. Denver, Colorado, 14–16 December 2005.

Scire, J.S. and F.R. Robe. 1997. Fine-scale application of the CALMET meteorological model to a complex terrain site. *Air and Waste Management Association's 90th Annual Meeting and Exhibitioin.* June 8 – 13, 1997. Toronto, Ontario.

Scire, J.S. et al. 2000. A User's Guide for the CALPUFF Dispersion Model. Earth Tech, Inc.

Scire, J.S. et al. 2000b. A User's Guide for the CALMET Meteorological Model. Earth Tech, Inc.

Scire, J.S. et al. 1999. CALPUFF Modeling System. Earth Tech, Inc.

Scire, J.S. et al. 1989. CALGRID: A Mesoscale Photochemical Grid Model Volume II: User's Guide. *California Air Resources Board.* Sacremento, California. http://www.src.com/calgrid/files/CALGRID_Users_Guide.pdf

Song, Y., Zhang, M., Cai, X. 2006. PM10 modeling of Beijing in the winter. *Atmospheric Environment* 40: 4126-4136.

Triantafyllou, AG and PA Kassomenos. 2002. Aspects of atmospheric flow and dispersion of air pollutants in a mountainous basin. *The Science of the Total Environment* 297: 85-103.

US EPA, US Environmental Protection Agency, Office of Air Quality Planning and Standards, 1996. Review of National Ambient Air Quality Standards for PM: Policy Assessment of Scientific and Technical Information. US EPA, Washington, DC. Report No. EPA-452/R-96-013.

Vedal, S. 1997. Critical review—ambient particles and health: lines that divide, *Journal of the Air and Waste Management Association* 47 (5): 551–581.

Vedal, S. 1995. Health Effects of Inhalable Particles: Implications for British Columbia. Air Resources Branch, British Columbia Ministry of Environment. Victoria B.C.

Venkatram, A. 1988. Topics in Applied Dispersion Modeling in *Lectures on Air Pollution Modeling.* eds. Venkatram, A. and J.C. Wyngaard . American Meteorological Society, Boston.

Watson, J.G. 2002. Visibility: Science and regulation, *of the Air and Waste Management Association* 52 (6): 628–713.

Whiteman, D.C. 2000. *Mountain Meteorology: Fundamentals and Applications.* Oxford University Press, New York.

WHO, World Health Organization, 1994. Update and Revision of the Air Quality Guidelines for Europe. WHO Regional Office for Europe, WHO, Copenhagen. Report no. EUR/ ICP/EHAZ 94-05/PB0, pp. 14.

Win Lee , S et al. 2004. Important aspects in source $PM_{2.5}$ emissions measurement and characterization from stationary combustion systems. *Fuel Processing Technology* 85 (6): 687-699.

Wyngaard, J.C. 1988. Structure of the PBL in *Lectures on Air Pollution Modeling.* eds. Venkatram, A. and J.C. Wyngaard . American Meteorological Society, Boston.

Yamartino, R.J., Scire, J., Carmichael, G., Chang, Y., 1992. The CALGRID mesoscale photochemical grid model: model formulation. *Atmospheric Environment* 26A (8): 1493–1512.